

Methods for Estimating Capacities and Rates of Gaussian Quantum Channels

Oleg V. Pilyavets, Cosmo Lupo and Stefano Mancini

Abstract—Optimization methods aimed at estimating the capacities of a general Gaussian channel are developed. Specifically evaluation of classical capacity as maximum of the Holevo information is pursued over all possible Gaussian encodings for the lossy bosonic channel, but extension to other capacities and other Gaussian channels seems feasible.

Solutions for both memoryless and memory channels are presented. It is first dealt with single use (single-mode) channel where the capacity dependence from channel's parameters is analyzed providing a full classification of the possible cases. Then it is dealt with multiple uses (multi-mode) channel where the capacity dependence from the (multi-mode) environment state is analyzed when both total environment energy and environment purity are fixed. This allows a fair comparison among different environments, thus understanding the role of memory (inter-mode correlations) and phenomenon like superadditivity of the capacity.

The developed methods are also used for deriving transmission rates with heterodyne and homodyne measurements at the channel output. Classical capacity and transmission rates are presented within a unique framework where the rates can be treated as logarithmic approximations of the capacity.

Index Terms—Classical capacity of quantum channels, Classical transmission rates of quantum channels, Gaussian quantum channels, Quantum information.

I. INTRODUCTION

QUANTUM channels are every means that convey quantum systems on whose states information is encoded. Formally they are quantum maps from input to output states [1]. The maximum rate at which information can be reliably transmitted through a quantum channel defines its capacity. Actually one can define several capacities depending on the kind of information transmitted (classical or quantum) and on the additional resources used in transmission [2].

Evaluation of quantum channel capacities is one of the most important and difficult problems of quantum information theory. Gaussian channels, which maps input Gaussian states into output Gaussian states, are among the simplest models allowing capacities investigation [3]. They are also relevant for experimental implementations in quantum optics [4] and

for security analysis in continuous variables quantum key distribution [5].

A paradigmatic example of Gaussian quantum channel is the lossy bosonic channel [3], [6] where states lose energy 'en route' from the sender to the receiver. The term bosonic arises because each input (respectively output) is represented by an optical bosonic field mode. In turn, the effect of losses is usually modeled by letting each input mode interact with an environment mode through a rotation (beam splitter) transform whose angle (transmissivity) determines the loss rate [4].

The classical capacity and the classical assisted capacity for such a channel were evaluated in Refs. [7], [8] by assuming each environment mode in the vacuum state. Subsequently, also the quantum capacity has been derived [9]. However, when more general states of the environment are taken into account, e.g. non-separable ones giving rise to memory effect [10], the evaluation of capacities becomes much more demanding. Attempts have been carried out in [11], [12] by resorting to specific parameters' ranges and numerics.

There are different ways to introduce memory effects in such channels (see e.g. [11] and [13]). Here, we shall refer to the method first presented in [10]. Moreover, we will solely consider classical capacity and classical information transmission rates.

Finding classical capacity results in the constrained maximization of Holevo information [14], [15], [16] over input states, where constraints appear due to the restriction on input energy. We shall confine our attention to Gaussian inputs which in practice are the most important set of states and are also conjectured to be optimal [17]. However, this gives rise to a maximization problem which in general might be not spectral, therefore we shall consider only that class of memory models which result in a spectral problem. The latter will allow us to split the maximization for memory channel in two steps: the maximization inside each channel's mode (use) respecting its own energy restriction (it gives the capacity for the single channel use (single-mode)), and a further optimization of the distribution of total input energy over different channel modes (uses). This essential simplification is possible thanks to the obtained proof of concavity for one-shot capacity over input energy and to the additivity of the Holevo function in the memoryless case (see also [18]).

As far as the first maximization step involves the optimization inside each channel mode separately, we shall first discuss the single channel use (single-mode). It can be shown that its environment is characterized by two parameters: the amount of squeezing and the average amount of thermal photons. To completely specify the channel usage we also have to consider

O. Pilyavets is with the School of Science and Technology, Physics Division, University of Camerino, I-62032 Camerino, Italy and with the P. N. Lebedev Physical Institute, Leninskii Prospect 53, Moscow 119991, Russia (email: pilyavets@gmail.com).

C. Lupo is with the School of Science and Technology, Physics Division, University of Camerino, 62032 Camerino, Italy (email: cosmo.lupo@unicam.it).

S. Mancini is with the School of Science and Technology, Physics Division, University of Camerino, 62032 Camerino, Italy (email: stefano.mancini@unicam.it).

the transmissivity value and the input energy restriction. Thus, the classical capacity is found to be a monotonic function of all these parameters except of the environment squeezing. This makes the latter a specific parameter indicating different channel's regimes. In particular, it turns out that the capacity does not depend on any parameters except of the input energy if the environment squeezing tends to infinity (see also [11], [12]). Then we shall deeply study this behavior putting forward the existence of *critical parameters* that characterize the general behavior of the channel. We will also find out *super-critical parameters*, which in turn characterize the behavior of the critical parameters, and can be somehow regarded as fundamental constants.

We shall then move to the multi-mode channel setting to address the second maximization step. This will be done by resorting to convex separable programming techniques [19], [20] and will allow us to draw conclusions about the memory channel. This has become a palatable subject because of the possibility of enhancing the memoryless capacity [21]. This fact gives evidence of the superadditive phenomenon for quantum memory channels. However, in order to establish the superadditivity of the memory channel, one has to fairly compare different environments, by e.g. using the same energy constraints and purity. We shall investigate this problem showing optimality of non-homogeneous distribution of energy over modes for some channel's parameters, which happens due to non-monotonic dependence of the one-shot capacity from the environment squeezing discussed above. That can be interpreted as violation of mode symmetry, because the optimization problem is completely symmetric over channel modes. In turn, this mode symmetry violation can be related to the quadrature symmetry violation occurring in the single-mode channel. Then we can conclude that capacity is super-additive if mode symmetry is violated and additive otherwise.

It worth noticing that also the recent study [22] about the effect of noise correlation on the capacity of additive Gaussian noise channel can be brought back to the above sketched approach.

Finally, we will make use of the developed methods for deriving transmission rates which are even more relevant than capacity for practical purposes. Specifically we will account for the most common continuous variable measurements at the channel output, namely heterodyne and homodyne measurements [23]. Preliminary studies on such rates for lossy memory channel have been performed in [24]. Here, throughout the paper, capacity and transmission rates are presented in the same framework showing an unexpected parallelism between these quantities. Actually, within this framework the rates result as logarithmic approximations to the capacity. Similarly to the capacity, in general they are also subjected to violation of quadrature and mode symmetry, which will allow us to pose the optimal memory problem and calculate the critical parameters for the rates as well.

The paper is organized as follows. In Sec. II Gaussian channels are introduced. In Sec. III the classical capacity together with the information transmission rates are defined. In Sec. IV classical capacity and transmission rates for single-mode lossy bosonic channel are evaluated. In Sec. V the role

of single-mode channel parameters is discussed by evaluating critical and supercritical parameters for capacity and rates. In Sec. VI the capacity and rates for the multi-mode channel are evaluated and a particular memory model is studied. Sec. VII is for conclusions.

II. GAUSSIAN QUANTUM CHANNELS

Quantum mechanics in continuous variables can be introduced independently from Dirac approach as Weyl star-product (also known as Weyl calculus [25]) which operates with Weyl symbols defined on system's phase space (\mathbf{q}, \mathbf{p}) . Quadratures \mathbf{q} and \mathbf{p} for the system with n degrees of freedom are n -dimensional vectors of canonical variables. Below it will be useful to consider a vector

$$\mathbf{x} := (\mathbf{q}, \mathbf{p}) = (q_1, \dots, q_n, p_1, \dots, p_n). \quad (1)$$

Any quantum state, usually represented as a density operator $\hat{\rho}$ in the Hilbert space $\mathcal{H} \equiv \otimes^n L_2(\mathbb{R})$, can be specified in the above framework by its *Wigner function* $W(\mathbf{q}, \mathbf{p})$, which is a Weyl symbol of $\hat{\rho}$. Its relation with the density matrix in the \mathbf{q} representation reads¹

$$W(\mathbf{q}, \mathbf{p}) = \int \rho \left(\mathbf{q} + \frac{\mathbf{u}}{2}, \mathbf{q} - \frac{\mathbf{u}}{2} \right) e^{-i\mathbf{p}\mathbf{u}} d\mathbf{u},$$

$$\rho(\mathbf{q}, \mathbf{q}') = \frac{1}{(2\pi)^n} \int W \left(\mathbf{p}, \frac{\mathbf{q} + \mathbf{q}'}{2} \right) e^{i\mathbf{p}(\mathbf{q} - \mathbf{q}')} d\mathbf{p}.$$

In this work we apply Weyl calculus to the system of n one-dimensional harmonic oscillators, therefore we will call these degrees of freedom as *modes*. Furthermore, we restrict all possible quantum states of these oscillators by *Gaussian* ones, which are defined as follows. The quantum state $\hat{\rho}$ is called Gaussian if its Wigner function is Gaussian, *i.e.* such state can be completely specified by quadratures covariance matrix V and vector \mathbf{a} which are parameters (the second and first moments) of its Wigner function²:

$$\hat{\rho} \leftrightarrow \{\mathbf{a}, V\} \leftrightarrow W(\mathbf{x}) = \frac{1}{\sqrt{\det V}} e^{-\frac{1}{2}(\mathbf{x} - \mathbf{a}, V^{-1}(\mathbf{x} - \mathbf{a}))}, \quad (2)$$

where (\cdot) stands for the real scalar product and the vector \mathbf{a} represents displacement in the phase space. The quantities to be studied do not depend on this displacement, therefore each quantum state and each classical³ Gaussian distribution will be solely labeled by their quadratures covariance matrices, e.g. $\hat{\rho} \leftrightarrow V$.

Notice, that any Gaussian distribution of the form (2) is the Wigner function of some quantum state if its covariance matrix V satisfies the Heisenberg uncertainty condition [25], [26]

$$V + \frac{i\Sigma}{2} \geq 0, \quad (3)$$

¹Throughout the paper it is assumed commutation relations between canonical operators \hat{q}_h, \hat{p}_l belonging to \mathcal{H} to be $[\hat{q}_h, \hat{p}_l] = i\delta_{hl}$ (with δ the Kronecker symbol and $\hbar = 1$), and normalization of a n -mode Wigner function to be $\int W(\mathbf{x}) d\mathbf{x} = (2\pi)^n$.

²Notice, that Eq. (2) completely specifies the ordering of covariances in matrix V as corresponding to the vector (1).

³We will use convention accepted in quantum information theory, where random variables and probability densities of standard (classical) information theory are called *classical* to distinguish them from *quasi-probability* distributions (and variables associated with them) appearing in quantum setting.

where

$$\Sigma = \begin{pmatrix} \mathbb{O}_n & \mathbb{I}_n \\ -\mathbb{I}_n & \mathbb{O}_n \end{pmatrix} \quad (4)$$

is the symplectic form with \mathbb{O}_n and \mathbb{I}_n the $n \times n$ null and identity matrices, respectively. The eigenvalues of ΣV are $2n$ purely imaginary numbers $\{\pm i\nu_k\}$, $k = 1, \dots, n$, where $\{\nu_k\}$ are called *symplectic eigenvalues* of V . The condition (3) can be equivalently written as inequalities $\nu_k \geq 1/2$, which are saturated by pure Gaussian states [4], [25].

A *Gaussian quantum channel* acting on n modes is by definition a *completely positive* and *trace preserving* map defined on the set of quantum states, which maps any n -mode Gaussian state into a n -mode Gaussian state. As a consequence, it is any map Φ_n of moments [6]

$$\{\mathbf{a}, V\} \mapsto \{X_n^\top \mathbf{a} + \mathbf{d}_n, X_n^\top V X_n + Y_n\} \quad (5)$$

characterized by the triad (\mathbf{d}_n, X_n, Y_n) , where X_n, Y_n are two real $2n \times 2n$ -matrices obeying the inequality

$$Y_n + \frac{i}{2} (\Sigma - X_n^\top \Sigma X_n) \geq 0$$

with $Y_n \geq 0$ and symmetric and $\mathbf{d}_n \in \mathbb{R}^{2n}$ a displacement vector.

A very special case is that of the *memoryless channel*, for which $\Phi_n = \Phi_1^{\otimes n}$ is the direct product of n identical maps, *i.e.* a single-mode Gaussian channel used n times. It is hence characterized by a triad

$$(\bigoplus^n \mathbf{d}_1, \bigoplus^n X_1, \bigoplus^n Y_1),$$

where we have denoted

$$\mathbf{d}_1 := (d_q, d_p)^\top, \\ \bigoplus^n \mathbf{d}_1 := (d_q, \dots, d_q, d_p, \dots, d_p)^\top \in \mathbb{R}^{2n}.$$

Notice, that X_1, Y_1 are 2×2 -matrices, whose entries are scalars, and the direct sums $\bigoplus^n X_1, \bigoplus^n Y_1$ are 2×2 matrices, whose entries are $n \times n$ diagonal matrices⁴. Loosely speaking, the memoryless channel acts equally and independently on each of its uses.

More generally we can consider the case of a *quantum channel with memory* (or simply a *memory channel*). It is any channel which is *not* memoryless. Making no assumption on additional structures that might be present (e.g. causality, invariance under time translations), we can only say that $\Phi_n \neq \Phi_1^{\otimes n}$ or

$$(\mathbf{d}_n, X_n, Y_n) \neq (\bigoplus^n \mathbf{d}_1, \bigoplus^n X_1, \bigoplus^n Y_1).$$

The memory channel can be interpreted as a framework to describe correlations between channel actions corresponding to different channel uses.

⁴Such a convention was chosen to be consistent with the ordering (1) and the symplectic form (4).

III. CLASSICAL CAPACITY

The Gaussian quantum channel can be used to transmit classical information by *encoding* a classical stochastic continuous variable $\alpha \in \mathbb{R}^{2n}$, distributed according to a probability density P_α , into a set of quantum states (Wigner functions) W_α . The maximum rate at which classical information can be reliably sent through the channel defines its *classical capacity*.

In the case of a memoryless quantum channel, its classical capacity is given by [15], [16]

$$C = \lim_{n \rightarrow \infty} \frac{\chi(\Phi_n)}{n}, \quad (6)$$

where the *Holevo function* χ evaluated on n channel uses is defined as⁵

$$\chi(\Phi_n) = \max_{\{W_\alpha, P_\alpha\}} \left\{ S \left[\int \Phi_n(W_\alpha) P_\alpha d\alpha \right] - \int S[\Phi_n(W_\alpha)] P_\alpha d\alpha \right\}, \quad (7)$$

with $\Phi_n = \Phi_1^{\otimes n}$ and S the von Neumann entropy. Thus, the computation of the memoryless capacity⁶ is based on the optimization over all input ensembles W_α , including those made of states which are entangled among different channel uses.

If the input states are restricted to an ensemble of product states, it is reasonable to consider the so-called *one-shot capacity*

$$C_1 = \chi(\Phi_1)$$

obtained from Eqs. (6) and (7) by assuming $n = 1$. Clearly the one-shot capacity is a lower bound on the memoryless capacity. If these two quantities coincide, the Holevo function is said to be additive. In turn, additivity of the Holevo function dramatically simplifies the problem of evaluating the memoryless capacity. Even though the Holevo function has been shown to be additive for several relevant channels, this property does not always hold [27].

Moving to the general case, one could be tempted to generalize the formulae (6) and (7) to the case of memory channels by applying them for $\Phi_n \neq \Phi_1^{\otimes n}$. Quite generally we can say that the relation (6) only provides an upper bound for the capacity of the memory channel [28]. Indeed, it has been proven [29] that it coincides with the memory channel capacity for the class of so-called *forgetful* channels.

Thus, on the one hand we can define the upper bound

$$\overline{C} := \lim_{n \rightarrow \infty} \overline{C}_n, \quad \overline{C}_n := \frac{\chi(\Phi_n)}{n}.$$

On the other hand, for any n , one can look at n uses of the channel described by Φ_n as a single n -mode memoryless channel. Its one-shot capacity found as maximum over the set of Gaussian states provides a lower bound on the capacity of the memory channel [12]

$$\underline{C}_n := \frac{\chi_G(\Phi_n)}{n}. \quad (8)$$

⁵Contrarily to the original definition [16], in this paper we incorporate the maximum over input states in the Holevo function.

⁶As far as we consider only classical channel capacity, it will be often called as simply the capacity.

Taking the limit over n , we can as well define the lower bound⁷

$$\underline{C} := \lim_{n \rightarrow \infty} \underline{C}_n. \quad (9)$$

Since the capacity (in sense of the above definitions) in continuous variables case turns out to be infinite, some physically motivated constraints must be specified to avoid meaningless results. A typical choice in the framework of Gaussian channels is to impose a restriction on the maximal average input energy per channel use. As far as we are considering the system of n single-mode oscillators (see Sec. II) with channel uses corresponding to oscillators modes, this constraint reads⁸

$$\frac{1}{2n(2\pi)^n} \int \left(\int W_\alpha(\mathbf{x}) P_\alpha d\alpha \right) \mathbf{x}^2 d\mathbf{x} \leq N + \frac{1}{2}, \quad (10)$$

where N represents the maximum number of excitations (photons) per mode in average.

Finally, let us consider *Gaussian encoding* W_α, P_α used to calculate χ_G . For n uses of the quantum channel, we fix a reference n -mode Gaussian state, with zero mean, which is described by the Wigner function $\{0, V_{\text{in}}\}$ (see the definition (2)). A classical variable α will be encoded by applying a displacement operation on the reference state, thus obtaining Wigner function $\{\sqrt{2}\alpha, V_{\text{in}}\}$. We assume the stochastic variable α to be itself distributed according to the Gaussian probability density distribution with zero mean:

$$P_\alpha = \frac{1}{(2\pi)^n \sqrt{\det V_{\text{mod}}}} e^{-(\alpha, V_{\text{mod}}^{-1} \alpha)}.$$

Hence, the corresponding ensemble state

$$\int W_\alpha P_\alpha d\alpha,$$

is also Gaussian and described by a Wigner function $\{0, \bar{V}_{\text{in}}\}$, where

$$\bar{V}_{\text{in}} = V_{\text{in}} + V_{\text{mod}}. \quad (11)$$

Quadratures covariance matrices of output state and output average state below will be labeled by V_{out} and \bar{V}_{out} , respectively:

$$\begin{aligned} V_{\text{out}} &\leftrightarrow \Phi_n(W_\alpha), \\ \bar{V}_{\text{out}} &\leftrightarrow \int \Phi_n(W_\alpha) P_\alpha d\alpha. \end{aligned} \quad (12)$$

The restriction to Gaussian states, which are mapped into Gaussian states by Gaussian channels, dramatically simplifies the problem, since the complexity of specifying Gaussian states is polynomial in the number n of modes (see Eq. (2)). Moreover, Gaussian states are conjectured to be optimal inputs for Gaussian channels [17].

The von Neumann entropy of a n -mode Gaussian state $\{\mathbf{a}, V\}$ is the function of symplectic eigenvalues ν_k of matrix V [4]:

$$S(V) = \sum_{k=1}^n g\left(\nu_k - \frac{1}{2}\right), \quad (13)$$

⁷Throughout the paper, for the sake of simplicity, we will often refer to this lower bound as simply the capacity.

⁸We assume quantum states to have zero mean, i.e. $\langle \mathbf{x} \rangle = 0$.

where g is defined as

$$g(v) := (v+1) \log_2(v+1) - v \log_2 v.$$

The Holevo- χ quantity for the set G of Gaussian states can be derived from Eqs. (7) and (13). It equals [3]

$$\chi_n = \max_{V_{\text{in}}, V_{\text{mod}}} \sum_{k=1}^n \left[g\left(\bar{\nu}_k - \frac{1}{2}\right) - g\left(\nu_k - \frac{1}{2}\right) \right], \quad (14)$$

where χ_n is a shorthand notation for $\chi(\Phi_n)$. In turn, the quantities $\bar{\nu}_k$ and ν_k are the symplectic eigenvalues of \bar{V}_{out} and V_{out} , respectively. Finally, the input energy constraint (10) for Gaussian states can be written in terms of the covariance matrices as

$$\frac{\text{Tr} \bar{V}_{\text{in}}}{2n} \leq N + \frac{1}{2}. \quad (15)$$

A. Estimating the classical capacity

As we have seen the evaluation of the classical capacity practically reduces to the evaluation of the function (13). Notice, that $g(v)$ is not analytic in the neighborhood of zero where its asymptotic value is $-v \log_2 v$. Also, the function $g\left(v - \frac{1}{2}\right)$ is not analytic in the neighborhood of infinity, where its asymptotic value is $\log_2 v$. By subtracting this logarithm part we get the analytic function in the region $v \geq \frac{1}{2}$ which has its Laurent series (see also [30])

$$g\left(v - \frac{1}{2}\right) = \log_2 v + \frac{1}{\ln 2} \left[1 - \frac{1}{2} \sum_{j=1}^{\infty} \frac{(2v)^{-2j}}{j(2j+1)} \right] \quad (16)$$

written in the neighborhood of infinity. In particular, to the zeroth-order approximation it is

$$g\left(v - \frac{1}{2}\right) \approx \log_2 v + \frac{1}{\ln 2}, \quad (17)$$

where we have neglected terms of the order $O(v^{-2})$. Allowing perturbation of logarithm by the first terms in the series (16) we can also construct next-order approximations.

In what follows, it will be convenient to introduce the function

$$g_j(v) := v^j g^{(j)}\left(v - \frac{1}{2}\right), \quad (18)$$

where $j = 0, 1, 2, \dots$. Thus,

$$\begin{aligned} g_0(v) &= g\left(v - \frac{1}{2}\right), \\ g_1(v) &= v g' \left(v - \frac{1}{2}\right) = v \log_2 \frac{v + \frac{1}{2}}{v - \frac{1}{2}}, \\ g_2(v) &= v^2 g'' \left(v - \frac{1}{2}\right) = -\frac{v^2}{(v^2 - \frac{1}{4}) \ln 2}, \end{aligned} \quad (19)$$

and so on. It also has simple rules for derivatives, e.g.:

$$g'_1(v) = \frac{g_1(v) + g_2(v)}{v}, \quad g'_2(v) = \frac{2g_2(v) + g_3(v)}{v}.$$

In particular, we have $g_1(v) \equiv (\ln 2)^{-1}$ at zeroth-order approximation and

$$g_1(v) = \frac{1}{\ln 2} \left[1 + \frac{1}{12v^2} \right], \quad (20)$$

at first-order approximation.

Notice, that by using (17) we have, at the lowest order,

$$\chi_n^{(\log)} = \max_{V_{\text{in}}, V_{\text{mod}}} \sum_{k=1}^n \log_2 \frac{\bar{\nu}_k}{\nu_k}. \quad (21)$$

The value \underline{C}_n calculated through approximation (21) below will be denoted as $\underline{C}_n^{(\log)}$ and called *logarithmic approximation to capacity*. In turn, the quantity \underline{C}_n will be called *zeroth-order approximation to capacity* and denoted by $\underline{C}_n^{(0)}$, if actual maximum over V_{in} and V_{mod} is not taken in Eq. (14), but symplectic eigenvalues ν_k and $\bar{\nu}_k$ are chosen instead to be those at which the maximum in (21) is achieved. Thus, $\underline{C}_n^{(0)}$ is given by substitution of the approximate symplectic eigenvalues into the exact relation for Holevo- χ quantity.

B. Examples of Gaussian channels

There are two types of noises that are mostly relevant for experimental setups: *attenuation* and *addition of classical noise*. The so-called *lossy (bosonic) channels* describe the attenuation, while the *additive (classical) noise channels* take into account only the addition of classical noise. For a discussion of the capacity of the other classes of Gaussian channels, in the single-mode case, see [31].

The lossy channels play a prominent role and below we will focus our attention to them. They are characterized by the map (5) with the matrices

$$X = \sqrt{\eta} \mathbb{I}_{2n}, \quad Y = (1 - \eta) V_{\text{env}}. \quad (22)$$

Here V_{env} denotes the $2n \times 2n$ covariance matrix of the channel environment that ‘contaminates’ the input signal, which is attenuated by the the channel’s *transmissivity* $\eta \in [0, 1]$. In particular the lossy bosonic channel acts as a rotation (beam splitter) on the canonical quadratures and gives rise to the following relation among the covariance matrices [6]:

$$V_{\text{out}} = \eta V_{\text{in}} + (1 - \eta) V_{\text{env}}, \quad (23)$$

$$\bar{V}_{\text{out}} = \eta (V_{\text{in}} + V_{\text{mod}}) + (1 - \eta) V_{\text{env}}. \quad (24)$$

In fact, these transformations follow from the definitions (5), (12) and (22). Below (see Eq. (112)) it will be shown that the capacity is a monotonically increasing function of the average number of input photons per mode (channel use) N , therefore we shall constrain the input energy using the equality in (15), *i.e.*

$$\frac{1}{2n} \text{Tr}(V_{\text{in}} + V_{\text{mod}}) = N + \frac{1}{2}. \quad (25)$$

The additive noise channels are described by similar transformations [6]

$$V_{\text{out}} = V_{\text{in}} + V_{\text{env}}, \quad (26)$$

$$\bar{V}_{\text{out}} = V_{\text{in}} + V_{\text{mod}} + V_{\text{env}} \quad (27)$$

following from Eq. (5) if $X = \mathbb{I}_{2n}$ and $Y = V_{\text{env}}$, where V_{mod} and V_{env} correspond to classical distribution, while V_{in} should satisfy the uncertainty relation. Notice, that similarity between Eqs. (26), (27) and (23), (24) makes the extension of the method we are going to develop to the additive noise channel straightforward. In particular, a similar approach has been recently used in Ref. [22].

C. Heterodyne and homodyne rates

As far as the general optimization approach to find the Holevo function (14) is also applicable to information transmission rates, we are going to consider these as well and compare them with the capacity.

Suppose, that the matrices V_{in} , V_{mod} and V_{env} are block diagonal, *i.e.* can be written in the form

$$V_{\text{ind}} = \begin{pmatrix} V_{\text{ind},qq} & \mathbb{O}_n \\ \mathbb{O}_n & V_{\text{ind},pp} \end{pmatrix}, \quad (28)$$

where \mathbb{O}_n was defined by Eq. (4) and ‘ind’ may stand for ‘in’, ‘mod’ or ‘env’. Moreover, let us assume that their diagonal blocks mutually commute (including blocks taken from different matrices). In such a case by considering the average information accessible by performing *heterodyne* measurement on each single channel output (joint measurement of q and p quadratures) one can get the *heterodyne rate* [11]

$$R^{(\text{het})} := \lim_{n \rightarrow \infty} R_n^{(\text{het})}, \quad (29)$$

$$R_n^{(\text{het})} = \frac{1}{2n} \max_{V_{\text{in}}, V_{\text{mod}}} \log_2 \det \left[\left(\bar{V}_{\text{out}} + \frac{\mathbb{I}_{2n}}{2} \right) \left(V_{\text{out}} + \frac{\mathbb{I}_{2n}}{2} \right)^{-1} \right]. \quad (30)$$

Analogously, by considering *homodyne* measurement on each single channel output (measurement of u_* quadrature, where u_* is a placeholder for q and p) one can find the *homodyne rate* [11]

$$R^{(\text{hom})} := \lim_{n \rightarrow \infty} R_n^{(\text{hom})},$$

$$R_n^{(\text{hom})} = \frac{1}{2n} \max_{V_{\text{in}}, V_{\text{mod}}} \log_2 \det \left[\bar{V}_{\text{out}, u_* u_*} V_{\text{out}, u_* u_*}^{-1} \right], \quad (31)$$

where notations of matrix blocks are the same as in Eq. (28).

IV. SINGLE CHANNEL USE

Let us consider single use (single mode) of the lossy bosonic channel. Its description requires the consideration of 2×2 covariance matrices of the general form to solve the optimization problem. However, all the properties can be found by taking all involved matrices in the diagonal form. This can be done thanks to the following *input purity theorems*:

Theorem 1: For the single use of the lossy bosonic channel, the 2×2 matrices V_{in} and V_{mod} at which the maximum of the Holevo function over Gaussian states is achieved, are simultaneously diagonalizable together with V_{env} . Moreover, the optimal matrix V_{in} corresponds to pure state.

Proof: The proof⁹ is reported in Appendix A. ■

Theorem 2: Let us consider the single use of the lossy bosonic channel characterized by 2×2 diagonal covariance matrices V_{env} , V_{in} , and V_{mod} , then the maxima for both

⁹In the generic setting, the optimality of pure input states has been proven in [15]. However, in our case the Holevo function has to be optimized under the constraint of Gaussian input states and energy restriction. For these reasons, it is worth proving this property explicitly for the considered setting.

heterodyne and homodyne rates are provided by pure input states¹⁰.

Proof: The proof is reported in Appendix B. ■

Let us discuss these theorems in the context of rates. Remember, that in the case of 2×2 -matrices the assumptions used to derive general relations (30) and (31) are equivalent to diagonality of all involved matrices, therefore optimality of pure input states for rates is guaranteed by theorem 2. Moreover, if one conjectures that the relations (30) and (31) hold also for 2×2 matrices of general form (*i.e.* non-diagonal), then commutativity of matrices together with input purity are guaranteed by theorem 1, whose extension to the case of rates is straightforward.

Thus, below it is always assumed without loss of generality that all the matrices are already diagonalized and the input state is pure. Furthermore, unless otherwise stated, in the following it is assumed¹¹ that $0 < \eta < 1$.

A. System of notations

Let us introduce the system of notations that will be used hereafter. Any single-mode state labeled by index “ind” will be referred to by its quadratures covariance matrix V_{ind} parametrized by $\mathcal{N}_{\text{ind}} \in \mathbb{R}_+$ and $s_{\text{ind}} \in \mathbb{R}$ as

$$V_{\text{ind}} := V(\mathcal{N}_{\text{ind}}, s_{\text{ind}}) = \left[\mathcal{N}_{\text{ind}} + \frac{1}{2} \right] \begin{pmatrix} e^{s_{\text{ind}}} & 0 \\ 0 & e^{-s_{\text{ind}}} \end{pmatrix}. \quad (32)$$

In particular, “ind” may stand for “in”, “mod”, “env” or “out” for the cases of input, modulation, environment or output covariance matrices, respectively. The quantity s_{ind} will be referred to as *squeezing* in “ind”. The quantity \mathcal{N}_{ind} will always be written in “EuScript” font and called *average amount of thermal photons* in the state “ind”. We also define the *average amount of photons* N_{ind} in the state “ind” as

$$\frac{1}{2} \text{Tr}(V_{\text{ind}}) = N_{\text{ind}} + \frac{1}{2}, \quad (33)$$

which is equivalent to the relation

$$N_{\text{ind}} = \left(\mathcal{N}_{\text{ind}} + \frac{1}{2} \right) \cosh s_{\text{ind}} - \frac{1}{2}. \quad (34)$$

Below we will usually omit the word “average” referring to the quantities \mathcal{N}_{ind} and N_{ind} . All the quantities related with some overlined matrix will be also overlined, *i.e.* $\overline{V}_{\text{ind}}$ equals $V(\overline{\mathcal{N}}_{\text{ind}}, \overline{s}_{\text{ind}})$ and has amount of photons $\overline{N}_{\text{ind}}$. In order to indicate that some channel parameters are related with homodyne or heterodyne rates (they are defined below in Subsec.IV-B) the upper indices “(hom)” and “(het)” will be used. The only exceptions from the above rules are: the index “env” will be omitted for quantities which represent the squeezing (or its particular values) in channel environment, *e.g.* $s \equiv s_{\text{env}}$; the index “in” and overlining will be omitted for

¹⁰Notice, that extension of theorem 2 to the case of Holevo function is straightforward, being it a particular case of theorem 1.

¹¹This is done because the limit case $\eta = 1$ (noiseless channel) is considered separately in Subsec. IV-I and the limit case $\eta = 0$ (infinitely noisy channel) is trivial giving zero capacity and rates.

the quantities which represent the average amount of photons (or its particular values, *e.g.* thresholds) in averaged input state \overline{V}_{in} (see Eq. (11)) and its “heterodyne analog” $\overline{V}_{\text{in}}^{(\text{het})}$, *e.g.* $N \equiv \overline{N}_{\text{in}} \equiv \overline{N}_{\text{in}}^{(\text{het})}$.

Notice, that the state $V(\mathcal{N}_{\text{ind}}, s_{\text{ind}})$ is *pure* if $\mathcal{N}_{\text{ind}} = 0$ and *mixed* otherwise, is *squeezed* if $s_{\text{ind}} \neq 0$, is *thermal* if $\mathcal{N}_{\text{ind}} \neq 0$ and $s_{\text{ind}} = 0$, is *thermal squeezed* if both $\mathcal{N}_{\text{ind}} \neq 0$ and $s_{\text{ind}} \neq 0$, and is *vacuum* if both $\mathcal{N}_{\text{ind}} = 0$ and $s_{\text{ind}} = 0$.

The eigenvalues of each matrix will be denoted by the first character of matrix index. Then, the eigenvalue which is the first diagonal element corresponds to quadrature q , therefore it will be labeled by index q (analogously, by p for the second diagonal element). However, as far as both quadratures enter all the relations in the same way, instead of specifying the quadrature q or p usually we will use index u as a placeholder for q or p . Also, we will use the rule: if $u = q$, then $u_* = p$, and vice versa. In particular, we will refer to the eigenvalues of matrices $V_{\text{in}}, V_{\text{mod}}, V_{\text{env}}, V_{\text{out}}$ and $\overline{V}_{\text{out}}$ as i_u, m_u, e_u, o_u and \overline{o}_u , respectively. For instance, we have $V_{\text{env}} = \text{diag}(e_q, e_p)$ for the environment matrix. Also, without loss of generality, below it is always assumed that if environment eigenvalues are non-equal, then $e_u > e_{u_*}$.

As far as only the single-mode case is discussed in this section, index k will be omitted for symplectic eigenvalues ν_k and $\overline{\nu}_k$ (they were introduced in Eq. (14)). Also, index n will be omitted for χ - and \underline{C} - and R -quantities (*e.g.*, see Eqs. (8), (14), (21), (30) and (31)). To simplify the notations, in what follows we allow each of these quantities to stand either for the result of the maximization or for the function to maximize, depending on context.

Taking into account that the symplectic eigenvalue for 2×2 -matrix V is $\sqrt{\det V}$, we have for the matrices V_{out} and $\overline{V}_{\text{out}}$ the relations

$$\nu = \sqrt{o_u o_{u_*}}, \quad \overline{\nu} = \sqrt{\overline{o}_u \overline{o}_{u_*}}, \quad (35)$$

where

$$\begin{aligned} o_u &= \eta i_u + (1 - \eta) e_u, \\ \overline{o}_u &= \eta (i_u + m_u) + (1 - \eta) e_u, \\ o_{u_*} &= \eta i_{u_*} + (1 - \eta) e_{u_*}, \\ \overline{o}_{u_*} &= \eta (i_{u_*} + m_{u_*}) + (1 - \eta) e_{u_*}. \end{aligned} \quad (36)$$

B. Heterodyne variables

In the following it will be convenient to introduce the *heterodyne environment matrix*

$$V_{\text{env}}^{(\text{het})} := V_{\text{env}} + \frac{\mathbb{I}_2}{2(1 - \eta)},$$

whose eigenvalues are

$$e_u^{(\text{het})} = e_u + \frac{1}{2(1 - \eta)}, \quad e_{u_*}^{(\text{het})} = e_{u_*} + \frac{1}{2(1 - \eta)}. \quad (37)$$

Replacing V_{env} by $V_{\text{env}}^{(\text{het})}$ in the relations (23) and (24), one can also define the “heterodyne version” of the other matrices:

$$V_{\text{out}}^{(\text{het})} = \eta V_{\text{in}}^{(\text{het})} + (1 - \eta) V_{\text{env}}^{(\text{het})}, \quad (38)$$

$$\overline{V}_{\text{out}}^{(\text{het})} := \eta \left(V_{\text{in}}^{(\text{het})} + V_{\text{mod}}^{(\text{het})} \right) + (1 - \eta) V_{\text{env}}^{(\text{het})}, \quad (39)$$

where the eigenvalues of matrices V_{out} , \bar{V}_{out} , $V_{\text{out}}^{(\text{het})}$ and $\bar{V}_{\text{out}}^{(\text{het})}$ are related as follows:

$$\begin{aligned} o_u^{(\text{het})} &= o_u + \frac{1}{2}, & o_{u_*}^{(\text{het})} &= o_{u_*} + \frac{1}{2}, \\ \bar{o}_u^{(\text{het})} &= \bar{o}_u + \frac{1}{2}, & \bar{o}_{u_*}^{(\text{het})} &= \bar{o}_{u_*} + \frac{1}{2}. \end{aligned}$$

Then, one can define symplectic eigenvalues in the heterodyne setting (similarly to Eqs. (35)) by the relations

$$\nu^{(\text{het})} = \sqrt{o_u^{(\text{het})} o_{u_*}^{(\text{het})}}, \quad \bar{\nu}^{(\text{het})} = \sqrt{\bar{o}_u^{(\text{het})} \bar{o}_{u_*}^{(\text{het})}}. \quad (40)$$

The average amount of photons $N_{\text{env}}^{(\text{het})}$ in the heterodyne environment

$$V_{\text{env}}^{(\text{het})} = V\left(\mathcal{N}_{\text{env}}^{(\text{het})}, s^{(\text{het})}\right)$$

(see Eq. (32)) can be introduced using the standard relation (33). The parameters of the environment matrices $V_{\text{env}} = V(\mathcal{N}_{\text{env}}, s)$ and $V_{\text{env}}^{(\text{het})}$ are related by

$$\left[\mathcal{N}_{\text{env}}^{(\text{het})} + \frac{1}{2}\right]^2 = \left[\mathcal{N}_{\text{env}} + \frac{1}{2} + \frac{1}{2(1-\eta)}\right]^2 + \frac{N_{\text{env}} - \mathcal{N}_{\text{env}}}{1-\eta}, \quad (41)$$

$$s^{(\text{het})} = \frac{1}{2} \ln \frac{1 + (1-\eta)(2\mathcal{N}_{\text{env}} + 1)e^s}{1 + (1-\eta)(2N_{\text{env}} + 1)e^{-s}}, \quad (42)$$

$$s = \frac{1}{2} \ln \frac{1 - (1-\eta)(2\mathcal{N}_{\text{env}}^{(\text{het})} + 1)e^{s^{(\text{het})}}}{1 - (1-\eta)(2N_{\text{env}}^{(\text{het})} + 1)e^{-s^{(\text{het})}}}, \quad (43)$$

$$N_{\text{env}}^{(\text{het})} = N_{\text{env}} + \frac{1}{2(1-\eta)}. \quad (44)$$

In particular, for thermal environment $V(\mathcal{N}_{\text{env}}, 0)$ we have $N_{\text{env}}^{(\text{het})} = \mathcal{N}_{\text{env}}^{(\text{het})}$ and

$$\mathcal{N}_{\text{env}}^{(\text{het})} = \mathcal{N}_{\text{env}} + \frac{1}{2(1-\eta)}.$$

Notice, that the heterodyne environment $V_{\text{env}}^{(\text{het})}$ is squeezed if and only if V_{env} is squeezed.

The quantities with upper index “(het)” defined in this subsection will allow us to simplify the relations for the heterodyne rate. We shall refer to them as *heterodyne variables*. The latter, which are eigenvalues will be also called *heterodyne eigenvalues* to distinguish them from *standard* eigenvalues (of V_{in} , V_{env} , V_{out} , etc.).

C. Heterodyne and homodyne rates

Let us consider the homodyne rate (31). It corresponds to a measurement of the u_* -quadrature, which is the less noisy according to the convention $e_u > e_{u_*}$ (obviously, there is no difference in the choice of quadrature if $e_u = e_{u_*}$). Such a choice gives higher rate in comparison with the measurement of u -quadrature. In what follows (see Subsec. IV-E), it will be shown that this case corresponds to eigenvalue $m_u = 0$ be optimal for homodyne rate. In explicit form it is

$$R^{(\text{hom})} = \frac{1}{2} \log_2 \frac{\bar{o}_{u_*}}{o_{u_*}}, \quad (45)$$

which coincides with $\log_2(\bar{\nu}/\nu)$ if $m_u = 0$. This property gives rise to the relation (see Eqs. (21) and (35))

$$R^{(\text{hom})} = \underline{C}^{(\log)} \quad (46)$$

if optimal m_u is also zero for logarithmic approximation to capacity¹² (we equalize the quantities $R^{(\text{hom})}$ and $\underline{C}^{(\log)}$ for the same channel parameters). This holds true for small values of N (see Eq. (81) below). Thus, in this case the homodyne rate coincides with the logarithmic approximation to capacity.

Analogously, Eq. (30) gives

$$R^{(\text{het})} = \log_2 \frac{\bar{\nu}^{(\text{het})}}{\nu^{(\text{het})}}, \quad (47)$$

for heterodyne measurement (see Eqs. (40)), *i.e.* the heterodyne rate is equal to the logarithmic approximation to capacity calculated with $V_{\text{env}}^{(\text{het})}$. One can also get for a fixed s that

$$\lim_{N_{\text{env}} \rightarrow \infty} R^{(\text{het})} = \underline{C}^{(\log)}. \quad (48)$$

Eqs. (46) and (48) define the values of parameters s and N_{env} for which the rates approach the capacity (the comparison between capacity, homodyne and heterodyne rates was discussed earlier in [7]).

The simple form of (47) explains why the description of heterodyne rate using heterodyne variables introduced in Subsec. IV-B is the most natural one. Keep in mind, that the heterodyne rate can be described using both approaches: as standard variables used for capacity and homodyne rate, or as heterodyne variables. Despite we shall usually work with heterodyne variables, sometimes standard variables will be used.

As far as quantities (30) and (47) are identical as functions of input and modulation eigenvalues, the latter do not depend on representation (type of variables) used for $R^{(\text{het})}$. It means that upper indices “(het)” written for input and modulation eigenvalues are used only to indicate that they are optimal for heterodyne rate (to distinguish from those optimal for capacity and homodyne rate). However, indices “(het)” written for environment, output and average output eigenvalues indicate both different variables used and optimality for heterodyne rate. Loosely speaking, $i_u^{(\text{het})} = i_u$ and $m_u^{(\text{het})} = m_u$, while $e_u^{(\text{het})} \neq e_u$, $o_u^{(\text{het})} \neq o_u$, $\bar{o}_u^{(\text{het})} \neq \bar{o}_u$ ($u \in \{q, p\}$) as *abstract variables*, but in our convention *all* of them are different, because $i_u^{(\text{het})}$ and $m_u^{(\text{het})}$ are used *only* for heterodyne case and are optimal for it¹³.

Below, we shall usually write the relations for capacity and then explain which replacements should be applied to get analogous relations for rates. These replacements can be some

¹²It will be shown in Subsec. IV-F, that if $m_u = 0$ is optimal for one of the quantities \underline{C} and $\underline{C}^{(\log)}$, then it is optimal also for the other. Then, remember (see Subsec. III-A) that optimal eigenvalues for $\underline{C}^{(\log)}$ and $\underline{C}^{(0)}$ are always the same by definition.

¹³Writing, e.g. $i_u^{(\text{het})} = i_u$ would be misleading, as i_u are those eigenvalues optimal for capacity, but not optimal for heterodyne rate. This is less problematic for homodyne rate, because its optimal eigenvalues coincide in some cases with that of the logarithmic approximation to capacity (see Eq. (46)) and therefore can be treated as a particular case of eigenvalues optimal for capacity.

of the following:

$$i_u \rightarrow i_u^{(\text{het})}, \quad i_{u_*} \rightarrow i_{u_*}^{(\text{het})}, \quad (49)$$

$$m_u \rightarrow m_u^{(\text{het})}, \quad m_{u_*} \rightarrow m_{u_*}^{(\text{het})}, \quad (50)$$

$$e_u \rightarrow e_u^{(\text{het})}, \quad e_{u_*} \rightarrow e_{u_*}^{(\text{het})}, \quad (51)$$

$$o_u \rightarrow o_u^{(\text{het})}, \quad o_{u_*} \rightarrow o_{u_*}^{(\text{het})}, \quad (52)$$

$$\bar{o}_u \rightarrow \bar{o}_u^{(\text{het})}, \quad \bar{o}_{u_*} \rightarrow \bar{o}_{u_*}^{(\text{het})}, \quad (53)$$

$$N_{\text{env}} \rightarrow N_{\text{env}}^{(\text{het})}, \quad \mathcal{N}_{\text{env}} \rightarrow \mathcal{N}_{\text{env}}^{(\text{het})}, \quad (54)$$

$$\nu \rightarrow \nu^{(\text{het})}, \quad \bar{\nu} \rightarrow \bar{\nu}^{(\text{het})}, \quad (55)$$

$$g_1 \rightarrow \frac{1}{\ln 2}, \quad g_2 \rightarrow -\frac{1}{\ln 2}. \quad (56)$$

Each of the above numbered lines specifies two replacements. However, only those replacements, which correspond to *explicit* variables of the relation (subjected to replacements) must be applied. Finally, when discussing about the rates, if we refer to relations written for the capacity, we should first apply the proper replacements.

D. Optimization problem

The optimization problem for the heterodyne rate can be formulated as follows. One needs to find the matrices $V_{\text{in}}^{(\text{het})}$ and $V_{\text{mod}}^{(\text{het})}$ (see Eqs. (38) and (39)), which provide the maximum for the function (47) and satisfy the energy constraint

$$\frac{1}{2} \text{Tr} \left(\bar{V}_{\text{in}}^{(\text{het})} \right) = N + \frac{1}{2}, \quad (57)$$

where

$$\bar{V}_{\text{in}}^{(\text{het})} = V_{\text{in}}^{(\text{het})} + V_{\text{mod}}^{(\text{het})}.$$

By substituting Eq. (38) into Eq. (33) written for $\bar{V}_{\text{out}}^{(\text{het})}$ and taking into account the energy constraint (57), we get the amount of photons in the average output state

$$\bar{N}_{\text{out}}^{(\text{het})} = \eta N + (1 - \eta) N_{\text{env}}^{(\text{het})}. \quad (58)$$

Analogously, for the case of capacity the relations (24) and (25) give

$$\bar{N}_{\text{out}} = \eta N + (1 - \eta) N_{\text{env}}. \quad (59)$$

Notice, that theorems 1 and 2 allow us to exclude the variables i_{u_*} and $i_{u_*}^{(\text{het})}$ from the optimization problems due to the purity of the input states:

$$i_u i_{u_*} = \frac{1}{4}, \quad i_u^{(\text{het})} i_{u_*}^{(\text{het})} = \frac{1}{4}.$$

Then, the optimization problems for the single-mode channel can be formulated as follows. One needs to find the maxima of functions (see definitions (8), (14), (45) and (47))

$$\underline{C} = g \left(\bar{\nu} - \frac{1}{2} \right) - g \left(\nu - \frac{1}{2} \right), \quad (60)$$

$$R^{(\text{het})} = \log_2 \bar{\nu}^{(\text{het})} - \log_2 \nu^{(\text{het})}, \quad (61)$$

$$R^{(\text{hom})} = \frac{1}{2} \left[\log_2 \bar{o}_{u_*} - \log_2 o_{u_*} \right], \quad (62)$$

over the variables i_u, m_u, m_{u_*} in the case of \underline{C} and $R^{(\text{hom})}$, and over the variables $i_u^{(\text{het})}, m_u^{(\text{het})}, m_{u_*}^{(\text{het})}$ in the case of $R^{(\text{het})}$, taking into account the constraints

$$i_u > 0, \quad (63)$$

$$m_u, m_{u_*} \geq 0, \quad (64)$$

$$i_u + \frac{1}{4i_u} + m_u + m_{u_*} = 2N + 1, \quad (65)$$

in the case of \underline{C} and $R^{(\text{hom})}$, and the constraints (63)-(65) after the replacements (49) and (50) in the case of $R^{(\text{het})}$. In Subsec. IV-F and IV-G we shall solve it using Lagrange multipliers method.

It is interesting to note that the relations for symplectic eigenvalues (35) and (40) allow the capacity (60) and heterodyne rate (61) to be represented as

$$\underline{C} = g \left(\bar{N}_{\text{out}} \right) - g \left(N_{\text{out}} \right), \quad (66)$$

$$R^{(\text{het})} = \log_2 \left(\bar{N}_{\text{out}}^{(\text{het})} + \frac{1}{2} \right) - \log_2 \left(N_{\text{out}}^{(\text{het})} + \frac{1}{2} \right), \quad (67)$$

where $\bar{N}_{\text{out}}, N_{\text{out}}, \bar{N}_{\text{out}}^{(\text{het})}$ and $N_{\text{out}}^{(\text{het})}$ are the amounts of thermal photons for the states $\bar{V}_{\text{out}}, V_{\text{out}}, \bar{V}_{\text{out}}^{(\text{het})}$ and $V_{\text{out}}^{(\text{het})}$, respectively.

E. The solution stages

Let us consider the capacity and the homodyne rate. In Subsec. IV-F and IV-G it will be shown that all the solutions of Lagrange equations, associated to the optimization problem stated in Subsec. IV-D, give positive i_u , that is $m_u, m_{u_*} \geq 0$ are the only inequalities to satisfy. This allows us to classify the solutions depending on the amount of positive optimal m -eigenvalues. The following terminology is used for this purpose.

Definition 1: The solution belongs to the *first stage* if the optimal m_u, m_{u_*} are both equal to zero, to the *second stage* if the optimal m_u, m_{u_*} are one equal to zero and the other is positive, and to the *third stage* if the optimal m_u, m_{u_*} are both positive.

As far as $R^{(\text{hom})}$ does not depend on m_u , due to the condition (65) the maximum is achieved for $m_u = 0$, which shows the absence of the third stage in homodyne rate. In other words, energy N should not be wasted in the quadrature unused for information transmission.

The first stage holds if and only if capacity is equal to zero, which can only be if $N = 0$ (if $N \neq 0$ one can always get non-zero capacity and rates by taking $i_u = \frac{1}{2}, m_u = m_{u_*} = N$). In particular, Eq. (65) applied for the first stage gives $i_u = \frac{1}{2}$. The same consideration holds true also for the homodyne rate.

Proposition 1: Given $\bar{o}_u \neq \bar{o}_{u_*}$ in the second stage, the eigenvalues $m_u = 0$ and $m_{u_*} > 0$ are optimal for capacity¹⁴ if and only if $\bar{o}_u > \bar{o}_{u_*}$.

¹⁴This proposition holds for both cases $e_u > e_{u_*}$ and $e_u < e_{u_*}$.

Proof: Suppose that $m_{u_*} = 0$ and $m_u > 0$ are optimal in the case of $\bar{o}_u > \bar{o}_{u_*}$. The energy constraint (65) is preserved by the change of variables $m'_u = m'_{u_*} = m_u/2$, $i'_u = i_u$. The new variables do not change the second term in Eq. (60) but increase the first term¹⁵. Thus, they give higher maximum for capacity. Similarly, one can prove that $m_u = 0$ and $m_{u_*} > 0$ are not optimal if $\bar{o}_u < \bar{o}_{u_*}$. Hence, the proposition is proved by contradiction. ■

Proposition 2: If $e_u > e_{u_*}$, then in the second stage $m_u = 0$ and $m_{u_*} > 0$ are optimal for capacity.

Proof: The proof is reported in Appendix C. ■

It follows from propositions 1 and 2 that the case of $e_u > e_{u_*}$ requires $o_u = \bar{o}_u$ and

$$o_u \geq \bar{o}_{u_*} > o_{u_*} \quad (68)$$

in the second stage.

Similar consideration gives $\bar{o}_u = \bar{o}_{u_*}$ in the third stage (by supposing $\bar{o}_u \neq \bar{o}_{u_*}$ one can always redistribute the energy N among m -eigenvalues so to decrease the difference $|\bar{o}_u - \bar{o}_{u_*}|$ thus giving higher maximum for capacity). Taking into account Eq. (65), we get in this case

$$\bar{o}_u = \bar{o}_{u_*} = \eta \left(N + \frac{1}{2} \right) + (1 - \eta) \left(N_{\text{env}} + \frac{1}{2} \right). \quad (69)$$

The equality $\bar{o}_u = \bar{o}_{u_*}$ is equivalent to the equation $\bar{N}_{\text{out}} = \bar{N}'_{\text{out}}$, where the latter is given by Eq. (59). Thus, for the third stage, the first term in the relation (66) is already found.

Notice, that the above considerations for the capacity (including definition 1, propositions 1 and 2, Eqs. (68) and (69)) hold also for the heterodyne rate if the replacements (49)–(54) and $g \rightarrow \log_2$ are applied, and if Eqs. (58), (61) and (67) are mentioned instead of Eqs. (59), (60) and (66), respectively. Below the solutions for the third and the second stages are presented.

F. The third stage

In the case of the third stage, the Lagrange multipliers method applied to the function \underline{C} with the constraint (65) leads to the following system of equations (see definition of g_k in Eq. (18)):

$$\begin{aligned} \frac{\partial L}{\partial i_u} &= \frac{\eta}{2} \left[g_1(\bar{\nu}) \left(\frac{1}{\bar{o}_u} - \frac{1}{4i_u^2 \bar{o}_{u_*}} \right) \right. \\ &\quad \left. - g_1(\nu) \left(\frac{1}{o_u} - \frac{1}{4i_u^2 o_{u_*}} \right) \right] - \varkappa \left[1 - \frac{1}{4i_u^2} \right] = 0, \quad (70) \end{aligned}$$

$$\frac{\partial L}{\partial m_u} = \frac{\eta}{2} \frac{g_1(\bar{\nu})}{\bar{o}_u} - \varkappa = 0, \quad (71)$$

$$\frac{\partial L}{\partial m_{u_*}} = \frac{\eta}{2} \frac{g_1(\bar{\nu})}{\bar{o}_{u_*}} - \varkappa = 0, \quad (72)$$

¹⁵The area of a rectangle with fixed perimeter is higher if the length of sides differs less. In the considered case $\bar{o}'_u + \bar{o}'_{u_*} = \bar{o}_u + \bar{o}_{u_*}$ but $|\bar{o}'_u - \bar{o}'_{u_*}| < |\bar{o}_u - \bar{o}_{u_*}|$. In addition, g is monotonically increasing and concave function.

where the Lagrange function is

$$L = \underline{C} - \varkappa \left(i_u + \frac{1}{4i_u} + m_u + m_{u_*} - 2N - 1 \right),$$

with \varkappa the Lagrange multiplier.

Eqs. (71) and (72) give $\bar{o}_u = \bar{o}_{u_*}$ which was obtained before from qualitative considerations. By substituting Eqs. (71) and (72) into Eq. (70) one can find that squeezing in input s_{in} equals that of environment s and output s_{out} :

$$\frac{i_{u_*}}{i_u} = \frac{e_{u_*}}{e_u} = \frac{o_{u_*}}{o_u}, \quad (73)$$

which allows us to find optimal input eigenvalues

$$i_u = \frac{1}{2} \sqrt{\frac{e_u}{e_{u_*}}}, \quad i_{u_*} = \frac{1}{2} \sqrt{\frac{e_{u_*}}{e_u}}. \quad (74)$$

Thus, given the environment state $V_{\text{env}} = V(N_{\text{env}}, s)$, the optimal input state is $V_{\text{in}} = V(0, s)$. Combining Eq. (69) with (74) one can obtain optimal m -eigenvalues

$$\begin{aligned} m_u &= N + \frac{1}{2} - i_u + \frac{1 - \eta}{\eta} \left(N_{\text{env}} + \frac{1}{2} - e_u \right), \\ m_{u_*} &= N + \frac{1}{2} - i_{u_*} + \frac{1 - \eta}{\eta} \left(N_{\text{env}} + \frac{1}{2} - e_{u_*} \right). \end{aligned} \quad (75)$$

In order to get analogous relations for the heterodyne rate, the replacements (49)–(54) and (56) must be applied to Eqs. (70)–(72) and (73)–(75). In particular, it gives

$$s_{\text{in}}^{(\text{het})} = s^{(\text{het})} = s_{\text{out}}^{(\text{het})}$$

and $V_{\text{in}}^{(\text{het})} = V(0, s^{(\text{het})})$. Notice, that Eqs. (37) and (44) give

$$\begin{aligned} N_{\text{env}}^{(\text{het})} + \frac{1}{2} - e_u^{(\text{het})} &= N_{\text{env}} + \frac{1}{2} - e_u, \\ N_{\text{env}}^{(\text{het})} + \frac{1}{2} - e_{u_*}^{(\text{het})} &= N_{\text{env}} + \frac{1}{2} - e_{u_*} \end{aligned}$$

for the relations (75).

Finally, the explicit relations for capacity and heterodyne rate in the third stage read

$$\begin{aligned} \underline{C} &= g[\eta N + (1 - \eta)N_{\text{env}}] - g[(1 - \eta)N_{\text{env}}], \quad (76) \\ R^{(\text{het})} &= \log_2 \left[\eta N + (1 - \eta)N_{\text{env}}^{(\text{het})} + \frac{1}{2} \right] \\ &\quad - \log_2 \left[(1 - \eta)N_{\text{env}}^{(\text{het})} + \frac{1}{2} \right], \quad (77) \end{aligned}$$

where Eq. (77) becomes

$$R^{(\text{het})} = \log_2 \left[1 + \frac{\eta N}{1 + (1 - \eta)N_{\text{env}}} \right] \quad (78)$$

for the case of thermal nonsqueezed environment. The relation (76) originally was found in [12] and generalizes that obtained for lossy bosonic channel with vacuum environment $g(\eta N)$ [7] and, later, with thermal nonsqueezed environment [10]. In turn, Eq. (77) generalizes the relation for the heterodyne rate, $\log_2(1 + \eta N)$, found in [32] for vacuum environment (see also discussion in [7]).

By comparing Eqs. (21), (60) and (76) we get the logarithmic approximation to the capacity¹⁶

$$\underline{C}^{(\log)} = \log_2 \left[\eta N + (1 - \eta) N_{\text{env}} + \frac{1}{2} \right] - \log_2 \left[(1 - \eta) N_{\text{env}} + \frac{1}{2} \right], \quad (79)$$

which coincides with the heterodyne rate (77) after the replacements (54) (it follows from Eqs. (41) and (44) that the limits of the ratios $N_{\text{env}}^{(\text{het})}/N_{\text{env}}$ and $N_{\text{env}}^{(\text{het})}/N_{\text{env}}$ for $N_{\text{env}} \rightarrow \infty$ are equal to one). Thus, the limit (48) actually holds. Notice, that eigenvalues (74) and (75) are optimal also for the quantity $\underline{C}^{(\log)}$, therefore we have $\underline{C} \equiv \underline{C}^{(0)}$ in the third stage.

In the case of pure environment, the capacity (76) can be written as

$$\underline{C} = g(\overline{N}_{\text{out}}), \quad (80)$$

where $\overline{N}_{\text{out}}$ is given by Eq. (59). The form of the relation (80) provides the most natural generalization of the noiseless channel capacity $g(N)$. Thus, in the third stage the capacity of the channel with pure environment is completely defined by the average amount of photons contained in the channel (*i.e.* in the system “environment plus input”), where probability weights η and $1 - \eta$ specify the contribution of input and environment states into the channel capacity.

Previously it was proved (see proposition 2) that $m_{u_*} \neq 0$ is optimal for the chosen convention ($e_u > e_{u_*}$), therefore the third stage holds if $m_u > 0$. This is the case for the capacity (for the quantities \underline{C} , $\underline{C}^{(\log)}$ and $\underline{C}^{(0)}$) if the amount N of input photons is higher than the threshold

$$N_{2 \rightarrow 3} = i_u - \frac{1}{2} - \frac{1 - \eta}{\eta} \left(N_{\text{env}} + \frac{1}{2} - e_u \right), \quad (81)$$

where i_u is defined by the first of Eqs. (74). It is equivalent to the restriction $s < s_{2 \rightarrow 3}$ for given values of η , N and N_{env} , where

$$s_{2 \rightarrow 3} = -\ln \left[\sqrt{1 + \phi_0 + (N + 1/2)^2 \phi_0^2} - (N + 1/2) \phi_0 \right]$$

with

$$\phi_0 := \frac{\eta}{(1 - \eta) \left(N_{\text{env}} + \frac{1}{2} \right)}. \quad (82)$$

Notice, that the quantity $s_{2 \rightarrow 3}$ has the limits

$$\begin{aligned} \lim_{\eta \rightarrow 1} s_{2 \rightarrow 3} &= \ln(2N + 1), \\ \lim_{\eta \rightarrow 0} s_{2 \rightarrow 3} &= 0. \end{aligned} \quad (83)$$

The threshold (81) holds also for the heterodyne rate if the replacements (49) and $N_{2 \rightarrow 3} \rightarrow N_{2 \rightarrow 3}^{(\text{het})}$ are applied, where $i_u^{(\text{het})}$ expressed through standard eigenvalues reads

$$i_u^{(\text{het})} = \frac{1}{2} \sqrt{\frac{1 + 2(1 - \eta)e_u}{1 + 2(1 - \eta)e_{u_*}}}. \quad (84)$$

The threshold $N_{2 \rightarrow 3}$ is a nonnegative number which equals zero only for the vacuum environment. As far as the third stage holds only if $N > N_{2 \rightarrow 3}$ and the first stage holds for

only $N = 0$, the second stage must correspond to values $0 < N \leq N_{2 \rightarrow 3}$. Thus, the type of solution increases its stage in sequence starting from the first stage and ending to the third one if N grows from zero to infinity. This explains the origin of the adopted term “stage”. Also, it can be interpreted as “the third stage is always the most preferable if energy N is sufficiently high, otherwise the second stage should be taken, and the first stage holds if only both the third and the second stage fail to satisfy the constraint”. This mnemonic rule, although trivial for the single-mode channel, will be useful when applied to the multi-mode memory channel. The above consideration is also valid for the heterodyne threshold $N_{2 \rightarrow 3}^{(\text{het})}$.

Similarly to the quantity $s_{2 \rightarrow 3}$, given the values of s , N and N_{env} , the relation for transmissivity $\eta_{2 \rightarrow 3}$ corresponding to transition from second to third stage can be written as

$$\eta_{2 \rightarrow 3}^{-1} = 1 - \frac{N + \frac{1}{2} - i_u}{N_{\text{env}} + \frac{1}{2} - e_u}, \quad (85)$$

where $0 < s \leq \ln(2N + 1)$ and i_u is defined by the first of Eqs. (74). Taking into account that $s_{\text{in}} = s$, $s \geq 0$, the limit (83) and monotonicity of $\eta_{2 \rightarrow 3}$ with respect to s , one can see that

$$\frac{1}{2} \leq i_u \leq N + \frac{1}{2}, \quad (86)$$

where higher values of i_u correspond to higher values of $\eta_{2 \rightarrow 3}$. The transmissivity $\eta_{2 \rightarrow 3}$ is plotted vs s in Fig.1-left.

G. The second stage

One can show that the Lagrange equations for the capacity (and heterodyne rate) in the second stage can be obtained from the system (70)-(72) by substituting $m_u = 0$ ($m_u^{(\text{het})} = 0$) in all equations and by removing Eq. (71) corresponding to derivative with respect to m_u ($m_u^{(\text{het})}$). This is because unknown variables enter in the Lagrange equations as linear combinations. For the homodyne rate the Lagrange equations are the same as for the capacity in the second stage if the replacement (56) is applied.

Then, solving the Lagrange equations for the homodyne rate one can find the ratio

$$\frac{i_{u_*}}{i_u} = \frac{o_{u_*}}{\overline{o}_{u_*}}, \quad (87)$$

which also holds for the heterodyne rate after replacements (49), (52) and (53). For the capacity the Lagrange equations give a *mode transcendental equation* on i_u

$$\mathcal{F}(i_u) = 0, \quad (88)$$

where

$$\mathcal{F} := g_1(\overline{\nu}) \left[\frac{1}{o_u} - \frac{1}{\overline{o}_{u_*}} \right] - g_1(\nu) \left[\frac{1}{o_u} - \frac{1}{4i_u^2 o_{u_*}} \right]. \quad (89)$$

Notice, that Eq. (88) results to Eq. (87) if the g_1 -function is taken to zeroth-order approximation (*i.e.* $g_1 \equiv (\ln 2)^{-1}$). Remember, that in the second stage the optimal eigenvalues for $\underline{C}^{(\log)}$, $\underline{C}^{(0)}$ and $R^{(\text{hom})}$ (see Eqs. (21) and (46)) are the

¹⁶Remember, that according to Eq. (17) $g(v) \approx \log_2(v + \frac{1}{2})$.

same. They follow from Eq. (87) solved for the variable i_u and equal to

$$m_u = 0, \quad (90)$$

$$m_{u_*} = 2N + 1 - i_u - \frac{1}{4i_u}, \quad (91)$$

$$i_u = \frac{1}{2} \left[\sqrt{1 + (2N + 1)\phi + (\phi/2)^2} - \phi/2 \right], \quad (92)$$

$$i_{u_*} = \frac{1}{4i_u}, \quad (93)$$

where

$$\phi = \frac{\eta}{1 - \eta} e_{u_*}^{-1} \quad (94)$$

is equal to ϕ_0 (see Eq. (82)) in the case of thermal environment ($s = 0$). The exact values of the optimal eigenvalues for the capacity \underline{C} are given by Eqs. (88), (90), (91) and (93). As far as eigenvalues (90)–(93) are optimal for the quantity $\underline{C}^{(0)}$, below we will call them as *the zeroth-order solution* (or *the zeroth-order eigenvalues*) for capacity. Thus, similarly to the third stage, in the second stage the quantity $\underline{C}^{(0)}$ is also expressed in an explicit form. In turn, the condition $m_{u_*} > 0$ (see Eq. (91)) restricts the admissible region for i_u to the interval

$$N + \frac{1}{2} - \sqrt{N^2 + N} < i_u < N + \frac{1}{2} + \sqrt{N^2 + N}.$$

The optimal eigenvalues for the heterodyne rate are given by the same relations (90)–(93) if the replacements (49), (50) and

$$\phi \rightarrow \phi^{(\text{het})}, \quad (95)$$

with

$$\phi^{(\text{het})} = \frac{\eta}{1 - \eta} \left[e_{u_*}^{(\text{het})} \right]^{-1} \quad (96)$$

are applied.

By comparing Eq. (62) with Eq. (87) one can get the homodyne rate

$$\begin{aligned} R^{(\text{hom})} &= \log_2(2i_u) \\ &= \log_2 \left[\sqrt{1 + (2N + 1)\phi + (\phi/2)^2} - \phi/2 \right]. \end{aligned} \quad (97)$$

Remember, that $R^{(\text{hom})} \equiv \underline{C}^{(\log)}$ (see Eq. (46)) in the second stage. Then, similarly, by comparing Eqs. (61) and (87) we get the same relation (97) for the heterodyne rate if the replacements (49) and (95) are applied to it.

The first-order approximation for mode transcendental equation (88) can be obtained by replacing the function g_1 with its first-order approximation (20). Since Eq. (88) cannot be exactly solved within this approximation, we will solve it in the neighborhood of the zeroth-order solution (90)–(93) as linear perturbation. In particular, by denoting input zeroth-order eigenvalue (92) as $i_u^{(0)}$ and substituting i_u with $i_u^{(0)} + \varepsilon_u$ in the first-order approximation of Eq. (88), we get a linear equation for small deviation ε_u . Its solution is

$$\varepsilon_u = \frac{\eta \bar{o}_{u_*} o_u i_u^{(0)} m_{u_*} (\bar{o}_{u_*} - o_u)}{2 \left[\eta^2 (o_u^2 + \bar{o}_{u_*}^2 - \bar{o}_{u_*} o_u) i_u^{(0)} m_{u_*} - \bar{o}_{u_*}^2 o_u^2 (12\nu^2 + 1) \right]}, \quad (98)$$

whose variables are the zeroth-order eigenvalues. Thus, we have found *the first-order solution*¹⁷ $i_u^{(1)} = i_u^{(0)} + \varepsilon_u$. Remember that in the second stage, by virtue of Eqs. (90), (91) and (93), the only degree of freedom is represented by i_u . Hence, it is sufficient to specify its value in order to have the complete solution of the optimization problem.

Similarly to the quantity $\underline{C}^{(0)}$ whose variables are the zeroth-order eigenvalues (90)–(93), the first-order solution has to be substituted into the exact¹⁸ relation (60) instead of its first-order approximation which was used to derive the first-order eigenvalues. Otherwise, the loss in accuracy becomes significant. In particular, although input and modulation eigenvalues calculated through exact and approximate approaches essentially differ each other, they give rise to almost equal values for capacity. This can be explained by the fact that the quantity (60), considered as a function of only one unknown variable¹⁹ i_u , has zero derivative in the neighborhood of its optimal value (*i.e.* the deviation of i_u affects maximum of the capacity only in the second order). The quantity (60) considered as a function of the first-order eigenvalues below will be called *the first-order approximation to capacity* $\underline{C}^{(1)}$.

The homodyne rate $\log_2 \sqrt{1 + 4\eta N}$ was found in [32] by supposing both the environment and input states to be vacuum (see also discussion in [7]). Indeed, it can be obtained without solving the optimization problem, by substituting in Eq. (62) $i_u = i_{u_*} = e_u = e_{u_*} = 1/2$ and $m_{u_*} = 2N$ as it follows from the constraint (65). However, since optimal input state is never vacuum according to Eq. (92), that rate holds (approximately) only if the value of N is close to zero.

H. \bar{o}_{u_*} -representation

We have solved the problem of finding the optimal eigenvalues i_u , i_{u_*} , m_u and m_{u_*} for given values of e_u , e_{u_*} , η and N . It is interesting to note, that the eigenvalue \bar{o}_{u_*} can be used as the equivalent replacement²⁰ of the quantity N . In fact, Eq. (69) makes it evident in the third stage. Let us show this also for the second stage. Combining Eqs. (36), (91), (93) and (94) one can get the relation

$$2N + 1 = i_u + \frac{\bar{o}_{u_*}}{\eta} - \frac{1}{\phi}. \quad (99)$$

By substituting it into Eq. (92) and then solving the latter for i_u one can obtain

$$i_u = \frac{1}{2} \left[\sqrt{(\phi/4)^2 + \bar{o}_{u_*} \phi / \eta} - \phi/4 \right]. \quad (100)$$

Hence, Eq. (97) can be equivalently rewritten through variable \bar{o}_{u_*} as

$$R^{(\text{hom})} = \log_2 \left[\sqrt{(\phi/4)^2 + \bar{o}_{u_*} \phi / \eta} - \phi/4 \right], \quad (101)$$

¹⁷Similarly, another first-order solution can be obtained if exact relation for g_1 function is used instead of approximation (20).

¹⁸Notice, that in order to get the zeroth-order and the first-order approximate solutions we replaced the exact g -function and its derivatives (everywhere in optimization problem) by their zeroth-order and the first-order approximations, respectively.

¹⁹The other input and modulation eigenvalues have to be expressed through i_u using Eqs. (90), (91) and (93).

²⁰This fact will be used in Sec. VI for discussing memory channels.

which coincides with the quantity $\underline{C}^{(\log)}$ in the second stage. Notice, that eigenvalue m_{u_*} can be expressed through \bar{o}_{u_*} as

$$m_{u_*} = \frac{\bar{o}_{u_*}}{\eta} - \frac{1}{\phi} - \frac{1}{4i_u}. \quad (102)$$

Thus, the eigenvalues (90), (93), (100) and (102) are optimal for the quantities $R^{(\text{hom})}$, $\underline{C}^{(\log)}$ and $\underline{C}^{(0)}$ in the second stage and expressed through the quantity \bar{o}_{u_*} instead of N . Eqs. (99)–(102) hold also for the heterodyne rate if the replacements (49), (50), (53) and (95) are applied.

Similarly, the mode transcendental equation (88) also does not depend on N if eigenvalue \bar{o}_{u_*} is assumed to be a known constant. In this case the admissible region for the eigenvalue i_u (root of Eq. (88)) can be estimated using inequalities $\bar{\nu} > \frac{1}{2}$ and $m_{u_*} > 0$ (see Eq. (102)), which can be rewritten as

$$i_u > \frac{1}{\eta} \left[\frac{1}{4\bar{o}_{u_*}} - (1 - \eta) e_u \right]$$

and

$$i_u > \frac{1}{4} \left[\frac{\bar{o}_{u_*}}{\eta} - \frac{1}{\phi} \right]^{-1},$$

respectively. Analogously to Eq. (98), by expressing N through \bar{o}_{u_*} in Eq. (88) and using approximation (20) one can get the first order solution $i_u^{(1)} = i_u^{(0)} + \varepsilon_u$ in terms of \bar{o}_{u_*} . In this case ε_u is given by the relation

$$\begin{aligned} \varepsilon_u &= (\bar{o}_{u_*} - o_u)(\bar{o}_{u_*} - o_{u_*}) o_u i_u^{(0)} \\ &\times \left\{ \left(2 [o_u^2 + \bar{o}_{u_*}^2 - (o_u + o_{u_*}) \bar{o}_{u_*}] + [12 o_u^2 + 1] \nu^2 \right) i_u^{(0)} \eta \right. \\ &\quad \left. - 2 [12 \nu^2 + 1] o_u^2 \bar{o}_{u_*} \right\}^{-1}, \quad (103) \end{aligned}$$

whose variables are the zeroth-order eigenvalues (93), (100) and (102). Notice, that despite the equations (92) and (100) are equivalent (one can be obtained from another), this is not the case for relations (98) and (103).

I. Noiseless channel

Let us demonstrate the above results on the particular case of noiseless (*i.e.* ideal) channel ($\eta=1$). Its capacity equals $C = g(N)$. The optimal eigenvalues for its homodyne rate can be found from Eqs. (87), (91) and (93) by substituting $\eta = 1$, which gives

$$i_u = N + \frac{1}{2}, \quad (104)$$

$$m_{u_*} = N \left(1 + \frac{1}{2N+1} \right) = \sinh(\ln(2N+1)). \quad (105)$$

The optimal eigenvalues for its heterodyne rate can be obtained from Eqs. (75) and (84) by substituting $\eta = 1$, which results in $i_u^{(\text{het})} = i_{u_*}^{(\text{het})} = \frac{1}{2}$ and $m_u^{(\text{het})} = m_{u_*}^{(\text{het})} = N$. Hence, we have $N_{2 \rightarrow 3}^{(\text{het})} = 0$ (see Eq. (81)), *i.e.* the second stage does not exist in this case.

The relations (78) and (97) applied to the noiseless channel give the inequalities [7]

$$R^{(\text{het})} < R^{(\text{hom})} < C, \quad (106)$$

where $R^{(\text{hom})} = \log_2(2N+1)$ and $R^{(\text{het})} = \log_2(N+1)$ [32]. It means that both heterodyne and homodyne rates never

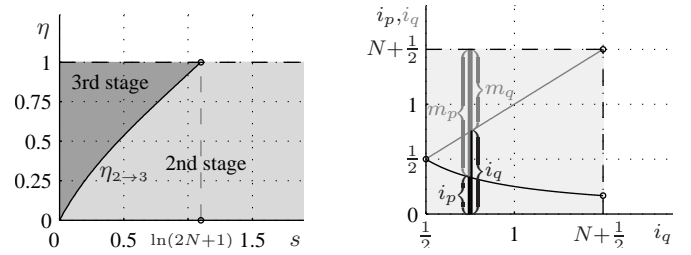


Fig. 1. On the left, two regions of the plane (s, η) corresponding to the third (darker background) and the second stage for $N = 1$ and $N_{\text{env}} = 1$. The regions are separated by the curve $\eta_{2 \rightarrow 3}$ (see Eq. (85)) plotted vs s (black curve), it splits the whole plane into two regions marked with different grey-scale backgrounds (the darker background corresponds to third stage). The curve $\eta_{2 \rightarrow 3}$ reaches the value $\eta = 1$ at squeezing value $s = \ln(2N+1)$. The horizontal dashed line plotted for $\eta = 1$ corresponds to noiseless channel. On the right, the eigenvalues i_p and i_q for the noiseless channel are plotted vs i_q for $N = 1$. The area of the square of grey color is equal to $\bar{\nu}^2 = (N + \frac{1}{2})^2$ which defines the capacity $g(\sqrt{\bar{\nu}^2} - \frac{1}{2}) = g(N)$. Depicted braces show that each value of i_q corresponds to two different methods to distribute the energy $N + \frac{1}{2}$ between input and modulation quadratures.

achieve the capacity for finite N even for the noiseless channel²¹. In particular, for large values of N inequalities (106) read

$$\log_2 N < \log_2 N + 1 < \log_2 N + \frac{1}{\ln 2},$$

where the difference between the rates and the capacity disappears in the limit $N \rightarrow \infty$. In addition, both capacity and rates of the noiseless channel are always higher than their values in the presence of losses (environment), *i.e.* when $\eta < 1$.

One can also notice that despite optimal input and modulation eigenvalues are unique for heterodyne and homodyne rate, this is not the case for noiseless channel capacity. The latter has infinite amount of solutions, which can be shown as follows. At first, since the theorem 1 holds also for $\eta = 1$, the optimal input state must be pure. At second, any pure input state zeros the second term in Holevo- χ quantity. As far as the area of a rectangle with fixed perimeter is maximal if and only if rectangle's sides are equal (see proof of proposition 2), we have the system of equations

$$\begin{aligned} i_u + m_u &= N + \frac{1}{2}, \\ \frac{1}{4i_u} + m_{u_*} &= N + \frac{1}{2}, \end{aligned} \quad (107)$$

where the energy restriction (65) is the “perimeter”. Thus, by taking any input eigenvalue from the interval

$$\frac{1}{4(N + \frac{1}{2})} \leq i_u \leq N + \frac{1}{2}, \quad (108)$$

and obtaining the eigenvalues i_{u_*} , m_u , m_{u_*} from the relations (93), (107) we arrive at the same value of capacity $g(N)$.

Taking into account that the capacity is symmetric over quadratures and considering as usual only positive values of s_{in} , we can parametrize the interval (108) as (see similarity

²¹It is shown in [32] that the capacity of the noiseless channel can be achieved by using Fock states for encoding and photon counting measurement for decoding.

with Eq. (86)) $s_{\text{in}} = \sigma \ln(2N + 1)$, where $\sigma \in [0, 1]$. Notice, that $\sigma = 1$ is the only solution corresponding to second stage in this interval. Then, the optimal eigenvalues can be expressed as functions of σ as

$$\begin{aligned} i_u &= \frac{1}{2}(2N + 1)^\sigma, \\ i_{u_*} &= \frac{1}{2}(2N + 1)^{-\sigma}, \\ m_u &= N + \frac{1}{2} [1 - (2N + 1)^\sigma], \\ m_{u_*} &= N + \frac{1}{2} [1 - (2N + 1)^{-\sigma}], \end{aligned} \quad (109)$$

The set of eigenvalues optimal for noiseless channel are plotted in Fig.1-right. The black point at the left part of the graph corresponds to well-known solution $i_u = i_{u_*} = \frac{1}{2}$, $m_u = m_{u_*} = N$ which is particular case of $\sigma = 0$ in Eqs. (109). Two black points at the right part of the graph correspond to solution (104), (105) following from Eqs. (109) for $\sigma = 1$.

Let us consider how the solution (*i.e.* the optimal input and modulation eigenvalues) changes if noise in the channel disappears ($\eta \rightarrow 1$). The loci (s, η) corresponding to different stages are shown in Fig.1-left. One can see, that if s belongs to the interval $(0, \ln(2N + 1))$, then by increasing η from 0 to 1 we always change the second stage to the third one. As far as $s_{\text{in}} = s$ in the third stage, the solutions for different values of s for noisy channel tend to different solutions for noiseless channel and remain in the third stage. These solutions of noiseless channel correspond to the interval $\sigma \in [0, 1]$. Then, all solutions for $s \geq \ln(2N + 1)$ of noisy channel tend to the same solution of the noiseless channel which corresponds to the second stage and to $\sigma = 1$.

J. Universal limit

Let us analyze the behavior of the capacity and rates in the limit of infinite environment squeezing ($s \rightarrow \infty$) if channel parameters η , N and N_{env} are fixed. Notice, that only the second stage is possible in this case according to Eq. (81). By substituting eigenvalues (90), (91) and (93) into mode transcendental equation (88) and then solving it for i_u in the case of $s \rightarrow \infty$ one can get the result (104). Thus, the eigenvalues maximizing the capacity in the limit of $s \rightarrow \infty$ are the same as for the noiseless channel and given by Eqs. (104) and (105). Substituting them into Eqs. (35) one can see that both symplectic eigenvalues ν and $\bar{\nu}$ tend to infinity if $s \rightarrow \infty$. This allows us to use the logarithmic approximation to the capacity to find the limit. Hence, by comparing Eqs. (46), (97) and (104) we obtain the result [12]

$$\lim_{s \rightarrow \infty} \underline{C}(s, \eta, N, N_{\text{env}}) = \log_2(2i_u) = \log_2(2N + 1), \quad (110)$$

which will be called below as *the universal limit*.

As far as $\lim_{\phi \rightarrow \infty} i_u$ (see Eq. (92)) gives the relation (104), the limit (110) also holds for homodyne rate $\lim_{s \rightarrow \infty} R^{(\text{hom})}$ [24]. Analogously, taking into account that $\lim_{s \rightarrow \infty} \phi^{(\text{het})} = 2\eta$ (see Eq. (96)), we get the limit

$$\lim_{s \rightarrow \infty} R^{(\text{het})} = \log_2 \left[\sqrt{1 + 2(2N + 1)\eta + \eta^2} - \eta \right]. \quad (111)$$

Notice, that the limiting value (110) of the capacity equals the homodyne rate in the case of perfect (noiseless) channel (see Eq. (106)). This fact can be understood by considering that, for $s \rightarrow \infty$, the quadrature u becomes infinitely noisy while the quadrature u_* becomes noiseless. Thus, by encoding the information in the quadrature u_* , the information transmission becomes noiseless.

K. Concavity of solution

The concavity over N for the capacity and rates will be essential below for discussing multiple channels uses. It is also the important property allowing to show additivity of the capacity and rates for the memoryless channels.

Let us show the concavity of the function $\underline{C}(N)$. In the second stage, the latter can be represented as $\underline{C}(N, i_u(N))$, therefore the first derivative with respect to N is

$$\frac{d\underline{C}}{dN} = \frac{\partial \underline{C}}{\partial N} + \frac{\partial \underline{C}}{\partial i_u} \frac{\partial i_u}{\partial N}.$$

However, since only the eigenvalues maximizing \underline{C} are of interest, we have $\partial \underline{C} / \partial i_u = (\eta/2)\mathcal{F} = 0$ (see definition (89)), therefore

$$\frac{d\underline{C}}{dN} = \frac{\partial \underline{C}}{\partial N}.$$

Then, one can show that for all values of N and for both second and third stages

$$\frac{d\underline{C}}{dN} = \frac{\eta}{\sigma_{u_*}} g_1(\bar{\nu}) > 0, \quad (112)$$

which proves that $\underline{C}(N)$ is a monotonically increasing function of its argument. Notice, that

$$\max_N \frac{\partial \underline{C}}{\partial N} = \lim_{N \rightarrow 0} \frac{\partial \underline{C}}{\partial N} \leq \infty, \quad (113)$$

where equality is achieved only by the pure environment state ($e_u = e_{u_*} = 1/2$).

It is shown in Appendix E that

$$\frac{d^2 \underline{C}}{dN^2} < 0. \quad (114)$$

Then, we deduce from Eqs. (112) and (114) that the function $\underline{C}(N)$ is concave on the whole region of $N \in [0, \infty)$. Thus, the single-mode (one-shot) capacity for fixed values of e_u, e_{u_*} and η can be considered as the concave function:

$$N \longrightarrow \boxed{\underline{C} = \underline{C}(N)} \longrightarrow \underline{C}, \quad (115)$$

i.e. as a “blackbox” returning the value of \underline{C} upon “input” N while respecting the concavity property.

The derivative (112) holds also for rates if the replacement (56) is applied. Besides it, for the heterodyne rate the replacements (53) and (55) must be applied. The concavity of both rates and logarithmic approximation to capacity can be deduced from explicit relations (77), (79) and (97). Hence, both heterodyne and homodyne rates are also concave functions which can be treated in the same “blackbox” form.

L. λ -representation

As far as function $\underline{C}(N)$ is concave and monotonically increasing, the value of the derivative (112) can be used as the equivalent replacement for the amount of photons N granted for the channel input. Such approach below will be called the λ -representation to distinguish it from the standard approach using the quantity N (N -representation). Thus, we can specify an input energy for capacity using

$$\lambda(N) := \frac{\partial \underline{C}}{\partial N} = \frac{\eta}{\bar{o}_{u_*}} g_1(\bar{\nu}). \quad (116)$$

Eq. (116) can be equivalently rewritten²² in the form of Planck distribution²³

$$\bar{N}_{\text{out}} = \frac{1}{e^{\omega/T} - 1}, \quad (117)$$

where $\bar{N}_{\text{out}} = \bar{\nu} - 1/2$, the ‘‘temperature’’ $T := \eta/(\lambda \ln 2)$ and ‘‘frequency’’ $\omega := \bar{\nu}/\bar{o}_{u_*}$. We will also use the ‘‘temperature’’ for the ideal channel

$$T_1 := (\lambda \ln 2)^{-1} \quad (118)$$

obtained from the relation for T with $\eta = 1$.

In the third stage $\omega = 1$ and $\bar{N}_{\text{out}} = \bar{N}_{\text{out}}$ (see Subsec. IV-E), *i.e.* the quantities λ and η completely define the average amount of photons (59) contained in channel and, if the environment is pure, its capacity (see Eq. (80)). Moreover, the dependence $N(\lambda)$ given by Eq. (117) is expressible in explicit form:

$$N = \frac{1}{\eta} \left[\frac{1}{e^{1/T} - 1} - (1 - \eta) N_{\text{env}} \right]. \quad (119)$$

Let us now consider the second stage. Following [22] one can substitute $g_1(\bar{\nu}) = \bar{o}_{u_*} \lambda / \eta$ (see Eq. (116)) in the relation (88). That leads to

$$\omega = \sqrt{1 + \frac{\eta g_1(\nu)}{\lambda} \left[\frac{1}{o_u} - \frac{1}{4i_u^2 o_{u_*}} \right]}, \quad (120)$$

where we used the relation $\omega^2 = \bar{o}_{u_*}/o_u$ (remember, that in the second stage we have $\bar{o}_u = o_u$). Then, by substituting Eq. (120) and the relation $\bar{\nu} = \omega o_u$ in Eq. (117) we get a transcendental equation which relates λ and i_u . Hence, Eq. (117) (after all substitutions) becomes the mode transcendental equation (88) written in λ -representation. If the value of i_u is found for a given value of λ , the input energy N reads

$$N = \frac{1}{2} \left[\frac{o_u \omega^2}{\eta} - \frac{1}{\phi} + i_u - 1 \right], \quad (121)$$

which is the relation (99) with $\bar{o}_{u_*} = o_u \omega^2$. Thus, in any representation (N -, \bar{o}_{u_*} - or λ -representation) we have to solve only a single transcendental equation to find all variables.

Similarly to the threshold value $N_{2 \rightarrow 3}$ defined by Eq. (81), one can consider the threshold $N_{1 \rightarrow 2} = 0$ which defines the amount of photons corresponding to the transition from first to

second stage. These thresholds in the λ -representation will be denoted by $\lambda_{2 \rightarrow 3}$ and $\lambda_{1 \rightarrow 2}$ and can be obtained as follows.

The threshold $\lambda_{1 \rightarrow 2}$ is the limit of λ for $N \rightarrow 0$. Remember, that $N = 0$ is the case of the first stage with optimal eigenvalues $i_u = i_{u_*} = \frac{1}{2}$ and $m_u = m_{u_*} = 0$ (see Subsec. IV-E). Then, the convention $e_u > e_{u_*}$ means for the first stage that u is the quadrature corresponding to $m_u = 0$ for infinitesimal non-zero values of N . Hence, the general relation (116) gives

$$\lambda_{1 \rightarrow 2} \equiv \lim_{N \rightarrow 0} \lambda = \frac{\eta}{o_{u_*}} g_1(\nu) = \eta \sqrt{\frac{o_u}{o_{u_*}}} g' \left(\nu - \frac{1}{2} \right), \quad (122)$$

where the input eigenvalues are those of vacuum. Analogously,

$$\lambda_{2 \rightarrow 3} \equiv \lambda(N_{2 \rightarrow 3}) = \eta g_1(\bar{\nu}) / \bar{\nu} = \eta g' \left[\eta \left(i_u - \frac{1}{2} \right) + (1 - \eta) \left(e_u - \frac{1}{2} \right) \right], \quad (123)$$

where i_u is given by (74).

Proposition 3: The function $\lambda_{1 \rightarrow 2}(e_u, e_{u_*})$ is monotonically decreasing over each of its arguments.

Proof: The dependence $\lambda_{1 \rightarrow 2}(e_u)$ is proportional to the function $g_1(\nu)$, and the dependence $\lambda_{1 \rightarrow 2}(e_{u_*})$ is proportional to the function $g_1(\nu)/\nu^2$. Both these functions are monotonically decreasing over the argument ν . In turn, ν is monotonically increasing over o_u and o_{u_*} which are linear functions of e_u and e_{u_*} , respectively. Taking into account that the composition of monotonically decreasing and monotonically increasing functions is monotonically decreasing, the proposition is proved. ■

Using the zeroth-order approximation for the g_1 -function in Eq. (116), one can consider the quantity

$$\lambda^{(0)} = \frac{\eta}{\bar{o}_{u_*} \ln 2}, \quad (124)$$

which will play the role of λ for both²⁴ the approximated quantities $\underline{C}^{(0)}$ and $\underline{C}^{(1)}$. Analogously to Eq. (118) we will use the notation

$$T_1^{(0)} := \left(\lambda^{(0)} \ln 2 \right)^{-1}.$$

Then, the thresholds $\lambda_{1 \rightarrow 2}^{(0)}$ and $\lambda_{2 \rightarrow 3}^{(0)}$ can be defined like the quantities (122) and (123).

Similarly to capacity (the derivatives $dR^{(\text{hom})}/dN$ and $dR^{(\text{het})}/dN$ were defined in Subsec. IV-K) one can introduce the quantities

$$\lambda^{(\text{hom})} := \frac{dR^{(\text{hom})}}{dN} = \frac{\eta}{\bar{o}_{u_*} \ln 2}, \quad (125)$$

$$\lambda^{(\text{het})} := \frac{dR^{(\text{het})}}{dN} = \frac{\eta}{\bar{o}_{u_*}^{(\text{het})} \ln 2} \quad (126)$$

²⁴Our purpose is to get (as much as possible) analytical relation for capacity in multi-mode setting discussed in Sec. VI. If the first-order approximation for g_1 -function is used (see Eq. (20)), then the inversion of the dependence $\lambda(N)$ given by Eq. (116) gives rise to algebraic equation of high order, therefore we use the quantity $\lambda^{(0)}$ also to derive $\underline{C}^{(1)}$.

²²Here we use the property: if $g'(v) = y$, then $v = 1/(e^{y \ln 2} - 1)$.

²³Similar result was obtained in Ref. [32] for a number-state channel, where the optimal photon-number distribution is Planck distribution parametrized by a Lagrange multiplier.

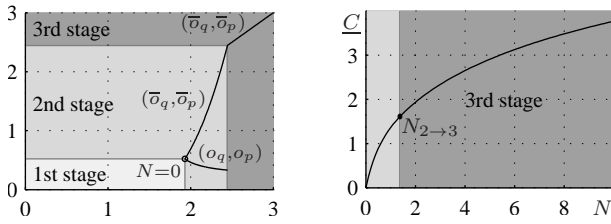


Fig. 2. On the left, the loci $(o_q(N), o_p(N))$ (bottom curve) and $(\bar{o}_q(N), \bar{o}_p(N))$ (top curve) for values of $N \in (0, 3)$ are plotted. The values of other parameters are $\mathcal{N}_{\text{env}} = s = 1$, $\eta = 0.6$. Different grey-scale backgrounds indicate the parameters' regions corresponding to different stages for given curves (the higher the stage is, the darker the color is). The first stage is a single point at $N = 0$, where $(o_q, o_p) = (\bar{o}_q, \bar{o}_p)$. In the third stage the locus (o_q, o_p) is mapped into a single point (situated at the border between the second and the third stages) for all values of N , since V_{in} does not depend on N . In turn, the locus (\bar{o}_q, \bar{o}_p) in the third stage is the line $\bar{o}_p = \bar{o}_q$. On the right, the quantity \underline{C} is plotted vs N . One can see that the dependence $\underline{C}(N)$ is actually concave. The values of $N \in (0, N_{2 \rightarrow 3})$ (marked using light grey color) corresponds to the second stage, and the values of $N \in (N_{2 \rightarrow 3}, 10)$ (marked with dark grey color) corresponds to the third stage.

for homodyne and heterodyne rates, respectively. Their threshold values will be denoted as $\lambda_{1 \rightarrow 2}^{(\text{hom})}$, $\lambda_{1 \rightarrow 2}^{(\text{het})}$ and $\lambda_{2 \rightarrow 3}^{(\text{het})}$. The “temperatures” for rates can be defined analogously to Eq. (118) as

$$T_1^{(\text{hom})} := \left[\lambda^{(\text{hom})} \ln 2 \right]^{-1}, \quad T_1^{(\text{het})} := \left[\lambda^{(\text{het})} \ln 2 \right]^{-1} \quad (127)$$

Then, in the third stage the quantities N and $\lambda^{(\text{het})}$ are related by equation

$$N = T_1^{(\text{het})} - \frac{1 - \eta}{\eta} \mathcal{N}_{\text{env}} - \frac{1}{\eta}.$$

It follows from Eqs. (99) and (100) that in the second stage N depends on $\lambda^{(0)}$ (for capacity $\underline{C}^{(0)}$) as

$$N = \frac{1}{2} [T_1^{(0)} - \phi^{-1} + i_u - 1], \quad (128)$$

where

$$i_u = \frac{1}{2} \left[\sqrt{(\phi/4)^2 + \phi T_1^{(0)}} - \phi/4 \right]. \quad (129)$$

Notice the similarity between Eqs. (121) and (128). In fact, the first term in Eq. (121) is equal to \bar{o}_{u_*}/η , which can be rewritten as (see Eq. (116)) $(g_1(\bar{v})/\eta) T \ln 2$. The latter is equal to T_1 if the replacement (56) is applied and η is set to 1. Taking into account the definitions (125)–(127) one can see that Eqs. (128) and (129) hold also for rates if $T_1^{(0)}$ is replaced by $T_1^{(\text{hom})}$ or $T_1^{(\text{het})}$, ϕ is given by Eq. (94) or replaced by $\phi^{(\text{het})}$ (see Eq. (96)), for homodyne and heterodyne rate, respectively.

M. Stage transition and quantum water filling

Finally, let us discuss the point of stage transition. As far as different stages correspond to solutions of different systems of Lagrange equations, it is natural that some properties (e.g. smoothness, see Eqs. (192) and (194) in Appendix E) are violated at this point. In fact, this can be seen from Fig.2-left, where the loci (\bar{o}_q, \bar{o}_p) and (o_q, o_p) are plotted for different

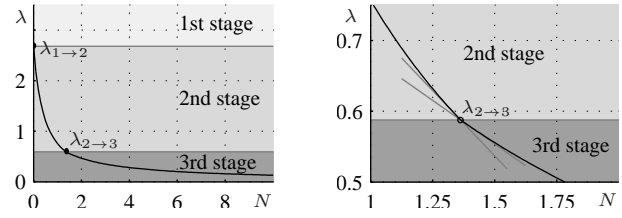


Fig. 3. The quantity λ is plotted vs N (the right is a magnification of the stage transition point $\lambda_{2 \rightarrow 3}$). The values of other parameters are $s = 1$, $\eta = 0.7$, $\mathcal{N}_{\text{env}} = 0.5$. One can see that $\lambda_{1 \rightarrow 2} = \lambda(N = 0) < \infty$. On the right, the left and right tangents are plotted at the point of $\lambda_{2 \rightarrow 3} = \lambda(N_{2 \rightarrow 3})$ (the left and right derivatives are different as it follows from Eqs. (192) and (194) in Appendix E).

values of N and fixed values of $s, \eta, \mathcal{N}_{\text{env}}$. The dependence of \bar{o}_p vs \bar{o}_q given by the locus (\bar{o}_q, \bar{o}_p) has a kink in the point of transition from second to third stage. Similarly, the function $\lambda(N)$ has a kink and the function $d\lambda/dN = d^2 \underline{C}/dN^2$ is discontinuous at this point (see Fig.3). However, the function $\underline{C}(N)$ is smooth at the point of stage transition, because its derivative (112) is continuous (see Fig.2-right).

In the third stage we have the equality (69), which can be written as

$$\eta(i_u + m_u) + (1 - \eta)e_u = \eta(i_{u_*} + m_{u_*}) + (1 - \eta)e_{u_*}.$$

It means that the energy spent for modulation is distributed between quadratures in a way to equalize the eigenvalues of the state \bar{V}_{out} . This type of solution is typical for optimization problems and it appears also for classical channels [35], where it was called “water filling”. Later such solution was shown to hold for some parameters also for quantum channel with additive noise [22], [30], [36], where it was called “quantum water filling”. For the case of lossy channel this type of solution was presented in [12].

Quite generally one can call “quantum water filling” all types of solutions for the optimal distribution of input energy between quadratures. It will be shown later in Sec. VI for memory channels that the input energy has to be distributed between many modes. In addition, all modes belonging to the third stage must possess equal average number of photons \bar{N}_{out} , and for all of them equality $\bar{o}_u = \bar{o}_{u_*}$ must hold. Furthermore, if almost all modes are in the third stage, the solution can be interpreted as a small perturbation of water filling. Thus, the term “quantum water filling” used for all types of solutions underlines the “physical” meaning of the performed optimization.

V. ROLE OF CHANNEL PARAMETERS

In this section we discuss the dependence from parameters of capacity and rates found in Sec. IV (i.e. for single channel use). Apart from characterizing the one-shot capacity this study is also relevant for the case of multiple channel uses and additivity problem discussed below in Sec. VI.

It is evident that both capacity and rates must be monotonic functions of parameters η , N and \mathcal{N}_{env} . In fact, higher transmissivity and input energy cannot result to less capacity or rates from physical point of view. In addition, it was

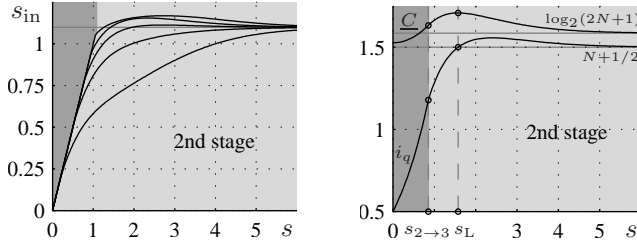


Fig. 4. On the left, the optimal input squeezing s_{in} is plotted vs s , for values of η going from 0.1 (bottom curve) to 0.9 (top curve) with step 0.2. The values of the other parameters are $N = 1$, $\mathcal{N}_{\text{env}} = 0$. On the right, both the capacity \underline{C} and optimal input eigenvalue i_q are plotted vs s . The value of the other parameters are $\mathcal{N}_{\text{env}} = 0$, $N = 1$, $\eta = 0.6$.

explicitly shown in Subsec. IV-K that both capacity and rates are monotonic concave functions of N .

In turn, monotonic dependence of capacity from \mathcal{N}_{env} can be shown as follows. Given the value $\mathcal{N}'_{\text{env}} > \mathcal{N}_{\text{env}}$ the lossy channel for the parameters s , η and $\mathcal{N}'_{\text{env}}$ can be represented as a channels composition $\mathcal{G}_N \circ \mathcal{G}_L$, where \mathcal{G}_L is a lossy channel with parameters s , η , \mathcal{N}_{env} and \mathcal{G}_N is an additive (classical) noise channel (see Eqs. (26) and (27)) with environment matrix

$$V_{\text{env}} = (1 - \eta)(\mathcal{N}'_{\text{env}} - \mathcal{N}_{\text{env}}) \begin{pmatrix} e^s & 0 \\ 0 & e^{-s} \end{pmatrix}.$$

Since the capacity of the composition of two channels cannot exceed that of each individual channel, we deduce that the capacity is non-increasing function of \mathcal{N}_{env} . Furthermore, the following *environment purity theorem* states that the optimal \mathcal{N}_{env} is zero:

Theorem 3: The maximum of capacity on the set of environment states $\{V_{\text{env}}\}$ whose elements have the same average amount of photons \mathcal{N}_{env} is achieved on pure environment state, i.e. $e_u e_{u_*} = 1/4$.

Proof: Proof is given in Appendix D. ■

Extension of this theorem to the case of rates is straightforward.

Thus, the only parameter which can make capacity and rates non-monotonic is the environment squeezing s . In this section we investigate this non-monotonic dependence. Below, the subsections V-A and V-B are mainly devoted to definitions, properties and numerical results on channel parameters, while the other subsections contain analytical results justifying the numerics.

A. Role of input and environment squeezing

Using the representation (32) for input covariance matrix $V_{\text{in}} = V(\mathcal{N}_{\text{in}}, s_{\text{in}})$, one can relate the optimal degree of input squeezing s_{in} to the degree of environment squeezing s . It follows from Eqs. (73) and (92) that $s_{\text{in}} = s$ for the third stage (for \underline{C} , $\underline{C}^{(0)}$, $\underline{C}^{(1)}$ and $\underline{C}^{(\log)}$) and

$$s_{\text{in}} = \ln \left[\sqrt{1 + (2N + 1)\phi + \phi^2/4} - \phi/2 \right] \quad (130)$$

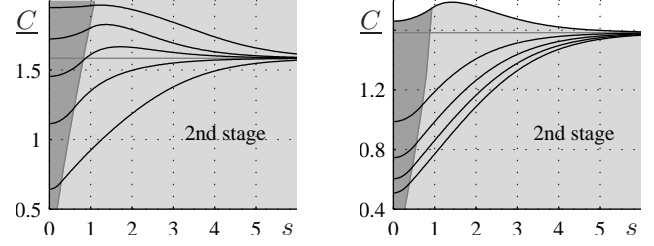


Fig. 5. On the left, capacity \underline{C} vs s , for values of η going from 0.15 (bottom curve) to 0.95 (top curve) with step 0.2. The values of the other parameters are $N = 1$, $\mathcal{N}_{\text{env}} = 0$. On the right, capacity \underline{C} vs s for values of \mathcal{N}_{env} going from 0 (top curve) to 4 (bottom curve) with step 1. The values of the other parameters are $\eta = 0.7$, $N = 1$.

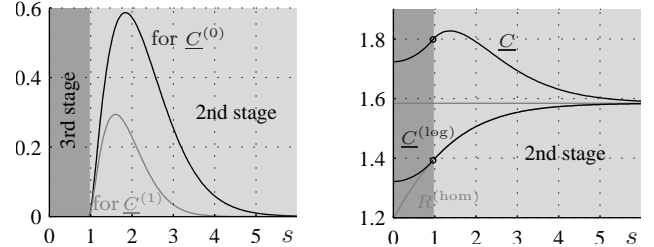


Fig. 6. On the left, the quantities $[(\underline{C} - \underline{C}^{(0)})/\underline{C}] \times 100\%$ (black) and $[(\underline{C} - \underline{C}^{(1)})/\underline{C}] \times 100\%$ (grey) are plotted vs s for $\eta = 0.75$, $N = 1$, $\mathcal{N}_{\text{env}} = 0$. On the right, the quantities \underline{C} , $\underline{C}^{(\log)}$ and $R^{(\text{hom})}$ are plotted vs s for $\eta = 0.75$, $N = 1$, $\mathcal{N}_{\text{env}} = 0$.

for the second stage (for $\underline{C}^{(0)}$ and $\underline{C}^{(\log)}$). Analogously, it follows from Eq. (73) that $s_{\text{in}} = s^{(\text{het})}$ (see Eq. (42)) for the heterodyne rate in the third stage. In the second stage both homodyne and heterodyne rates result to the same relation (130), where the replacement (95) must be applied for the heterodyne case. At the transition point between different stages there is a *kink* in the function $s_{\text{in}}(s)$ (see Fig.4-left). It reflects the fact that different stages correspond to solution of different systems of equations. The dependence $i_q(s)$ is shown in Fig.4-right (this is discussed in the following subsections in a more detailed way).

The capacity \underline{C} found by the exact analytical solution is shown in Fig.5 for fixed N as function of s and for different values of η (at left) and \mathcal{N}_{env} (at right). One can see that the squeezed environment ($s \neq 0$) may result to capacity enhancement. This phenomenon shows similarity with the improvement of the signal to noise ratio achieved by squeezed vacuum injection in an optical wave-guide tap [33]. The highest enhancement occurs at either finite value of s or at $s \rightarrow \infty$ depending on the value of η . In any case, the capacity in the limit of large s becomes only function of the energy constraint N (see Eq. (110)) explaining why all curves $\underline{C}(s)$ flow together to the same value²⁵ when $s \rightarrow \infty$. Similarly, s_{in} tends to the value (104) for $s \rightarrow \infty$ because it follows from Eq. (130) (see also Fig.4).

The difference among quantities $\underline{C}^{(0)}$, $\underline{C}^{(1)}$ and \underline{C} is shown in Fig.6-left. In Fig.6-right the quantities \underline{C} , $\underline{C}^{(\log)}$ and $R^{(\text{hom})}$

²⁵This behavior originally was observed in [11] for the capacity of particular memory channel found as maximum over a small subset of Gaussian states.

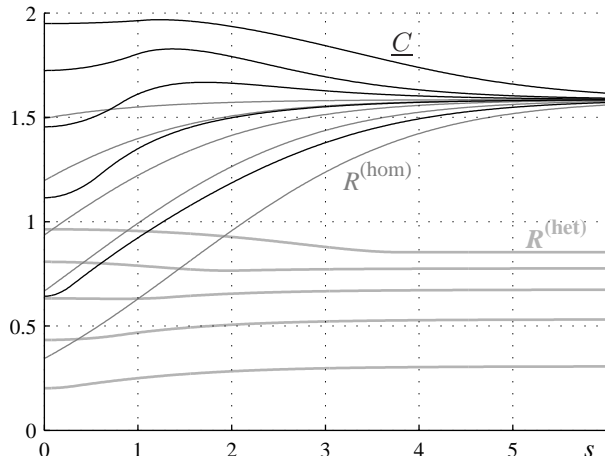


Fig. 7. Classical capacity \underline{C} (solid curves), homodyne $R^{(\text{hom})}$ (thin grey curves) and heterodyne $R^{(\text{het})}$ (bold grey curves) rates vs s , for values of η going from 0.15 (bottom curve) to 0.95 (top curve) with step 0.2. The values of the other parameters are $N = 1$, $N_{\text{env}} = 0$.

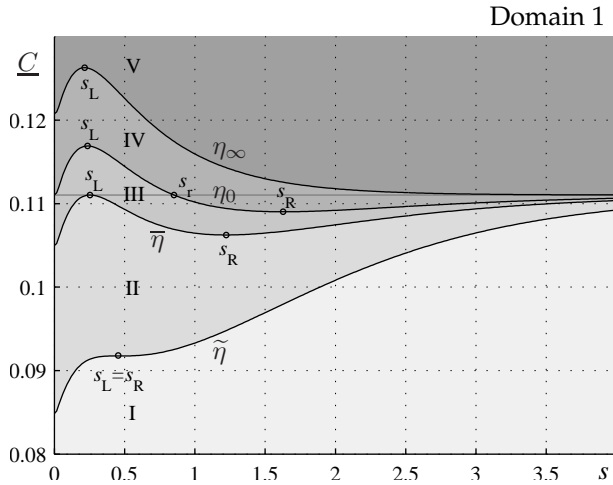


Fig. 8. The dependence $C(s)$ for channel parameters N and N_{env} belonging to the first domain ($N = 0.04$, $N_{\text{env}} = 0.001$) is plotted for values of transmissivity $\eta = 0.28, 0.359, 0.384$ and 0.424 (from bottom to top), which approximately correspond to border values between different regimes ($\tilde{\eta}$, $\bar{\eta}$, η_0 and η_∞ , respectively). Regimes are indicated with roman numbers (I-V) and different gray scale colors. Any curve $C(s)$ corresponding to a particular regime would completely lie in the area with the background color corresponding to that regime.

are shown together. One can see that $\underline{C}^{(\log)}$ coincides with homodyne rate in the second stage (see Eq. (46)).

The rates $R^{(\text{hom})}$ and $R^{(\text{het})}$ together with the exact solution for capacity are shown in Fig.7 for fixed N as functions of s and for different values of η . One can see that in the second stage both rates are monotonically growing functions of s which is in agreement with the Eq. (97). In the third stage the heterodyne rate may be non-monotonic achieving its minimum. As it can be seen from Fig.7, the optimal heterodyne rate is achieved at either $s \rightarrow \infty$ or $s = 0$. Analytical description of this behavior is given in Subsec.V-I. A similar (to Fig.7) family of curves can be obtained if $R^{(\text{het})}$ or $R^{(\text{hom})}$ is plotted versus s for different values of N_{env} and

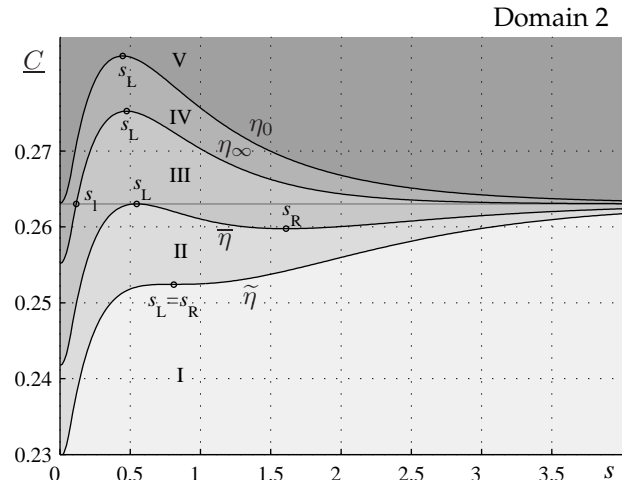


Fig. 9. The dependence $C(s)$ for channel parameters N and N_{env} belonging to the second domain ($N = 0.1$, $N_{\text{env}} = 0$) is plotted for values of transmissivity $\eta = 0.369, 0.394, 0.423, 0.44$ (from bottom to top), which approximately correspond to border values between different regimes ($\tilde{\eta}$, $\bar{\eta}$, η_∞ and η_0 , respectively). Regimes are indicated with roman numbers (I-V) and different gray scale colors. Any curve $C(s)$ corresponding to a particular regime would completely lie in the area with the background color corresponding to that regime.

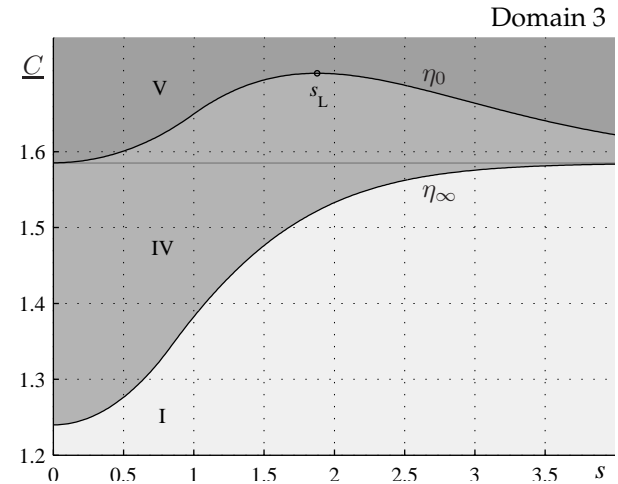


Fig. 10. The dependence $C(s)$ for channel parameters N and N_{env} belonging to the third domain ($N = 1$, $N_{\text{env}} = 1$) is plotted for values of transmissivity $\eta = 0.808$ (bottom curve) and 0.919 (top curve), which approximately correspond to border values between different regimes (η_∞ and η_0 , respectively). Regimes are indicated with roman numbers (I, IV and V); other regimes do not exist in the third domain and different gray scale colors. Any curve $C(s)$ corresponding to particular regime would completely lie in the area with the background color corresponding to that regime.

fixed η . One can see that the universal limit (110) holds also for this case.

Despite the behavior shown in Fig.5 is the most typical, there are parameters values giving more complicated dependence for $\underline{C}(s)$ (all possible cases are plotted at Figs.8, 9, 10 and 11). In particular, the capacity may have both minimum and maximum each of them attained at finite environment squeezing $0 < s < \infty$. Such behavior and the parameters related with its description are discussed in the following subsections.

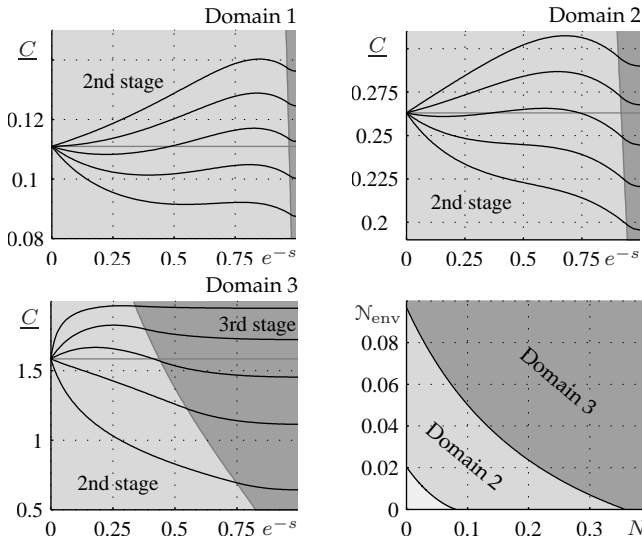


Fig. 11. The dependence $\underline{C}(e^{-s})$ for different values of η and fixed values of N and N_{env} . In particular, $N = 0.04$ and $N_{\text{env}} = 0$ (corresponding to the first domain), η goes from 0.275 (bottom) to 0.475 (top) with step 0.05 (top-left figure); $N = 0.1$ and $N_{\text{env}} = 0$ (corresponding to the second domain), η goes from 0.3 (bottom) to 0.5 (top) with step 0.05 (top-right figure); $N_{\text{env}} = 0$ and $N = 1$ (corresponding to the third domain), η goes from 0.15 (bottom) to 0.95 (top) with step 0.2 (bottom-left figure). The parts corresponding to different backgrounds belongs to different stages (lighter color states for second stage, and darker color states for third stage). Bottom-right: the loci $(N_0, N_{\text{env},0})$ (bottom curve) and $(\bar{N}, \bar{N}_{\text{env}})$ (top curve), corresponding to transitions between different channel domains. The points (N, N_{env}) belonging to the area between these curves correspond to the domains indicated with different grey scale backgrounds colors.

B. Role of transmissivity for capacity

It was shown in Fig.5 that both η and N_{env} can be chosen to parametrize the family of curves $\underline{C}(s)$. In order to completely characterize how capacity depends on squeezing we will use η . All “qualitative” possibilities for the dependence $\underline{C}(s)$ are shown in Figs.8, 9, 10 and 11. Such a dependence can be interpreted as crossing different *regimes* by increasing η from zero to one. In turn, the set of regimes depend on the *domain* which N and N_{env} values belong to (see Fig.11-bottom-right). Let us consider this behavior in more detail (in the relations below the argument of \underline{C} is assumed to be s).

Let us define the specific values of squeezing and transmissivity in a formal way. First we notice that from numerical calculations it results:

Proposition 4: The function $\underline{C}(s)$ may have at maximum two extrema for the values of squeezing $0 < s < \infty$.

Evidently, if the function $\underline{C}(s)$ has two extrema, then one of them must be maximum and the other minimum. They can be formally defined as follows.

Definition 2: The finite positive value of squeezing s will be denoted by s_L or s_R if the function $\underline{C}(s)$ has its local maximum or minimum at that values, respectively:

$$\begin{aligned} \underline{C}'(s_L) &= 0, & \underline{C}''(s_L) &< 0, \\ \underline{C}'(s_R) &= 0, & \underline{C}''(s_R) &> 0. \end{aligned}$$

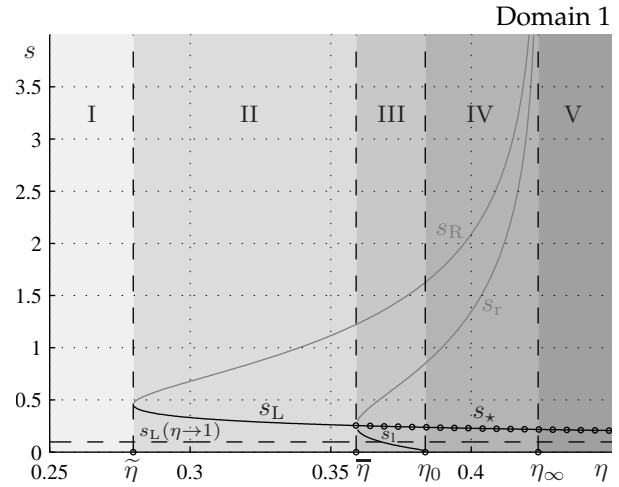


Fig. 12. The dependence of the quantities s_r , s_l , s_R , s_L and s_* vs η for capacity \underline{C} . The value of the other parameters are $N = 0.04$ and $N_{\text{env}} = 0.001$ (corresponding to the first domain). Different gray scale backgrounds corresponds to transmissivities η from different regimes (indicated with roman numbers). Vertical asymptotes are plotted for the critical transmissivities, and the horizontal asymptote shows the limit $\lim_{\eta \rightarrow 1} s_L$. The part of the curve $s_L(\eta)$ coinciding with $s_*(\eta)$ is shown with dots. At the point $\eta = \bar{\eta}$ the quantity s_* jumps to infinity and for all values of $\eta \leq \bar{\eta}$ is equal to infinity.

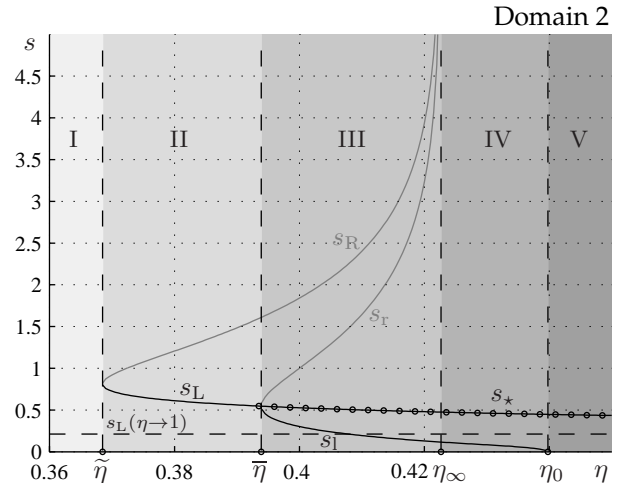


Fig. 13. The dependence of the quantities s_r , s_l , s_R , s_L and s_* vs η for capacity \underline{C} . The value of the other parameters are $N = 0.1$ and $N_{\text{env}} = 0$ (corresponding to the second domain). Different gray scale backgrounds corresponds to transmissivities η from different regimes (indicated with roman numbers). Vertical asymptotes are plotted for the critical transmissivities, and the horizontal asymptote shows the limit $\lim_{\eta \rightarrow 1} s_L$. The part of the curve $s_L(\eta)$ coinciding with $s_*(\eta)$ is shown with dots. At the point $\eta = \bar{\eta}$ the quantity s_* jumps to infinity and for all values of $\eta \leq \bar{\eta}$ is equal to infinity.

One of our purpose is to study the value of squeezing giving highest capacity, which can be defined as written below.

Definition 3: The value of squeezing s will be denoted by s_* and called *optimal* if it corresponds to global maximum of the function $\underline{C}(s)$:

$$\underline{C}(s_*) = \max_{0 \leq s \leq \infty} \underline{C}(s).$$

Finite values of squeezing providing the same value of

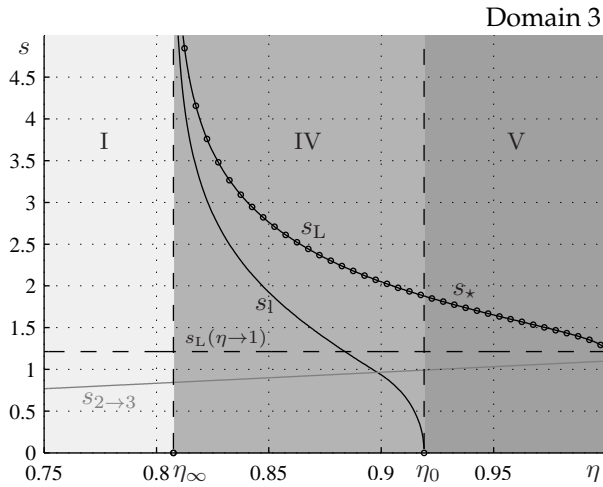


Fig. 14. The dependence of the quantities s_r , s_1 , s_R , s_L , s_* and $s_{2 \rightarrow 3}$ vs η for capacity \underline{C} . The value of the other parameters are $N = 1$ and $N_{\text{env}} = 1$ (corresponding to the third domain). Different gray scale backgrounds corresponds to transmissivities η from different regimes (indicated with roman numbers, the second and the third regimes do not exist). Vertical asymptotes are plotted for the critical transmissivities, and the horizontal asymptote shows the limit $\lim_{\eta \rightarrow 1} s_L$. The part of the curve $s_L(\eta)$ coinciding with $s_*(\eta)$ is shown with dots (s_* coincides with s_L on the whole region of transmissivities where s_L is defined, i.e. for $\eta \in (\eta_\infty, 1)$, and s_* equals infinity if $\eta \in (0, \eta_\infty)$). At the point $\eta = \bar{\eta}$ the quantity s_* together with s_L asymptotically tends to infinity. Also notice, that $s_{2 \rightarrow 3} \neq s_L$ in the limit $\eta \rightarrow 1$.

capacity as infinite squeezing can exist:

Definition 4: The finite positive value of squeezing s will be denoted by s_1 (s_r) if both the value of function $\underline{C}(s)$ at that squeezing coincides with the value at infinity and $\underline{C}(s)$ is increasing (decreasing) function at this point:

$$\begin{aligned} \underline{C}(s_1) &= \underline{C}(\infty), & \underline{C}'(s_1) &> 0, \\ \underline{C}(s_r) &= \underline{C}(\infty), & \underline{C}'(s_r) &< 0. \end{aligned}$$

As far as $\underline{C}(s)$ belongs to the third stage for small values of s and $\underline{C}(s)$ is always increasing function of s in the third stage, the extremum corresponding to the smallest value of squeezing must be the maximum. Hence, the minimum must correspond to higher value of squeezing which exists only if the maximum does. This also makes the function $\underline{C}(s)$ increasing in s_1 and decreasing in s_r . Thus, if both extrema exist, we have $s_L < s_R$ and $s_1 < s_r$ which explains the notations introduced in the definitions 2 and 4). In the general case it follows from numerical results that the function $\underline{C}(s)$ in the interval $0 < s < \infty$ can be one of the following:

- Monotonic function without stationary points.
- Monotonic function with single saddle-point.
- Function with one maximum.
- Function with one maximum and one minimum.

In order to study the case with the saddle-point we define the following transmissivity:

Definition 5: The transmissivity η will be denoted by $\tilde{\eta}$ and called *saddle-point transmissivity* if $\underline{C}(s)$ has saddle-point in

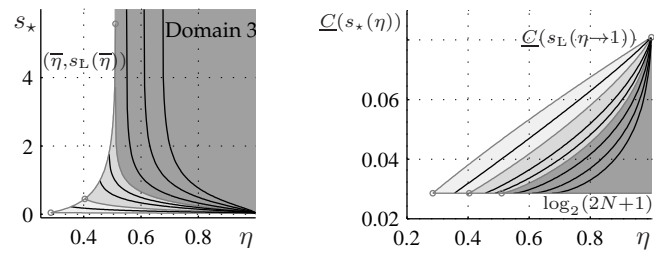


Fig. 15. Optimal environment squeezing s_* (left) and capacity $\underline{C}(s_*(\eta))$ (right) are plotted vs η for values of N_{env} equal to 0, 0.0055, 0.0165, 0.0413, 0.066, 0.0898, 0.1403, 0.2393 and 0.3879 (from bottom to top at left, and from top to bottom at right). The value of the other parameter is $N = 0.01$. Curves, corresponding to different backgrounds belongs to different domains (darker background corresponds to higher domain). The curves corresponding to transition between different domains are plotted using grey color. At the left: each curve belonging to the first or the second domain jumps to infinity at some finite value and equals infinity for all transmissivities to the left of that jump. Then, curves, corresponding to the third domain tend asymptotically to infinity and are equal to infinity for all values of η which are to the left of that asymptote. The whole region occupied by the finite dependences $s_*(\eta)$ is bounded to the left by the locus $(\bar{\eta}, s_L(\bar{\eta}))$. The values of $s_*(\min \eta) < \infty$ corresponding to borders between different domains are indicated with grey points. It is interesting to note that the area corresponding to the second domain is bounded from the top, i.e. for the values of N and N_{env} corresponding to transition from second to third domain, the value of s_* is still finite at the point $\eta = \bar{\eta}$. The area occupied by curves is bounded from the bottom by the curve $s_*(\eta)$ for $N_{\text{env}} = 0$ which is not zero. At the right: the whole region occupied by family of possible curves $\underline{C}(s_*(\eta))$ is bounded from the bottom by the limit (110). Here we plotted capacity corresponding to finite values of s_* (for small values of η we have $s_* = \infty$, therefore each curve $\underline{C}(s_*(\eta))$ is equal to $\log_2(2N+1)$ – this is not plotted). By increasing η from zero to one, we reach the point of $\eta = \bar{\eta}$ (for the first and second domain) or $\eta = \eta_*$ (for the third domain) where the curve $\underline{C}(s_*(\eta))$ is detached from horizontal line $\log_2(2N+1)$. And finally, when η tends to 1, all curves $\underline{C}(s_*(\eta))$ tend to the same value $\lim_{\eta \rightarrow 1} \underline{C}(s_L(\eta))$. One can see from numerics that this value does not depend on N_{env} .

some finite positive value of squeezing:

$$\exists \tilde{s} \in (0, \infty) \mid \underline{C}'(\tilde{s}) = \underline{C}''(\tilde{s}) = 0.$$

It follows from the results of numerical study that $\tilde{\eta}$ exists if and only if the following transmissivity does:

Definition 6: The transmissivity η will be denoted by $\bar{\eta}$ and called $\bar{\eta}$ -transmissivity if a finite positive value of squeezing exists such that $\underline{C}(s)$ has maximum at that squeezing and the value of maximum is equal to $\underline{C}(\infty)$:

$$\exists \bar{s} \in (0, \infty) \mid \underline{C}(\bar{s}) = \underline{C}(\infty), \underline{C}'(\bar{s}) = 0, \underline{C}''(\bar{s}) < 0.$$

Then, by considering the behavior of $\underline{C}(s)$ for zero and infinite squeezings the following definitions can be introduced.

Definition 7: The transmissivity η will be denoted by η_0 and called η_0 -transmissivity if the values of $\underline{C}(s)$ for zero and infinite squeezing coincide: $\underline{C}(0) = \underline{C}(\infty)$.

Definition 8: The transmissivity η will be denoted by η_∞ and called η_∞ -transmissivity if $\underline{C}'(\infty) = 0$, i.e. in neighborhood of infinite squeezing $\underline{C}(s)$ is decreasing for $\eta > \eta_\infty$ and increasing for $\eta < \eta_\infty$.

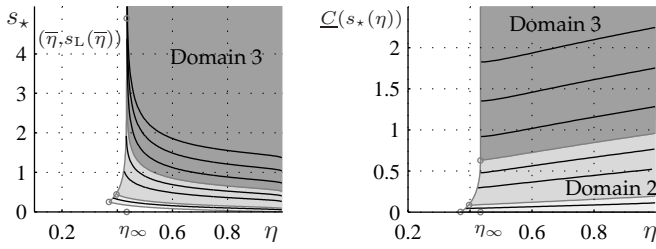


Fig. 16. Optimal environment squeezing s_* (left) and capacity $\underline{C}(s_*(\eta))$ (right) are plotted vs η for values of N equal to 10^{-6} , 0.0149, 0.0298, 0.1127, 0.1956, 0.2755, 0.4443, 0.7760, 1.2734 (from bottom to top for both: left and right graphs). The value of the other parameter is $\mathcal{N}_{\text{env}} = 0.01$. Curves, corresponding to different backgrounds belongs to different domains (darker background corresponds to higher number of domain). The curves corresponding to transition between different domains are plotted using grey color. At the left: each curve belonging to the first or the second domain jumps to infinity at some finite value and equals infinity for all transmissivities which are to the left of that value. Then, curves, corresponding to the third domain tend asymptotically to infinity (when η tends to η_∞ from the right) and are equal to infinity to the left of that asymptote. The whole region occupied by the finite dependences $s_*(\eta)$ is bounded to the left by the locus $(\bar{\eta}, s_L(\bar{\eta}))$. The values of $s_*(\min \eta) < \infty$ corresponding to borders between different domains are indicated with grey points. It is interesting to note that the area corresponding to the second domain is bounded by the finite value from the top, *i.e.* for the values of N and \mathcal{N}_{env} corresponding to transition from the second to the third domain, the value of s_* is still finite at the point $\eta = \bar{\eta}$. The area occupied by curves is bounded from the bottom by the curve $s_*(\eta)$ for $N \rightarrow 0$ which is not zero. One can see that in the third domain the value of $\eta = \eta_\infty$ is the same for all curves. This is in fact in agreement with the analytical result (obtained in subsequent subsections) that η_∞ does not depend on N . At the right: the whole region occupied by family of possible curves $\underline{C}(s_*(\eta))$ is bounded from the bottom by the zero. Here we plotted the capacity corresponding to finite values of s_* (for small values of η we have $s_* = \infty$, therefore each curve $\underline{C}(s_*(\eta))$ should be continued horizontally to the left being at the same level as in left border – this is not plotted).

One can note that some properties (e.g. saddle-point) can be observed only for particular “domains” of the parameters N and \mathcal{N}_{env} , which requires to introduce further classification. It follows from the results of numerical study that the following definitions allow to divide the quadrant ($N > 0$, $\mathcal{N}_{\text{env}} \geq 0$) into three non-overlapping *domains* (see Fig.11-bottom-right), thus providing consistent classification of all possible cases.

Definition 9: The parameters $(N, \mathcal{N}_{\text{env}})$ belong to the *first* or to the *second domain* if $\eta_0 < \eta_\infty$ or $\eta_0 > \eta_\infty$, respectively.

Definition 10: The parameters $(N, \mathcal{N}_{\text{env}})$ belong to the *third domain* if the function $\underline{C}(s)$ has at maximum one extremum in the interval $0 < s < \infty$ for all values of transmissivity $\eta \in (0, 1)$.

These domains correspond to the following relations between transmissivities:

- *First domain:* $\tilde{\eta} < \bar{\eta} < \eta_0 < \eta_\infty$.
- *Second domain:* $\tilde{\eta} < \bar{\eta} < \eta_\infty < \eta_0$.
- *Third domain:* $\eta_\infty < \eta_0$ ($\tilde{\eta}$ and $\bar{\eta}$ do not exist).

In order to characterize the transitions from one domain to another we will use the following definitions.

Definition 11: The value of N will be denoted by N_0 and called *supercritical* for a given value of \mathcal{N}_{env} , if the point $(N_0, \mathcal{N}_{\text{env}})$ corresponds to the transition from first to second

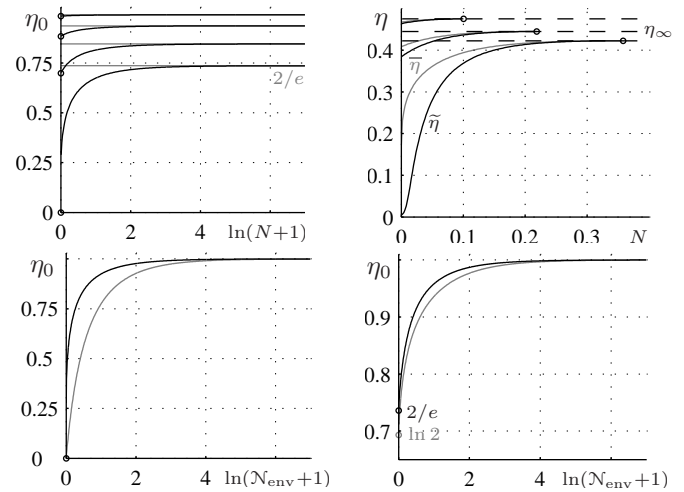


Fig. 17. Top-left: the quantity η_0 is plotted vs $\ln(N+1)$ for the values of \mathcal{N}_{env} equal to 0, 0.2, 1, 10 (from bottom to top). Top-right: the quantities $\tilde{\eta}$ (black solid), $\bar{\eta}$ (grey) and η_∞ (horizontal dashed black lines) are plotted vs N for the values \mathcal{N}_{env} equal to 0, 0.02, 0.05 (from bottom to top for all curves). The points where $\tilde{\eta}$ and $\bar{\eta}$ touch the line corresponding to η_∞ are indicated with bold points. Bottom-left: function $\lim_{N \rightarrow 0} \eta_0$ vs $\ln(\mathcal{N}_{\text{env}}+1)$ as exact (black curve, see Eq. (142)) and approximate (grey curve, see Eq. (145)) quantities. Bottom-right: function $\lim_{N \rightarrow \infty} \eta_0$ as exact (black curves, Eq. (146)) and approximate (grey curve, see Eq. (148)) quantities. The values of all the quantities for all the graphs for zero argument are shown by bold point.

domain. Similarly, the value of \mathcal{N}_{env} will be denoted by $\mathcal{N}_{\text{env},0}$ and called *supercritical* for a given value of N , if the point $(N, \mathcal{N}_{\text{env},0})$ corresponds to transition from first to second domain.

Definition 12: The value of N will be denoted by \tilde{N} and called *supercritical* for a given value of \mathcal{N}_{env} , if the point $(\tilde{N}, \mathcal{N}_{\text{env}})$ corresponds to transition from second to third domain. Similarly, the value of \mathcal{N}_{env} will be denoted by $\tilde{\mathcal{N}}_{\text{env}}$ and called *supercritical* for a given value of N , if the point $(N, \tilde{\mathcal{N}}_{\text{env}})$ corresponds to transition from second to third domain.

Definition 13: The function $f(N, \mathcal{N}_{\text{env}}) = 0$ will be denoted by f_0 and called *supercritical* if it corresponds to the boundary between the first and second domain. Similarly, the function $f(N, \mathcal{N}_{\text{env}}) = 0$ will be denoted by \tilde{f} and called *supercritical* if it corresponds to the boundary between the second and third domain.

As far as the boundary between domains characterize the critical parameters (transmissivities), e.g. appearance of some critical parameters or the relations between them, the term “supercritical” was used in the definitions 11, 12 and 13. One can also say that supercritical parameters are those critical parameters which characterize the other critical parameters.

The mnemonic rule to remember the notations used for the critical and supercritical parameters is the following. The quantities η_0 and η_∞ are defined by considering the behavior of capacity at the points of zero and infinite squeezing, therefore these values are used as subscripts. The supercritical

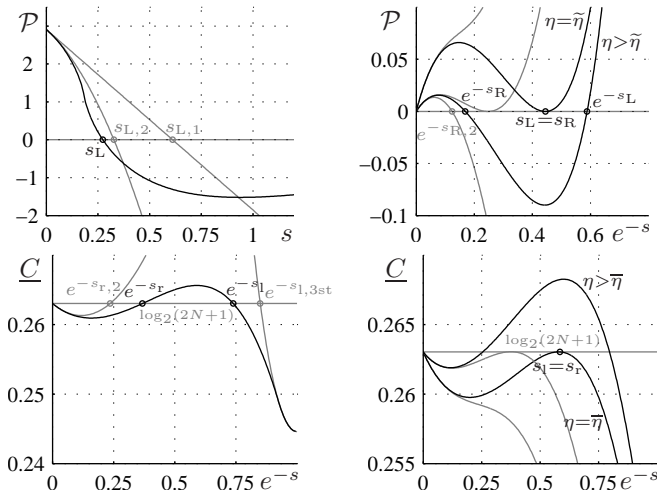


Fig. 18. Top-left (analytical method of estimation of s_L): quantity \mathcal{P} vs s together with its linear and quadratic approximations at the point $s = 0$. The value of parameters are $\eta = 0.8$, $N = 0.1$, $\mathcal{N}_{\text{env}} = 0$. Top-right (analytical method of estimation of $\tilde{\eta}$): quantity \mathcal{P} vs e^{-s} for the values $\eta = 0.3985$ (bottom black curve, its quadratic and cubic approximations at point $e^{-s} = 0$ through partial Taylor sum – grey color) and $\eta = 0.3685$ (top black curve and its third approximation at point $e^{-s} = 0$ – grey color). The value of other parameters are $N = 0.1$, $\mathcal{N}_{\text{env}} = 0$. The points, where quadratic and linear approximations cross the line $\mathcal{P} = 0$ defines quadratic and linear approximations for the corresponding s -quantities: approximations $s_{L,2}$ and $s_{L,1}$ for the quantity s_L , and approximation $s_{R,2}$ for the quantity s_R . Similarly, the value of transmissivity at which cubic approximation has two roots (touches the line $\mathcal{P} = 0$) defines approximation for $\tilde{\eta}$. Bottom-left (method of estimation of s_1 and s_r): \underline{C} vs e^{-s} for the values of $\eta = 0.4$, $N = 0.1$ and $\mathcal{N}_{\text{env}} = 0$. Bottom-right (method of estimation of $\tilde{\eta}$): \underline{C} vs e^{-s} for the values of $\eta = 0.3939$ (bottom black curve) and $\eta = 0.4062$ (top black curve). The value of other parameters are $N = 0.1$, $\mathcal{N}_{\text{env}} = 0$. For the top black curve its cubic approximation gives an estimation for the quantity $\tilde{\eta}$.

values N_0 and $\mathcal{N}_{\text{env},0}$ correspond to transition between the domains which have different relations between η_0 and η_∞ , therefore subscript zero is used. The $\tilde{\eta}$ -transmissivity corresponds to the case when $\underline{C}(s)$ decays into maximum to the left and minimum to the right if transmissivity η is slightly above the value $\tilde{\eta}$, i.e. $\underline{C}(s)$ forms a “wave” in such case. This explains the usage of tilde sign. The transmissivity $\tilde{\eta}$ corresponds to the case when the curve $\underline{C}(s)$ “touches” the upper line $\underline{C}(s) = \log_2(2N+1)$, therefore overlining is used. Finally, the transition from the third to the second domain corresponds to the appearance of the quantity $\tilde{\eta}$, i.e. “wave” behavior of the curve $\underline{C}(s)$, therefore the tilde sign is used for supercritical parameters \tilde{N} and $\tilde{\mathcal{N}}_{\text{env}}$.

Thus, we have defined four critical transmissivities ($\tilde{\eta}$, $\tilde{\eta}$, η_0 and η_∞) and four specific values of squeezing (s_R , s_L , s_r and s_l). Similarly, by considering the family of functions $\underline{C}(s)$ parametrized by \mathcal{N}_{env} (for fixed values of η and N) or by N (for fixed values of η and \mathcal{N}_{env}), the corresponding critical values for environment thermal or input photons can be considered, respectively. All these approaches can be generalized and considered as particular cases of *critical functions*. The latter are functions of the form $\delta(\eta, N, \mathcal{N}_{\text{env}}) = 0$, where any of the parameters η , N and \mathcal{N}_{env} is critical if the others are considered to be constants. In particular, by assuming N and \mathcal{N}_{env} to be constants and using notations for critical functions

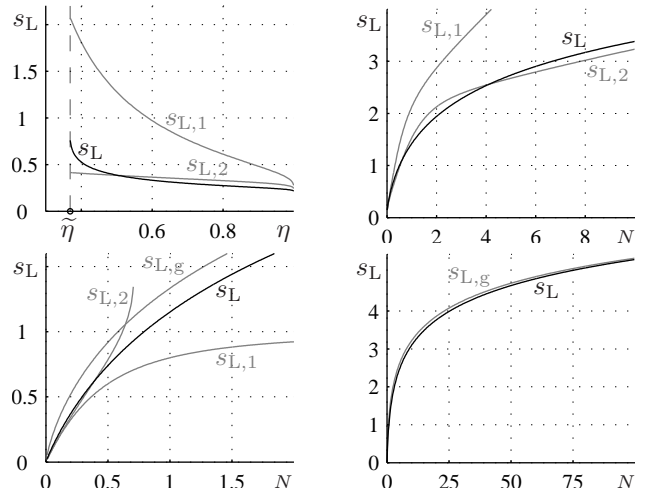


Fig. 19. Top: the dependence of the quantities s_L , $s_{L,1}$ and $s_{L,2}$ vs η (left) and vs N (right). The value the other parameters are: $N = 0.1$ and $\mathcal{N}_{\text{env}} = 0$ (left), $\eta = 0.9$ and $\mathcal{N}_{\text{env}} = 0.1$ (right). Bottom (left and right): the quantity $\lim_{\eta \rightarrow 1} s_L$ vs N (the value of \mathcal{N}_{env} was set to zero, but numerically this limit does not depend on \mathcal{N}_{env}). To the left it is plotted together with the approximations $s_{L,1}$, $s_{L,2}$, $s_{L,g} = \frac{2}{3}g(N)$, and to the right it is plotted together only with $s_{L,g} = \frac{2}{3}g(N)$ (see Eqs. (138) and (139)). Approximations $s_{L,1}$ and $s_{L,2}$ are plotted only for those values of the argument where they are applicable.

similarly to transmissivities, we get the following relations:

$$\begin{aligned} \tilde{\delta}(\tilde{\eta}, N, \mathcal{N}_{\text{env}}) &= 0, \\ \bar{\delta}(\tilde{\eta}, N, \mathcal{N}_{\text{env}}) &= 0, \\ \delta_0(\eta_0, N, \mathcal{N}_{\text{env}}) &= 0, \\ \delta_\infty(\eta_\infty, N, \mathcal{N}_{\text{env}}) &= 0. \end{aligned}$$

Now that we have introduced all necessary definitions we can discuss how $\underline{C}(s)$ is varying with the increasing of η from zero to one. As one can see from Figs.8, 9, 10 and 11 it passes in sequence the following five *regimes*:

- I. $0 < \eta \leq \tilde{\eta}$ (for the third domain one can consider η_∞ instead of $\tilde{\eta}$).

Capacity is monotonically increasing function of $s \in \mathbb{R}_+$ and tends to its universal limit (110) from the bottom. Optimal squeezing s_* is equal to ∞ . In particular, when $\eta = \tilde{\eta}$, capacity has its saddle-point for the value of squeezing $s = s_L = s_R$.

- II. $\tilde{\eta} < \eta \leq \tilde{\eta}$ (this regime does not exist for the third domain).

The saddle-point decays into two extrema – the capacity maximum to the left at the point of $s = s_L$ and the capacity minimum to the right at the point of $s = s_R$, where it is

$$\underline{C}(0) < \underline{C}(s_R) < \underline{C}(s_L) < \underline{C}(s_*) = \underline{C}(\infty).$$

Higher values of η correspond to lower values s_L and to higher values of s_R . Thus, despite we still have $s_* = \infty$, the value of $s = s_L$ could be more preferable because it is finite. When $\eta = \tilde{\eta}$, the local maximum at the point $s = s_L$ reaches the value of global maximum:

$$\underline{C}(s_L) = \underline{C}(s_*) = \underline{C}(\infty) = \log_2(2N+1).$$

III. $\bar{\eta} < \eta < \eta_0$ or $\bar{\eta} < \eta \leq \eta_\infty$ for the first and the second domains, respectively (this regime does not exist for the third domain).

Optimal squeezing s_* becomes finite and equal to s_L . Two values of squeezing s_l and s_r providing the same capacity as in the universal limit appear:

$$\underline{C}(s_l) = \underline{C}(s_r) = \underline{C}(\infty).$$

Higher values of η correspond to higher s_r and lower s_l . Capacity approaches its universal limit from the bottom: $\underline{C}(0 \ll s < \infty) < \underline{C}(s = \infty)$.

- *The first domain.* With the increasing of η the value of s_l is decreasing. It tends to zero when η tends to η_0 and then disappears (does not exist for $\eta \geq \eta_0$). The global capacity minimum for $\eta \rightarrow \eta_0 - 0$ is achieved at the value s_R .
- *The second domain.* When $\eta \rightarrow \eta_\infty$ both values of s_l and s_R tend to infinity, *i.e.*

$$\underline{C}(s_l) = \underline{C}(s_R) = \underline{C}(\infty)$$

and one of capacity extrema disappears. The global capacity minimum is still achieved at $s = 0$, therefore any squeezed environment is still more preferable.

IV. $\eta_0 \leq \eta \leq \eta_\infty$ (for the first domain) or $\eta_\infty < \eta \leq \eta_0$ (for the second and the third domains).

- *The first domain.* The capacity has two minima at values of zero and $s = s_R$, where $\underline{C}(0) > \underline{C}(s_R)$. When η tends to η_∞ , both s_l and s_R tend to infinity and the right extremum of $\underline{C}(s)$ disappears.
- *The second and the third domains.* The capacity has two minima at values of zero and infinite squeezing, where $\underline{C}(0) < \underline{C}(\infty)$. Starting from this regime it will have only one extremum for finite non-zero values of s which is maximum at $s = s_L$. When η reaches η_0 , we have

$$\underline{C}(0) = \underline{C}(\infty) = \log_2(2N + 1).$$

V. $\eta > \eta_\infty$ (for the first domain) or $\eta > \eta_0$ (for the second and the third domains).

The global capacity minimum is at infinite squeezing, *i.e.* $\underline{C}(\infty) < \underline{C}(0)$.

The notion of regime can be also clarified by considering specific values of squeezing as functions of transmissivity for fixed values of N and \mathcal{N}_{env} . In fact, one can see that these values of squeezing appear and disappear at some critical values of transmissivity which can also correspond to asymptotic lines (see Figs.12, 13 and 14). In particular, the optimal squeezing equals

$$s_* = \begin{cases} \infty, & \text{if } 0 < \eta < \eta'. \\ s_L, & \text{if } \eta' < \eta < 1, \end{cases} \quad (131)$$

where $\eta' = \bar{\eta}$ for the case of first and second domains and $\eta' = \eta_\infty$ for the case of third domain. Moreover, the optimal squeezing asymptotically tends to infinity for the case of third domain, but discontinuously jumps to infinity for first and

second domains. This transition behavior of optimal squeezing is shown in Fig.15-left and Fig.16-left, where $s_* < \infty$ is plotted as function of η for different values of \mathcal{N}_{env} and N respectively. The capacity corresponding to these finite values of s_* is plotted in Fig.15-right and Fig.16-right, respectively.

Finally, let us consider how critical transmissivities depend on N and \mathcal{N}_{env} . One can see that η_∞ does not depend on N and has non-trivial minimum for $\mathcal{N}_{\text{env}} = 0$ (see Fig.17-top-right). Then, both $\tilde{\eta}$ and $\bar{\eta}$ (we have always $\tilde{\eta} < \bar{\eta} < \eta_\infty$) are monotonically growing functions of $N \in (0, \tilde{N})$ which disappear for the values of $N \geq \tilde{N}$ and tend to η_∞ if N tends to \tilde{N} from the left. Notice, that the values of $\tilde{\eta}$ and $\bar{\eta}$ do not tend to zero for $N \rightarrow 0$ if $\mathcal{N}_{\text{env}} > 0$.

The η_0 -transmissivity is plotted vs $\ln(N + 1)$ for different values of \mathcal{N}_{env} in Fig.17-top-left. One can see that η_0 has non-trivial limits for the values of N tending to zero and infinity. These limits are plotted in Fig.17-left and Fig.17-right, respectively. It is interesting to note that the quantity $\eta_0(N \rightarrow \infty)$ also has non-trivial minimum.

The next subsections will be devoted to analytical estimation of critical and supercritical parameters as well as to estimation of the specific values of squeezing. This will eventually allow us to prove most of their properties discussed in this subsection.

C. Stationary points for capacity

Let us consider the quantities s_L , s_R , δ_∞ and $\tilde{\delta}$ analytically.

The critical function δ_∞ which characterize the behavior of the channel in the neighborhood of infinite environment squeezing $s \rightarrow \infty$ can be found as follows. We first note that only eigenvalues maximizing \underline{C} are of interest, therefore it is $\partial \underline{C} / \partial i_u = (\eta/2)\mathcal{F} = 0$, where $\mathcal{F} = 0$ is the mode transcendental equation (88). This allows us to simplify the derivative over s as

$$\frac{d\underline{C}}{ds} = \frac{\partial \underline{C}}{\partial s} + \frac{\partial \underline{C}}{\partial i_u} \frac{\partial i_u}{\partial s} = \frac{\partial \underline{C}}{\partial s}.$$

Its asymptotic behavior is

$$\frac{\partial \underline{C}}{\partial s} = \frac{[2N + 1 - (2N + 1)^{-1}] \delta_\infty}{\eta(1 - \eta)(\mathcal{N}_{\text{env}} + \frac{1}{2}) \ln 2} e^{-s},$$

where

$$\delta_\infty = (1 - \eta)^2 \left(\mathcal{N}_{\text{env}} + \frac{1}{2} \right)^2 - \frac{1}{12}. \quad (132)$$

Thus, η and \mathcal{N}_{env} are the only parameters which define how capacity tends to its universal limit (110). In particular, given a value of \mathcal{N}_{env} , the capacity tends to this limit from the top if $\eta > \eta_\infty$ and from the bottom if $\eta < \eta_\infty$, where η_∞ -transmissivity can be found from the relation

$$(1 - \eta_\infty) \left(\mathcal{N}_{\text{env}} + \frac{1}{2} \right) = \frac{1}{\sqrt{12}}. \quad (133)$$

In particular, for the vacuum environment it is

$$\eta_\infty = 1 - \frac{1}{\sqrt{3}} \approx 0.42265.$$

Analogously, if the value of η is fixed, the capacity tends to the universal limit (110) from the top or bottom depending

on the value of \mathcal{N}_{env} , which follows from Eq. (133). Consequently, this value plays a role similar to critical transmissivity if the family of curves $\underline{C}(s)$ parametrized by \mathcal{N}_{env} for fixed η and N is considered (compare the curves in Fig.5-left and Fig.5-right). It is interesting to note that this effect also exists for additive noise Gaussian channel where the quantity \mathcal{N}_{env} has the same meaning and its critical value equals $1/\sqrt{12}$ [34]. Thus, the critical parameters and the behavior shown in Fig.5 may be relevant for a general Gaussian channel.

In order to specify the region where environment squeezing increases the capacity, in the following we estimate the values of s corresponding to extrema of function $\underline{C}(s)$. Let us consider the system of equations $\partial\underline{C}/\partial s = 0$, $\partial\underline{C}/\partial i_u = 0$ taken for the eigenvalues maximizing \underline{C} and belonging to the second stage (extremum cannot be in the third stage since $\partial\underline{C}/\partial s \neq 0$ according to Eq. (76)). Its solution results to the value $i_u = N + 1/2$ and the value of s defined by the equation

$$\mathcal{P}(s) = 0, \quad (134)$$

where

$$\mathcal{P} = \frac{g_1(\bar{\nu})}{\bar{\nu}^2} \sinh s - \frac{g_1(\nu)}{\nu^2} \frac{\sinh(s - \ln(2N + 1))}{2N + 1}.$$

Thus, we have the same value of i_u for both local extrema of $\underline{C}(s)$ and the point of $s = \infty$.

Solving Eq. (134) in neighborhood of zero or infinite values of s one can estimate both its roots (s_L and s_R). In particular, after the expansion of Eq. (134) in powers of e^{-s} in the neighborhood of $s \rightarrow \infty$, where terms higher than the second order are neglected, it takes the form $z_2(e^{-s}) = 0$ with $z_2(e^{-s}) = be^{-2s} + ce^{-s}$ (b and c are some constants). The function $z_2(e^{-s})$ is the partial sum for Laurent series of the function $Z(e^{-s})$, where $Z = 0$ is the equation (134). Both functions $z_2(e^{-s})$ and $Z(e^{-s})$ are concave in the neighborhood of $s \rightarrow \infty$ (see Fig.18-top-right), therefore their nontrivial²⁶ roots are close each other. The latter property explains why the approximation $z_2(e^{-s}) = 0$ is applicable and leads to the result

$$s_R = \ln \frac{[1 + (2N + 1)^2] [\delta_\infty^2 + \frac{1}{180}] - \frac{\eta^2}{6} [N + \frac{1}{2}]^2}{\eta(1 - \eta)(N + \frac{1}{2})(\mathcal{N}_{\text{env}} + \frac{1}{2})\delta_\infty}, \quad (135)$$

where critical function δ_∞ is given by Eq. (132) and characterizes the ‘‘criticality’’ of the given channel parameters (their vicinity to the transition point). Notice, that according to estimation (135) we have

$$\lim_{\eta \rightarrow \eta_\infty} s_R = \lim_{\delta_\infty \rightarrow 0} s_R = \infty.$$

Analogously, considering the next order approximation for Eq. (134), one can construct the function $z_3(e^{-s}) = ae^{-3s} + be^{-2s} + ce^{-s}$ and find the condition when both nontrivial roots of the equation $z_3(e^{-s}) = 0$ coincide. This is the case of $s_L = s_R$ (both s_L and s_R are taken from approximation z_3 , see Fig.18), *i.e.* the saddle-point of the curve $\underline{C}(s)$ where both the derivatives $\partial\underline{C}/\partial s$ and $\partial^2\underline{C}/\partial s^2$ equal zero. In Subsec.V-H this approach will be used in order to provide analytical estimation of the saddle-point transmissivity $\tilde{\eta}$.

²⁶The trivial solution which we imply is $e^{-s} = 0$ corresponding to $s = \infty$.

Similarly, expanding Eq. (134) in powers of s in the neighborhood of $s = 0$ we get an equation of the form $as^3 + bs^2 + cs = 0$ (a , b and c are some constants depending on channels parameters), whose nontrivial root is an estimation for the left extremum s_L (see Subsec. V-D for its value and derivation).

Analyzing the equation $\underline{C}(s) = 0$ instead of Eq. (134) and applying the same method (expansion in powers of e^{-s} in the neighborhood of $s = \infty$ and in powers of s in the neighborhood of $s = 0$) one can estimate both left (s_l) and right (s_r) roots. In particular, one can get the relation

$$s_r = s_R - \ln 2.$$

Estimation of s_l is given in Subsec. V-F. The case when s_l and s_r (considered for this approximation) coincide corresponds to $\tilde{\eta}$ -transmissivity, which is estimated below in Subsec.V-H.

D. Estimation of s_L

Let us estimate the quantity s_L . Our purpose is to solve Eq. (134) in the neighborhood of $s = 0$ taking into account that all eigenvalues in extrema points are known. At first, notice that squares of symplectic eigenvalues as functions of s in the extrema points read

$$\begin{aligned} \nu_e^2(s) &= \Omega \left[\frac{\eta}{2}, (1 - \eta) \left(\mathcal{N}_{\text{env}} + \frac{1}{2} \right), s - \ln(2N + 1) \right], \\ \bar{\nu}_e^2(s) &= \Omega \left[\eta \left(N + \frac{1}{2} \right), (1 - \eta) \left(\mathcal{N}_{\text{env}} + \frac{1}{2} \right), s \right], \end{aligned}$$

where

$$\Omega(a, b, \varphi) := a^2 + b^2 + 2ab \cosh(\varphi).$$

Below we use the notations $\nu_{e,0} = \nu_e(0)$ and $\bar{\nu}_{e,0} = \bar{\nu}_e(0)$. Let us define the function

$$\mathcal{Y}(x_1, x_2) = \frac{x_1}{\nu_{e,0}^2} + \frac{x_2}{(\nu_{e,0}^2 - \frac{1}{4}) g_1(\nu_{e,0})}$$

and introduce the following notations:

$$\begin{aligned} \mathcal{X} &:= \frac{\eta}{2}(1 - \eta) \left(\mathcal{N}_{\text{env}} + \frac{1}{2} \right), \\ \text{cn} &:= \cosh(\ln(2N + 1)), \\ \text{sn} &:= \sinh(\ln(2N + 1)). \end{aligned}$$

By representing Eq. (134) as $\mathcal{P}(s) = as^2 + bs + c = 0$ we can find both linear (supposing $a = 0$) and quadratic ($a \neq 0$) approximations. They result as estimations of squeezing in left extremum of $C(s)$ (denoted as $s_{L,1}$ for linear approximation and $s_{L,2}$ for quadratic one):

$$s_{L,1}^{-1} = \mathcal{K}_1, \quad s_{L,2}^{-1} = \frac{1}{2} \left(\sqrt{\mathcal{K}_1^2 - 2\mathcal{K}_2 + \mathcal{K}_1} \right),$$

where

$$\begin{aligned} \mathcal{K}_1 &= \frac{\text{cn}}{\text{sn}} - \mathcal{X}\mathcal{Y}(1, 1) \text{sn} - \frac{(2N + 1) \nu_{e,0}^2 g_1(\bar{\nu}_{e,0})}{\text{sn} \bar{\nu}_{e,0}^2 g_1(\nu_{e,0})}, \\ \mathcal{K}_2 &= 1 - 3\mathcal{X}\mathcal{Y}(1, 1) \text{cn} + \text{sn}^2 \mathcal{X}^2 \mathcal{Y} \left(3\mathcal{Y}(1, 1), \frac{2}{\nu_{e,0}^2 - \frac{1}{4}} \right). \end{aligned} \quad (136)$$

(137)

Approximation $s_{L,1}$ is applicable only if $\mathcal{K}_1 > 0$ and $s_{L,2}$ is applicable only if $\mathcal{K}_1^2 > 2\mathcal{K}_2$ (it is equivalent to $N < (\sqrt{2})^{-1}$ if $\eta \rightarrow 1$). These regions of applicability follow from the condition that proper equations must have their roots positive.

Let us consider the limit $\lim_{\eta \rightarrow 1} s_L$. First, note that both second and third terms in relations Eq. (136) and (137) disappear when $\eta \rightarrow 1$, therefore we have

$$\lim_{\eta \rightarrow 1} s_{L,1} = \frac{\text{sn}}{\text{cn}} = \frac{2N(N+1)}{2N(N+1)+1} = \frac{1}{1+\phi_{s_L}}, \quad (138)$$

where

$$\phi_{s_L} = \frac{1}{2N(N+1)}.$$

The quantity $\lim_{\eta \rightarrow 1} s_{L,1}$, in turn, tends to 1 for $N \rightarrow \infty$ and to zero for $N \rightarrow 0$. Analogously,

$$\lim_{\eta \rightarrow 1} s_{L,2}^{-1} = \frac{1}{2} \left(1 + \phi_{s_L} + \sqrt{\phi_{s_L}^2 + 2\phi_{s_L} - 1} \right). \quad (139)$$

Notice, that the approximations (138) and (139) do not depend on thermal photons \mathcal{N}_{env} . This is an argument in support of the behavior observed numerically in Fig.15 for the exact limit.

The dependence of s_L and its approximation from parameters is shown in Fig.19. One can see that s_L is monotonically decreasing function of η , which indeed has non-trivial limit for $\eta \rightarrow 1$.

E. Estimation of η_0

As it follows from a definition 7 the transmissivity η_0 is given by the equation

$$\mathcal{O}(\eta) = 0, \quad (140)$$

where

$$\mathcal{O}(\eta) := g[\eta N + (1-\eta)\mathcal{N}_{\text{env}}] - g[(1-\eta)\mathcal{N}_{\text{env}}] - \log_2(2N+1). \quad (141)$$

Note that for $s = 0$ we have the case of the third stage and $N_{\text{env}} = \mathcal{N}_{\text{env}}$.

We can have the following cases: $\eta_0 < \eta_\infty$ (see Fig.8), $\eta_0 > \eta_\infty$ (see Fig.9) and $\eta_0 = \eta_\infty$. The latter case corresponds to transition from first to second domain and defines the locus $(N, \mathcal{N}_{\text{env}})$ where equality $\eta_0 = \eta_\infty$ holds. One can see from Fig.11-bottom-right that the limit value $\mathcal{N}_{\text{env}} = \mathcal{N}_{\text{env},0}$, which still can have $\eta_0 = \eta_\infty$ is achieved at $N = 0$. However, since Eq. (140) is satisfied by any values of η and \mathcal{N}_{env} if $N = 0$, we have to solve it for the limit $N \rightarrow 0$. By expanding Eq. (140) over N we get equation $N\partial\mathcal{O}/\partial N = 0$. Then, by substituting $N = 0$ into $\partial\mathcal{O}/\partial N = 0$ we get the equation

$$\eta_0 \ln \left(1 + \frac{1}{(1-\eta_0)\mathcal{N}_{\text{env}}} \right) = 2. \quad (142)$$

The joint solution of the system of Eqs. (142), (133) and $\eta_0 = \eta_\infty$ results to the equation

$$\left(1 - \frac{1}{\sqrt{3}(2\mathcal{N}_{\text{env}}+1)} \right) \ln \left(1 + \frac{\sqrt{3}(2\mathcal{N}_{\text{env}}+1)}{\mathcal{N}_{\text{env}}} \right) = 2.$$

Its solution is the supercritical value

$$\mathcal{N}_{\text{env},0}(N=0) \approx 0.0204.$$

1) *Limit values of \mathcal{N}_{env}* : For high values of \mathcal{N}_{env} Eq. (140) has its asymptotic behavior given by the relation

$$\log_2 \frac{\eta N + (1-\eta)\mathcal{N}_{\text{env}} + \frac{1}{2}}{(1-\eta)\mathcal{N}_{\text{env}} + \frac{1}{2}} = \log_2(2N+1),$$

from which one can get

$$(1-\eta)(1+2\mathcal{N}_{\text{env}}) = 0,$$

i.e.

$$\lim_{\mathcal{N}_{\text{env}} \rightarrow \infty} \eta_0 = 1. \quad (143)$$

In the case of pure (i.e. $\mathcal{N}_{\text{env}} = 0$) environment η_0 is equal to (see Eq. (140))

$$\eta_0 = \frac{1}{N} g^{-1}[\log_2(2N+1)]. \quad (144)$$

In turn, by supposing $\eta_0 = \eta_\infty$ we get the equation for N

$$\frac{1}{N} g^{-1}[\log_2(2N+1)] = 1 - \frac{1}{\sqrt{3}},$$

whose solution is supercritical value

$$N_0(\mathcal{N}_{\text{env}} = 0) \approx 0.0817.$$

Thus, $\eta_0 > \eta_\infty$ if $N > N_0(0)$, and $\eta_0 < \eta_\infty$ if $N < N_0(0)$ (see examples in Figs. 8, 9 and 10). In other words, if and only if $N \geq N_0(0)$, we have

$$\forall s \quad C(s, \eta \geq \eta_0) \geq \log_2(2N+1).$$

In particular, if the environment is pure, $\eta > \eta_0$ and $N \geq N_0(0)$, then the universal limit gives the global minimum for $C(s)$, and s_L gives the global maximum:

$$\begin{aligned} \min_{0 \leq s \leq \infty} C(s) &= \log_2(2N+1), \\ \max_{0 \leq s \leq \infty} C(s) &= C(s_L). \end{aligned}$$

2) *The case $N \rightarrow 0$* : By considering Eq. (142) for $\mathcal{N}_{\text{env}} \gg 0$ we obtain, to linear approximation in $\mathcal{N}_{\text{env}}^{-1}$, that

$$\lim_{N \rightarrow 0} \eta_0(\mathcal{N}_{\text{env}} \gg 0) = \frac{2\mathcal{N}_{\text{env}}}{2\mathcal{N}_{\text{env}}+1}. \quad (145)$$

Using Eq. (144) we get for pure environment

$$\lim_{N \rightarrow 0} \eta_0(\mathcal{N}_{\text{env}} = 0) = 0.$$

3) *The case $N \rightarrow \infty$* : By taking the limit $N \rightarrow \infty$ in Eq. (140) (we use expansion of g -function) one can get that it is equivalent to

$$\log_2 \frac{\eta e}{2} - g[(1-\eta)\mathcal{N}_{\text{env}}] = 0. \quad (146)$$

In particular, for pure environment we get

$$\lim_{N \rightarrow \infty} \eta_0(\mathcal{N}_{\text{env}} = 0) = \frac{2}{e}. \quad (147)$$

The function $g(x)$ behaves like $-x \log_2 x$ for small values of x . Using this property and expanding the logarithm in the first term of Eq. (146) in powers of $\varepsilon := 1-\eta$ up to the first order one can obtain the equation

$$\ln \frac{e}{2} - \varepsilon + \varepsilon \mathcal{N}_{\text{env}} \ln(\varepsilon \mathcal{N}_{\text{env}}) = 0.$$

Its solution gives an estimation of $\lim_{N \rightarrow \infty} \eta_0$:

$$\lim_{N \rightarrow \infty} \eta_0 = 1 - \left[\mathcal{N}_{\text{env}} W_{-1} \left(e^{-\mathcal{N}_{\text{env}}^{-1}} \ln \frac{2}{e} \right) \right]^{-1} \ln \frac{2}{e}, \quad (148)$$

where W_{-1} is -1 branch of Lambert W function which is solution of $W(z)e^{W(z)} = z$ and whose properties are well known [37]. One can show that the approximation (148) has the limits

$$\begin{aligned} \lim_{\mathcal{N}_{\text{env}} \rightarrow \infty} \lim_{N \rightarrow \infty} \eta_0 &= 1, \\ \lim_{\mathcal{N}_{\text{env}} \rightarrow 0} \lim_{N \rightarrow \infty} \eta_0 &= \ln 2. \end{aligned} \quad (149)$$

The first limit coincides with the exact value (see Eq. (143)), but the second one is different (see Eq. (147)). Maximal error of estimation (148) is about 5% and achieved by $\mathcal{N}_{\text{env}} = 0$. As far as $\lim_{N \rightarrow \infty} \eta_0$ is monotonic over \mathcal{N}_{env} (see Eq. (148)), Eq. (147) gives its minimum:

$$\lim_{N \rightarrow \infty} \eta_0 \geq \frac{2}{e}.$$

Eq. (149) can be obtained as follows. First, note that the following limit holds:

$$\lim_{z \rightarrow 0-0} \frac{\ln(-z)}{W_{-1}(z)} = 1. \quad (150)$$

It can be obtained by applying logarithm to both parts of equation

$$-W_{-1}(z)e^{W_{-1}(z)} = -z, \quad z < 0,$$

and then dividing it on $W_{-1}(z)$. Notice, that $W_{-1}(z) < 0$ for $z \in [-e^{-1}, 0]$ and has the limit

$$\lim_{z \rightarrow 0-0} W_{-1}(z) = -\infty.$$

Let us define a new variable $x < 0$ to be equal to the argument of W_{-1} in Eq. (148) and consider the limit of Eq. (148) for $x \rightarrow 0 - 0$ which corresponds to $\mathcal{N}_{\text{env}} \rightarrow 0$. Taking into account Eq. (150), we arrive at the result (149).

The dependence of η_0 on parameters is shown in Fig.17.

F. Estimation of s_1

The definition $C(s_1) = \log_2(2N + 1)$ results to

$$\cosh s_l = \frac{g^{-1} \left[\log_2(2N + 1) + g((1 - \eta) \mathcal{N}_{\text{env}}) \right] - \eta \left(N + \frac{1}{2} \right) + \frac{1}{2}}{(1 - \eta) \left(\mathcal{N}_{\text{env}} + \frac{1}{2} \right)},$$

which for pure environment reads

$$\cosh s_l = 1 + \frac{2N(\eta_0 - \eta)}{1 - \eta}, \quad (151)$$

where $\eta_0 = \eta_0(\mathcal{N}_{\text{env}} = 0)$ is given by Eq. (144). In particular, it is clear from Eq. (151) that

$$\lim_{\eta \rightarrow \eta_0 - 0} s_1 = 0,$$

which is in full correspondence with the definition and properties of s_1 .

G. Full channel characterization

Let us summarize the results that we obtained for channel characterization. We started from the point that squeezing s is the only parameter which gives rise to non-monotonic dependence of capacity \underline{C} . We have analyzed this behavior for typical values of N and \mathcal{N}_{env} (see Fig.5) and found that $\underline{C}(s)$ has maximum in the interval $0 < s < \infty$ if $\eta > \eta_\infty$, and is monotonic otherwise. Then, we have shown that the family of curves $\underline{C}(s)$ can be considered also for different values of \mathcal{N}_{env} and fixed η . Both these cases can be described using the parameter δ_∞ (see Eq. (132)). Thus, we get the pair of parameters $(\eta_\infty, \mathcal{N}_{\text{env}})$ characterizing the behavior of $\underline{C}(s)$ in the neighborhood of infinity. Then, we considered also other critical parameters, namely, $\tilde{\eta}$, $\bar{\eta}$ and η_0 by analyzing the family of curves $\underline{C}(s)$ for different values of η and fixed \mathcal{N}_{env} . However, by considering the family of curves $\underline{C}(s)$ for different values of \mathcal{N}_{env} (or N) and fixed η one can also introduce analogous critical parameters as the values of \mathcal{N}_{env} (or N). Hence, we finally have four triads of critical parameters to characterise the channel. After that we have analyzed how these critical parameters depend on N and \mathcal{N}_{env} by introducing supercritical parameters.

On the other hand, one can also say that critical parameters have allowed us to split the total space $(0 \leq \eta \leq 1, 0 \leq N \leq \infty, 0 \leq \mathcal{N}_{\text{env}} \leq \infty)$ into *regimes* with different properties of the dependence $\underline{C}(s)$, while supercritical parameters have allowed us to split the total space $(0 \leq N \leq \infty, 0 \leq \mathcal{N}_{\text{env}} \leq \infty)$ into *domains* with different properties of the critical parameters. Finally, note, that given the type of domain, regime and stage for parameters $\eta, N, \mathcal{N}_{\text{env}}$, one can qualitatively plot the family of curves $\underline{C}(s)$ (for different values of η) without numerical calculations and put forward all important points and extrema of these curves.

This classification completely characterises the role of environment squeezing. E.g. ‘‘supernonmonotonic’’ behavior of $\underline{C}(s)$ (when it has two extrema in the interval $0 < s < \infty$) is only possible in the first and the second domains, as in the third domain $\underline{C}(s)$ has at maximum a single extremum. Most of practically interesting channel parameters belong to the third domain, however, this classification is useful, as it provides exact conditions *when it is so* (expected behavior of $\underline{C}(s)$ from the third domain). The global optimal squeezing s_* has sudden jump to infinity at $\bar{\eta}$ in the first and second domain, but tends asymptotically to infinity in the third domain.

It is quite nontrivial that despite this difficult classification scheme the existence of supercritical parameters can be shown analytically (see Subsec. V-H). Moreover, in some important cases they can be found exactly and analytically (be expressed through radicals). Thus, despite we have started from numerical analysis of the dependence $\underline{C}(s)$, there are analytical results which support the found properties (see Subsec.V-H).

H. Supercritical parameters

First, we have to remember that $\tilde{\eta}$ tends to η_∞ when channel passes from second to third domain (see Fig.17-top-right). In

particular, the limits

$$\lim_{(N, \mathcal{N}_{\text{env}}) \rightarrow (\tilde{N}, \tilde{\mathcal{N}}_{\text{env}})} \lim_{\eta \rightarrow \tilde{\eta}^+} s_L(\eta) = \infty, \quad (152)$$

$$\lim_{(N, \mathcal{N}_{\text{env}}) \rightarrow (\tilde{N}, \tilde{\mathcal{N}}_{\text{env}})} \lim_{\eta \rightarrow \tilde{\eta}^+} s_R(\eta) = \infty \quad (153)$$

are supported by numerical calculations (here the notation “ $(N, \mathcal{N}_{\text{env}}) \rightarrow (\tilde{N}, \tilde{\mathcal{N}}_{\text{env}})$ ” means that we consider the values $(N, \mathcal{N}_{\text{env}})$ belonging to the second domain and tending to the border between second and third domain). The relations (152) and (153) are equivalent to the following statement: the value of squeezing corresponding to saddle-point transmissivity tends to infinity if the values of the channel parameters $(N, \mathcal{N}_{\text{env}})$ tend to those from the third domain. Consequently, in this case the quantities e^{-s_L}, e^{-s_R} tend to zero. Thus, we can say that the transition between second and third domain is completely characterized by the behavior of the function (134) in the neighborhood of the point $e^{-s} = 0$ (remember, that e^{-s_L} and e^{-s_R} are zeros of the function (134)). Let us now consider the Taylor expansion of (134) in the neighborhood of that point. To the third order it gives rise to the relation

$$ae^{-3s} + be^{-2s} + ce^{-s} = 0 \quad (154)$$

which is an approximate form of Eq. (134) in the neighborhood of $e^{-s} = 0$. Remember, that the coefficient c is proportional to δ_∞ (see Eq. (132)) and defines the transition from “undercritical” to “uppercritical” parameters of transmissivity and thermal photons. If we neglect a constant factor, c is just a denominator of the fraction under logarithm in s_R (see Eq. (135)). The case when $\tilde{\eta}$ disappears corresponds to the case when the function (134) has no roots in the neighborhood of $e^{-s} = 0$ except of the point $e^{-s} = 0$ itself. As far as (134) in this neighborhood is the polynomial (154), this condition is equivalent to the statement that this polynomial has no other extrema except of the point $e^{-s} = 0$. It is exactly so if both $b = c = 0$. Thus, by substituting $\delta_\infty = 0$ and $\eta = \eta_\infty$ in the relation $b = 0$ (up to a constant factor b is a numerator in the fraction under logarithm of Eq. (135)) we get

$$\frac{1 + (2N + 1)^2}{180} - \frac{1}{6} \left[\left[1 - \frac{1}{\sqrt{3}(2\mathcal{N}_{\text{env}} + 1)} \right] \left[N + \frac{1}{2} \right] \right]^2 = 0.$$

This relation between the values of N and \mathcal{N}_{env} is that defined by the function $\tilde{f}(\tilde{N}, \tilde{\mathcal{N}}_{\text{env}}) = 0$, therefore it can be rewritten as (see the parallelism with relation (133))

$$(1 - \tilde{\eta}_\infty) \left(\tilde{\mathcal{N}}_{\text{env}} + \frac{1}{2} \right) = \frac{1}{\sqrt{12}},$$

where the *effective supercritical transmissivity* $\tilde{\eta}_\infty$ is

$$\tilde{\eta}_\infty = \sqrt{\frac{2}{15} \left(\frac{1}{(2\tilde{N} + 1)^2} + 1 \right)}.$$

The quantity $\tilde{\mathcal{N}}_{\text{env}}$ as function of \tilde{N} was plotted in Fig.11-bottom-right. Finally, let us write down explicitly the above

supercritical values for the particular important cases:

$$\tilde{\mathcal{N}}_{\text{env}}(\tilde{N} = 0) = \frac{1}{2} \left[\left(\sqrt{3} - \frac{2}{\sqrt{5}} \right)^{-1} - 1 \right] \approx 0.0969, \quad (155)$$

$$\tilde{N}(\tilde{\mathcal{N}}_{\text{env}} = 0) = \frac{1}{2} \left[\sqrt{\frac{3}{2} + \frac{5}{2\sqrt{3}}} - 1 \right] \approx 0.3578 \quad (156)$$

where the value (155) is the maximum amount of thermal photons admissible in environment which still allows to obtain effects from first and second domain (e.g., existence of saddle-point transmissivity), and the value (156) is the maximum amount of input photons which still allows to observe the same behavior. These are fundamental constants of lossy bosonic channel providing its description on the top level of “hierarchy of characterization”.

Remember, that Eq. (134) (and hence its approximation (154)) is the derivative of the equation $\underline{C}(s) = 0$. Therefore, the analogous expansion of equation $\underline{C}(s) = 0$ in the neighborhood of $s \rightarrow \infty$ has the form

$$\mathfrak{A}e^{-3s} + \mathfrak{B}e^{-2s} + \mathfrak{C}e^{-s} + \log_2(2N + 1) = 0, \quad (157)$$

where $\mathfrak{C} = -c$, $\mathfrak{B} = -\frac{b}{2}$ and $\mathfrak{A} = -\frac{a}{3}$. Eq. (157) allows to interpret both critical and supercritical parameters in the same framework. In particular, zero-order coefficient $\log_2(2N + 1)$ is the universal limit (110), zero-equal linear coefficient ($\mathfrak{C} = 0$) defines critical parameter η_∞ , and if both linear and quadratic coefficients are zero ($\mathfrak{C} = \mathfrak{B} = 0$) we get supercritical parameters \tilde{N} and $\tilde{\mathcal{N}}_{\text{env}}$. In explicit form they read

$$\underline{C} = K_0 + K_1 x + K_2 x^2 + K_3 x^3,$$

$$K_0 = \log_2(2N + 1),$$

$$K_1 = T_1 \delta_\infty,$$

$$K_2 = T_2 \left[(1 + M^2) \left(\delta_\infty^2 + \frac{1}{180} \right) - \frac{\eta^2 M^2}{24} \right],$$

$$K_3 = T_3 \left[(1 + M^2 + M^4) \left(\delta_\infty^3 + \frac{\delta_\infty}{60} - \frac{1}{3780} \right) + (1 + M^2) \left(\frac{1}{60} - \frac{\delta_\infty}{4} \right) \frac{\eta^2 M^2}{4} - \frac{\eta^4 M^4}{64} \right],$$

where $M := 2N + 1$ and

$$T_j := \frac{2N(N + 1)(-1)^j}{j \left[\eta(1 - \eta) \left(N + \frac{1}{2} \right) \left(\mathcal{N}_{\text{env}} + \frac{1}{2} \right) \right]^j \ln 2}$$

with $j = 1, 2, 3$. The equation (discriminant) $K_2^2 - 4K_1K_3 = 0$ can be rewritten as

$$\begin{aligned} & (1 + M^4) \left(\frac{1}{900} + \frac{16}{315} \delta_\infty - \frac{14}{5} \delta_\infty^2 - 156 \delta_\infty^4 \right) \\ & + M^2 \left(\frac{1}{450} + \frac{16}{315} \delta_\infty - \frac{12}{5} \delta_\infty^2 - 120 \delta_\infty^4 \right) \\ & - \eta^2 M^2 (1 + M^2) \left(\frac{1}{60} + \frac{4}{5} \delta_\infty - 9 \delta_\infty^2 \right) \\ & + \eta^4 M^4 \left(\frac{1}{16} + 3 \delta_\infty \right) = 0, \end{aligned}$$

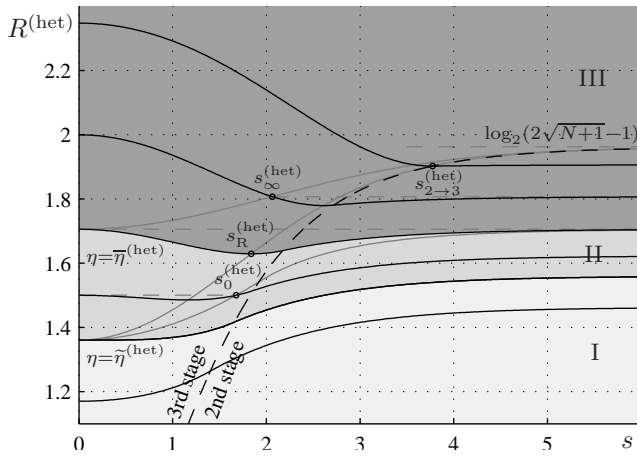


Fig. 20. Heterodyne rate $R^{(\text{het})}$ (black) vs s for the values of η equal to 0.4, 0.4774, 0.5356, 0.623, 0.75, 0.9 (from bottom to top). The values of other parameters are $N = 5$, $\mathcal{N}_{\text{env}} = 1$. The grey curves are the loci $(s_0^{(\text{het})}(\eta), R^{(\text{het})}(s_0^{(\text{het})}(\eta)))$, $(s_R^{(\text{het})}(\eta), R^{(\text{het})}(s_R^{(\text{het})}(\eta)))$ and $(s_\infty^{(\text{het})}(\eta), R^{(\text{het})}(s_\infty^{(\text{het})}(\eta)))$ where parameter η is varying over whole definitional domain of the quantities $s_0^{(\text{het})}$, $s_R^{(\text{het})}$ and $s_\infty^{(\text{het})}$, respectively. Dotted balck curve divide this quadrant into areas corresponding to different stages. The curves $R^{(\text{het})}(s)$ corresponding to the same regime have the same gray background color (the higher the regime the darker the color).

$$D = K_1' x + K_2'^2 x^2 + K_3'^3 x^3,$$

$$K_j' = -\frac{j}{\eta(1-\eta)(N+\frac{1}{2})(\mathcal{N}_{\text{env}}+\frac{1}{2})} K_j.$$

The equation (discriminant) $K_2'^2 - 4K_1'K_3' = 0$ can be rewritten as

$$(1+M^4) \left(\frac{1}{900} + \frac{4}{105} \delta_\infty - 2\delta_\infty^2 - 108\delta_\infty^4 \right) + M^2 \left(\frac{1}{450} + \frac{4}{105} \delta_\infty - \frac{8}{5} \delta_\infty^2 - 72\delta_\infty^4 \right) - \eta^2 M^2 (1+M^2) \left(\frac{1}{60} + \frac{3}{5} \delta_\infty - 6\delta_\infty^2 \right) + \eta^4 M^4 \left(\frac{1}{16} + \frac{9}{4} \delta_\infty \right) = 0.$$

Roots of these discriminants provide approximations for the quantities $\tilde{\eta}$ and $\bar{\eta}$.

Notice, that all of these results (universal limit, critical and supercritical parameters) are given by exact explicit analytical relations.

In turn, the supercritical parameters N_0 and $\mathcal{N}_{\text{env},0}$ are found in Appendix V-E, where the values

$$N_0(\mathcal{N}_{\text{env},0} = 0) \approx 0.0817,$$

$$\mathcal{N}_{\text{env},0}(N_0 = 0) \approx 0.0204$$

are obtained as numerical solutions of a transcendental equations.

I. Critical parameters for heterodyne rate

Let us analyze the behavior of the function $R^{(\text{het})}(s)$ versus s (below the argument of $R^{(\text{het})}$ is assumed to be s) for different values of η and fixed \mathcal{N}_{env} (see Fig.20). By solving

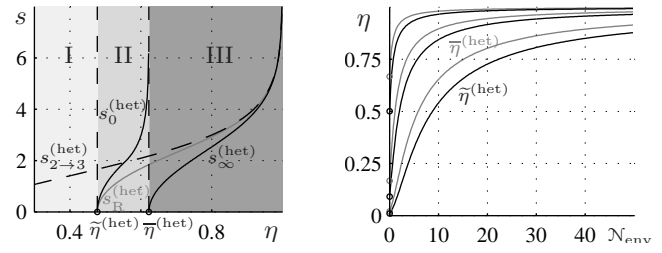


Fig. 21. Left: The quantities $s_{2 \rightarrow 3}^{(\text{het})}$, $s_0^{(\text{het})}$, $s_\infty^{(\text{het})}$ (black) and $s_R^{(\text{het})}$ (grey) are plotted vs η for $N = 5$, $\mathcal{N}_{\text{env}} = 1$. Right: $\tilde{\eta}^{(\text{het})}$ and $\bar{\eta}^{(\text{het})}$ are plotted vs \mathcal{N}_{env} for the values of N equal to 1, 10, 100 (from top to bottom).

Eq. $\partial R^{(\text{het})}/\partial s = 0$ in the third stage (see Eq. (77)), one can show that $R^{(\text{het})}(s)$ is monotonically increasing function if transmissivity belongs to the interval²⁷ $0 < \eta \leq \tilde{\eta}^{(\text{het})}$ (we will call this the *first regime* analogously to capacity), where

$$\tilde{\eta}^{(\text{het})} = \left[(2\mathcal{N}_{\text{env}} + 1)^2 + N - \sqrt{N^2 + (2N + 1)(2\mathcal{N}_{\text{env}} + 1)^2} \right] \times \left[2\mathcal{N}_{\text{env}}(2\mathcal{N}_{\text{env}} + 1) \right]^{-1}, \quad (158)$$

which is equal to $(N + 1)^{-1}$ in the case of squeezed vacuum state (one needs to take the limit $\mathcal{N}_{\text{env}} \rightarrow 0$ in Eq. (158)). Then, by equating the heterodyne values taken for $s = 0$ and $s = \infty$ (see Eqs. (78) and (111)), we obtain the corresponding transmissivity value

$$\bar{\eta}^{(\text{het})} = \left[8\mathcal{N}_{\text{env}}(\mathcal{N}_{\text{env}} + 1) + N + 2 - \sqrt{(N + 2)^2 + 16\mathcal{N}_{\text{env}}(\mathcal{N}_{\text{env}} + 1)(N + 1)} \right] \times \left[4\mathcal{N}_{\text{env}}(2\mathcal{N}_{\text{env}} + 1) \right]^{-1}, \quad (159)$$

which becomes $2(N + 2)^{-1}$ in the case of $\mathcal{N}_{\text{env}} = 0$. The latter can be obtained by taking the limit $\mathcal{N}_{\text{env}} \rightarrow \infty$ in Eq. (159) or by equating the relations $\log_2(1 + \eta N)$ and (111).

If $\tilde{\eta}^{(\text{het})} < \eta \leq \bar{\eta}^{(\text{het})}$ (the *second regime*), one can consider squeezing value $s_0^{(\text{het})}$ defined by the equality $R^{(\text{het})}(s_0^{(\text{het})}) = R^{(\text{het})}(0)$. In the second stage it equals

$$s_0^{(\text{het})} = \ln \left[1 + 2\eta N \left[\phi_0^{(\text{het})} \right]^{-1} \times \left\{ \left(2 \left[\phi_0^{(\text{het})} \right]^{-1} + 1 \right) \left(2\eta \left[\phi_0^{(\text{het})} \right]^{-1} - 1 \right) - N \right\}^{-1} \right],$$

where $\phi_0^{(\text{het})}$ is defined similarly to ϕ_0 (see Eq. (82)) as the value of $\phi^{(\text{het})}$ (see Eq. (96)) taken in the point $s = 0$. In explicit form $\phi_0^{(\text{het})}$ reads

$$\phi_0^{(\text{het})} = \frac{2\eta}{1 + (1 - \eta)(2\mathcal{N}_{\text{env}} + 1)}$$

²⁷Notations for critical parameters of heterodyne rate are chosen to be similar to those for capacity if saddle-point is imagined at $s = 0$.

In the third stage $s_0^{(\text{het})}$ is given by the relation

$$s_0^{(\text{het})} = \text{arcosh}[\eta N F_0 - 1],$$

where

$$F_0 = \frac{8 \left[N - \left(\eta \left[\phi_0^{(\text{het})} \right]^{-1} - 1 \right) \left(2 \left[\phi_0^{(\text{het})} \right]^{-1} + 1 \right) \right]}{\eta \left(2\eta \left[\phi_0^{(\text{het})} \right]^{-1} - 1 \right) \left(2 \left[\phi_0^{(\text{het})} \right]^{-1} + 1 \right)^2}.$$

One can show that $s_0^{(\text{het})} \rightarrow \infty$ if $\eta \rightarrow \bar{\eta}^{(\text{het})} - 0$, and $s_0^{(\text{het})} \rightarrow 0$ if $\eta \rightarrow \bar{\eta}^{(\text{het})} + 0$ (see also Fig.21). If the environment is pure ($\mathcal{N}_{\text{env}} = 0$), $s_0^{(\text{het})}$ can be rewritten as

$$s_0^{(\text{het})} = \ln \frac{(1 - \eta)(\eta N + 2)}{2 - \eta(N + 2)}$$

in second stage and as

$$s_0^{(\text{het})} = \text{arcosh} \frac{\eta^2(2N + 1)^2 - (1 - \eta)^2 - 1}{2(1 - \eta)}$$

in third stage.

Analogously, if $\bar{\eta}^{(\text{het})} < \eta \leq 1$ (the *third regime*), one can consider the quantity $s_\infty^{(\text{het})}$, such that $R^{(\text{het})}(s_\infty^{(\text{het})}) = R^{(\text{het})}(\infty)$. Due to the monotonicity of $R^{(\text{het})}(s)$ in the second stage, the value $s_\infty^{(\text{het})}$ can only correspond to the third stage, and it is equal to

$$s_\infty^{(\text{het})} = \text{arcosh} \left[F_\infty \phi_0 - \sqrt{1 + 4\eta F_\infty} \right],$$

where

$$F_\infty = N + \frac{1 + \eta}{2} - \sqrt{\eta N + \left(\frac{1 + \eta}{2} \right)^2}.$$

In particular, we have the limits

$$\lim_{\eta \rightarrow \bar{\eta}^{(\text{het})} + 0} s_\infty^{(\text{het})} = 0$$

and

$$\lim_{\eta \rightarrow 1} s_\infty^{(\text{het})} = \infty.$$

Also, if $\eta > \bar{\eta}^{(\text{het})}$ there is a minimum of $R^{(\text{het})}$ in the third stage corresponding to the value

$$s_{\text{R}}^{(\text{het})} = \text{arcosh} \left[\left\{ N + \frac{1 + \eta}{2} - \sqrt{\eta(1 + N) - \mathcal{N}_{\text{env}}(1 + \mathcal{N}_{\text{env}})(1 - \eta)^2} \right\} \phi_0 - (2\mathcal{N}_{\text{env}} + 1)(1 - \eta) \right],$$

which has its limits

$$\lim_{\eta \rightarrow \bar{\eta}^{(\text{het})} + 0} s_{\text{R}}^{(\text{het})} = 0$$

and

$$\lim_{\eta \rightarrow 1} s_{\text{R}}^{(\text{het})} = \infty.$$

Taking into account the above considerations we have for optimal squeezing in environment $s_\star^{(\text{het})}$ (providing the highest heterodyne rate for a given transmissivity) the equality

$$s_\star^{(\text{het})} = \begin{cases} \infty, & \text{if } 0 < \eta \leq \bar{\eta}^{(\text{het})}, \\ 0, & \text{if } \bar{\eta}^{(\text{het})} \leq \eta < 1, \end{cases}$$

which is similar to the analogous relation for capacity (131).

VI. MULTIPLE CHANNEL USES

Let us now move to the case of multiple uses (multi-mode) of the lossy bosonic channel. We will consider those types of memory channel environments which give rise to spectral problems (in general, symplectic eigenvalues are not functions of matrix spectrum). One of the simplest models of this class is

$$V_{\text{env}} = \bigoplus_{k=1}^n V_{\text{env},k}, \quad (160)$$

where each $V_{\text{env},k} = V(\mathcal{N}_{\text{env},k}, s_{\text{env},k})$ (see Eq. (32)) is the single-mode environment corresponding to k th channel use. It follows from [18] that optimal matrices V_{in} and V_{mod} have the same form as (160), *i.e.* they are direct sums of some single-mode matrices. Then, the average amount of photons per mode in V_{in} is related with the amount taken for each mode (see Eq. (33)) as

$$N = \frac{1}{n} \sum_{k=1}^n N_k. \quad (161)$$

In the following it will be useful to work with *total amount of input photons*

$$\mathcal{N} := nN,$$

which will always be written in calligraphic font. Note, that $\mathcal{N} = N$ for the single channel use. Similarly, we will search the maximum for *total capacity*

$$\mathcal{C} := n\mathcal{C}_n,$$

where

$$\mathcal{C}_n = \frac{1}{n} \sum_{k=1}^n C_k \quad (162)$$

with C_k the capacity of the single (k th) channel use (mode) as studied in Sec. IV. Below we use the system of notations introduced in Subsec. IV-A for the case of single channel use by adding extra index (usually, k) to all quantities in order to indicate which channel use the quantities are referred to.

Notice, that apart from the model (160), also environment model of the form (28) (with commuting blocks $V_{\text{env},qq}$ and $V_{\text{env},pp}$) gives rise to spectral problem. It particular, in this case it also follows from [18] that the maximum of χ -quantity (14) is achieved with matrices V_{in} and V_{mod} of the same form as (28), *i.e.* with null off-diagonal blocks. Furthermore, all diagonal blocks of all matrices will be mutually commuting. Such form of covariance matrices makes symplectic eigenvalues functions of the usual eigenvalues, specifically

$$\nu_k = \sqrt{o_{qk} o_{pk}}, \quad \bar{\nu}_k = \sqrt{\bar{o}_{qk} \bar{o}_{pk}}, \quad (163)$$

where

$$o_{uk} = \eta i_{uk} + (1 - \eta) e_{uk}, \\ \bar{o}_{uk} = \eta (i_{uk} + m_{uk}) + (1 - \eta) e_{uk}.$$

Both energy constraint (25) and symplectic spectrum (163) are preserved under orthogonal transformations. Thus, without affecting the final result, below we can consider all the involved matrices to be diagonal (see also the discussion in the appendix of [12]). Notice, that if all matrices are diagonal,

then the optimal input state is pure (it straightforwardly follows from the theorem 2 applied to each channel use).

More generally, according to the Williamson decomposition theorem, any covariance matrix can be put in a diagonal form by acting with a symplectic transformation [39]. However, such a symplectic transformation may not preserve the energy constraint. One can hence restrict the consideration to the class of models for which the symplectic transformation preserves the energy constraint (these are jointly symplectic and orthogonal). In particular, the models (28) belong to this class. The general form of such V_{env} matrices is presented in the Appendix of [12] (see also [38]).

A. Convex separable programming

The optimization problem for multiple channel uses is formulated as follows. One needs to find the maximum over the variables i_{uk} , m_{uk} , and m_{u_*k} for the following functions²⁸:

$$\begin{aligned} \underline{C}_n &= \frac{1}{n} \sum_{k=1}^n \left[g \left(\bar{\nu}_k - \frac{1}{2} \right) - g \left(\nu_k - \frac{1}{2} \right) \right], \\ R_n^{(\text{het})} &= \frac{1}{n} \sum_{k=1}^n \left[\log_2 \bar{\nu}_k^{(\text{het})} - \log_2 \nu_k^{(\text{het})} \right], \\ R_n^{(\text{hom})} &= \frac{1}{2n} \sum_{k=1}^n \left[\log_2 \bar{o}_{u_*k} - \log_2 o_{u_*k} \right] \end{aligned}$$

with the constraints

$$\begin{aligned} i_{uk} &> 0, \\ m_{uk}, m_{u_*k} &\geq 0, \\ \frac{1}{n} \sum_{k=1}^n \left[i_{uk} + \frac{1}{4i_{uk}} + m_{uk} + m_{u_*k} \right] &= 2N + 1. \end{aligned}$$

Then, the problem of finding the capacity²⁹ can be reformulated as finding the maximum for sum of concave³⁰ functions (each of them depending on one variable)

$$\mathcal{C}(N) = \sum_{k=1}^n C_k \quad (164)$$

over the distribution $P(N_k)$ of positive numbers N_k satisfying the constraint

$$\begin{aligned} \mathcal{N} &= \sum_{k=1}^n N_k, \\ N_k &= \frac{1}{2} \left[i_{uk} + \frac{1}{4i_{uk}} + m_{uk} + m_{u_*k} - 1 \right] \geq 0, \end{aligned} \quad (165)$$

where N_k is the amount of energy granted for k th mode (see Eq. (161)), and $C_k = C_k(i_{uk}, m_{uk}, m_{u_*k})$ (see the definition (162)) is parametrized by fixed parameters e_{uk}, e_{u_*k}

²⁸Here the homodyne rate corresponds to the measurement of (generally) different quadratures for different channel uses, where less noisy quadratures are used for information transmission. Such definition of homodyne rate is different from those given by the relation (31), where the same quadrature is measured in all modes.

²⁹The case of rates is completely analogous to that of capacity, therefore here it is omitted.

³⁰The concavity of single-use capacity C_k over its energy constraint N_k was proved in Subsec. IV-K.

and η , *i.e.* C_k only depends on the eigenvalues belonging to k th mode. Thus, the total optimization problem is splitted in two tasks: the first task is the ‘‘internal optimization’’ solved in Sec. IV, *i.e.* optimization inside each mode (see ‘‘box’’ (115)) and the second task is the ‘‘external optimization’’, *i.e.* finding the optimal distribution $P(N_k)$ of the total energy \mathcal{N} over ‘‘boxes’’ to get maximal output sum $\sum_{k=1}^n C_k$:

$$\begin{aligned} N_1 &\longrightarrow \boxed{C_1 = C_1(N_1)} \longrightarrow C_1 \\ &\dots\dots\dots \\ N_n &\longrightarrow \boxed{C_n = C_n(N_n)} \longrightarrow C_n \end{aligned}$$

This ‘‘external optimization’’ problem is known in mathematics as *convex separable programming* which was solved in [19], [20]. In particular, the following theorem based on concavity of target function was proved [19]:

Theorem 4: A feasible solution $\{N_k\}$ is an optimal solution to the problem (164), (165) if and only if there exists a $\lambda \in \mathbb{R}$ such that

$$N_k = 0, \quad \text{if } \lambda \geq \frac{\partial C_k}{\partial N_k}(N_k = 0), \quad (166)$$

$$N_k | \lambda = \frac{\partial C_k}{\partial N_k}(N_k), \quad \text{if } \lambda < \frac{\partial C_k}{\partial N_k}(N_k = 0). \quad (167)$$

Thus, the theorem states that any solution of ‘‘external optimization’’ problem satisfying its Lagrange equations is optimal because it is unique. Also, it follows from the theorem that the dependence $\lambda(N)$ is monotonic. Indeed, if λ is increasing, then some modes can change their ‘‘case’’ from (167) to (166), which results to zeroing their contribution to $N = \sum_{k=1}^n N_k$. Even if some modes remain in the case (167), their contribution N_k is decreasing because of the concavity and the monotonically increasing behavior of functions $C_k(N_k)$. Analogously, lower λ corresponds to higher N .

Below it will be convenient to use the *threshold functions* (see also [22])

$$\begin{aligned} \lambda_{1 \rightarrow 2,k} &\equiv \frac{dC_k}{dN_k}(N_k = 0) = \frac{\eta}{o_{u_*k}} g_1(\nu_k), \\ \lambda_{2 \rightarrow 3,k} &\equiv \frac{dC_k}{dN_k}(N_{2 \rightarrow 3,k}) = \frac{\eta}{\bar{\nu}_k} g_1(\bar{\nu}_k) \end{aligned} \quad (168)$$

defined analogously to single-mode relations (122) and (123), where quantity $N_{2 \rightarrow 3,k}$ is given by Eq. (81) applied to k th mode. Thus, the threshold functions are generalizations of the single-use threshold values written in λ -representation (see Subsec. IV-L). Taking into account (113) one can see that $\lambda \in (0, \lambda_{\text{max}})$ for $N > 0$, where

$$\lambda_{\text{max}} = \max_k \frac{\partial C_k}{\partial N_k}(N_k = 0) = \max_k \lambda_{1 \rightarrow 2,k}.$$

In the following the notion of *stage* will be referred to each mode (in complete analogy with the single use case presented in Sec. IV). It allows the optimization problem to be interpreted as the search for the optimal *distribution of modes across stages*. In particular, the case $N_k = 0$ holds if and only if k th mode belongs to the first stage, and the case $\lambda = \lambda_{\text{max}}$

corresponds to zero capacity, where all modes are in the first stage. Analogously, it follows from theorem 4, that if it is

$$\lambda < \min_k \frac{\partial C_k}{\partial N_k}(N_k = 0) = \min_k \lambda_{1 \rightarrow 2, k},$$

only the second and third stages exist (by comparing N_k granted for k th mode with its threshold value $N_{2 \rightarrow 3, k}$ one can obtain its actual stage).

The proposition 3 (see Subsec. IV-L) applied to multiple uses threshold functions (168) shows the relationship between the level of noise in particular quadratures and their participation to information transmission. For example, for fixed value of total energy N , the k th mode can change its stage from first to second if the noise in quadrature e_{uk} or $e_{u,k}$ is sufficiently decreased. More generally, one can say that it is the most optimal case when less noisy modes get more input energy and thus transfer more information, which is similar to the case of classical channels.

The “external optimization” problem is reducible to single transcendental equation on λ

$$\mathcal{N} = \sum_{k=1}^n N_k(\lambda), \quad (169)$$

which has single root because of theorem 4. It can be solved by using, e.g., method of bisection. Remember, that $N_k(\lambda) = 0$ if $\lambda > \lambda_{1 \rightarrow 2, k}$. Then, $N_k(\lambda)$ is given by Eq. (121) if $\lambda_{2 \rightarrow 3, k} < \lambda < \lambda_{1 \rightarrow 2, k}$. Finally, $N_k(\lambda)$ is given by Eq. (119) if $\lambda < \lambda_{2 \rightarrow 3, k}$. Thus, equation (169) can be considered as giving feasible solution for *any* λ , the only difference is that such a solution corresponds to another value of \mathcal{N} .

As far as the solution is unique it is sufficient to prove the convergence of the bisection method applied to Eq. (169), which can be done as follows. Notice, that λ and \mathcal{N} are related each other by one-to-one correspondence, and the dependence $\lambda(\mathcal{N})$ is monotonic. In particular, the limit $\lambda \rightarrow 0$ corresponds to the limit $\mathcal{N} \rightarrow \infty$, and the value $\lambda = \lambda_{\max}$ corresponds to $\mathcal{N} = 0$. Thus, as far as a unique λ corresponds to a given \mathcal{N} , the method of bisection applied to the transcendental equation (169) for the variable $\lambda \in (0, \lambda_{\max}]$ always converges to the solution.

Apart from the considered “blackbox” approach, the given optimization problem can be also interpreted in the following way. There are two effective unknown “variables” for the systems of Lagrange equations³¹: distribution of modes across stages and λ . In the simplest case, one of these variables can be set as internal and the another one as external during optimization process. The algorithm proposed in [19] uses λ as internal variable, while the above algorithm uses distribution of modes across stages for that. Since the latter algorithm is usually faster, below we will make use of it.

³¹Note, that each distribution of modes across stages results to its own system of Lagrange equations, where unknown variables are the eigenvalues of V_{in} and V_{mod} . As far as the system of Lagrange equations itself does not provide effective method to find distribution of modes across stages, some *a priori* properties are necessary to write a fast algorithm. In particular, concavity and monotonic behavior of capacity are such properties for the given problem.

B. Classical capacity and rates

Remember, that explicit analytical solution of the optimization problem is not possible and depends on the form of the threshold functions $\lambda_{1 \rightarrow 2, k}$, $\lambda_{2 \rightarrow 3, k}$ defined by environment matrix V_{env} and transmissivity η . However, if we are interested in finding approximate values of capacity, e.g. $\underline{C}_n^{(0)}$ or $\underline{C}_n^{(1)}$ relying on quantity $\lambda^{(0)}(N)$ (see Eq. (124)), some simplification of general method is possible. Below we show this using $\underline{C}_n^{(0)}$ and $\underline{C}_n^{(1)}$ as examples, but the generalization to the case of rates is straightforward.

Notice, that mode transcendental equation (88) can be formally written as the dependence $\bar{o}_{u,h} = f_h(i_{uh})$ for the h th channel use. Then, remember, that $\lambda^{(0)}$ (which is the amount of input photons granted for each channel use in the λ -representation) is the same for all modes in the third and the second stages. As far as the variable $\bar{o}_{u,k}$ for any mode k can be used as an equivalent replacement of $\lambda^{(0)}$ (see Eq. (124)), we can introduce a new variable

$$\begin{aligned} x &:= \bar{o}_{qm} = \bar{o}_{pm} = \bar{o}_{ql} = \bar{o}_{pl} = \dots \\ &= \bar{o}_{qh} = f_h(i_{ph}) = \bar{o}_{pt} = f_t(i_{qt}), \end{aligned} \quad (170)$$

getting a chain of equalities linking *all* modes of the second and third stages. Here modes m and l belong to the third stage, while modes h and t to the second stage ($m_{ph} = m_{qt} = 0$). Modes of the first stage are not included in (170) and all give V_{in} -eigenvalues equal to $\frac{1}{2}$. If some mode belongs to the third stage, its V_{in} -eigenvalues can be found from the relations (74). If some mode belongs to the second stage, its input eigenvalues are given in Subsec. IV-G (see Eqs. (100) and (103)).

Taking into account stages discrimination, equation (24) can be rewritten as

$$\sum_{\{2,3|m_{uk} \neq 0\}} [\eta(i_{uk} + m_{uk}) + (1 - \eta)e_{uk}] = [2n_3 + n_2]x, \quad (171)$$

where n_j is the number of modes belonging to j -th stage ($j = 1, 2, 3$; $n = n_1 + n_2 + n_3$) and $\sum_{\{2,3|m_{uk} \neq 0\}}$ stands for the summation over all eigenvalues of second and third stages, except for the uk -th ones corresponding to $m_{uk} = 0$. Also, the energy constraint (25) can be rewritten as

$$\sum_{\{2,3|m_{uk} \neq 0\}} [i_{uk} + m_{uk}] = 2n \left[N + \frac{1}{2} \right] - n_1 - \sum_k'' i_{uk}, \quad (172)$$

where $i_{uk} = f_k^{-1}(x)$ and the double prime sum extends over uk -th eigenvalues of the second stage, such that $m_{uk} = 0$. Substituting Eq. (172) into Eq. (171) we get a transcendental equation for the single variable x . Since all unknown eigenvalues can be expressed through x (see Eqs. (170)) we can formally arrive at $\underline{C}_n^{(0)}$ and $\underline{C}_n^{(1)}$.

Notice, that as far as the relation $i_{uk} = f_k^{-1}(x)$ is explicit in the zeroth-order and the first-order approximations (see Eqs. (100), and (103)), one can express the quantities $\underline{C}_n^{(0)}$ and $\underline{C}_n^{(1)}$ as functions of solution of only one algebraic equation (see Eqs. (171) and (172)) for one variable x .

When all modes are in the third stage we have the explicit analytical solution and the equalities $\underline{C}_n = \underline{C}_n^{(0)} = \underline{C}_n^{(1)}$. In

particular, it is

$$\underline{C}_n = g[\eta N + (1 - \eta)N_{\text{env}}] - \frac{1}{n} \sum_{k=1}^n g[(1 - \eta)\mathcal{N}_{\text{env},k}], \quad (173)$$

where

$$N_{\text{env}} = \frac{1}{n} \sum_{k=1}^n N_{\text{env},k} \quad (174)$$

is the average number of photons in the multiple uses environment. The analytical lower bound given by Eq.(173) generalizes the expression presented in [12]. Analogously, in the case of all modes belonging to the third stage the heterodyne rate reads

$$R_n^{(\text{het})} = \log_2 \left[\eta N + (1 - \eta)N_{\text{env}}^{(\text{het})} + \frac{1}{2} \right] - \frac{1}{n} \sum_{k=1}^n \log_2 \left[(1 - \eta)\mathcal{N}_{\text{env},k}^{(\text{het})} + \frac{1}{2} \right],$$

where $N_{\text{env}}^{(\text{het})}$ is defined similarly to Eq. (174).

If all modes are in the second stage, the homodyne rate reads (see Eq. (101))

$$R_n^{(\text{hom})} = \frac{1}{n} \sum_{k=1}^n \log_2 \left[\sqrt{(\phi_k/4)^2 + \phi_k T_1^{(\text{hom})}} - \phi_k/4 \right],$$

where $T_1^{(\text{hom})}$ (see Eq. (127)) is given by the root of equation (see the relations (128) and (129))

$$\frac{1}{n} \sum_{k=1}^n [i_{uk} - \phi_k^{-1}] = 2N + 1 - T_1^{(\text{hom})}$$

with

$$i_{uk} = \frac{1}{2} \left[\sqrt{(\phi_k/4)^2 + \phi_k T_1^{(\text{hom})}} - \phi_k/4 \right].$$

If the number of channel uses tends to infinity the discussed procedure can be properly generalized by changing the transcendental equations (e.g. Eqs. (171) and (172)) to equations on functions (spectral densities). However, if the considered model has some symmetry over stages, the general solution can be further simplified by considering some parameters which mark the boundaries between regions of modes belonging to different stages. In Subsec. VI-C we will show an example along this line.

C. Application to a particular memory channel

In this subsection we look for the capacity of channels whose environment is described by a covariance matrix of the form

$$V_{\text{env}} = \left[N_{\text{env}} + \frac{1}{2} \right] \begin{pmatrix} e^{s\Omega} & 0 \\ 0 & e^{-s\Omega} \end{pmatrix}, \quad (175)$$

where Ω is a real symmetric $n \times n$ matrix and $s \in \mathbb{R}$ is a parameter describing the environment properties. In particular, we will consider the case of environment model (175) with

$$\Omega_{ij} = \delta_{i,j+1} + \delta_{i,j-1}; \quad i, j = 1, \dots, n$$

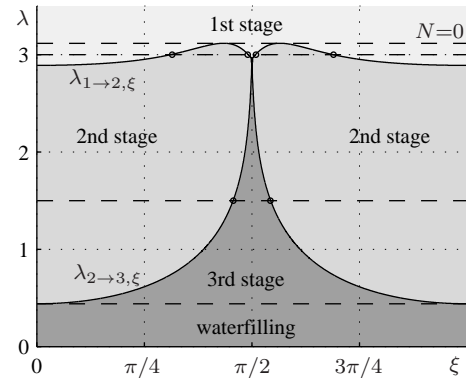


Fig. 22. Threshold functions $\lambda_{1 \rightarrow 2, \xi}$ and $\lambda_{2 \rightarrow 3, \xi}$ vs ξ for Ω -model. The value of other parameters are $\eta = 0.4$, $s = 0.5$, $N_{\text{env}} = 0.01$. The horizontal dashed lines correspond to different values of N , where the top line is the case of $N = 0$ and the bottom line is the border-case when all modes are in the third stage (below it we have “waterfilling solution”). The points at which horizontal lines (corresponding to some values of λ or, equivalently, N) cross threshold functions $\lambda_{1 \rightarrow 2, \xi}$ and $\lambda_{2 \rightarrow 3, \xi}$ mark borders between modes with different stages. The regions corresponding to different stages are filled by different grey colors.

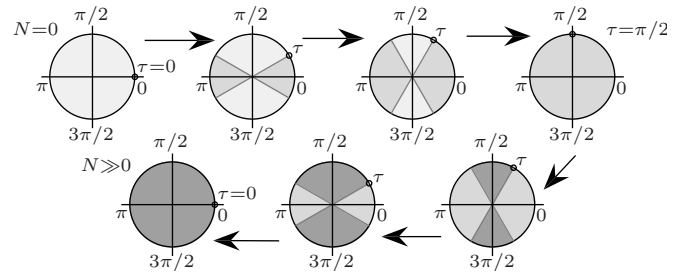


Fig. 23. Schematic representation of the “quantum water filling” for the capacities $\underline{C}^{(0)}$ and $\underline{C}^{(1)}$ and the environment model $\Omega_{ij} = \delta_{i,j+1} + \delta_{i,j-1}$ (it follows from the threshold functions $\lambda_{1 \rightarrow 2, \xi}$ and $\lambda_{2 \rightarrow 3, \xi}$ of variable ξ). The angle ξ parametrizing the spectral density corresponds to polar angle. White, grey and black sectors correspond to the first, second and third stages, respectively. Arrows show change of stages with increasing of N . The parameter τ marks the points of stage change.

describing a specific lossy bosonic channel with memory [11], which will be referred to as Ω -model of the environment. Notice, that by taking $\Omega_{ij} = \delta_{ij}$ we recover the case of the memoryless channel.

The parameter s in Eq. (175) represents the degree of correlation among environment modes. We are interested in the asymptotic behavior of this channel. That implies to take the limit $n \rightarrow \infty$ in the equations of Subsec. VI-B. It can be treated for some relations as the limit of Riemann sums resulting to the integral expressions. Thus, instead of a set of equations on eigenvalues we get a set of equations on functions which are spectral densities for the involved (infinite-dimensional) matrices. Below we denote the spectral densities by the same symbols as proper eigenvalues, but written in calligraphic and replacing the mode number h by a continuous parameter ξ , i.e., $i_{uh} \rightarrow \mathcal{I}_{u\xi}$, $o_{qh} \rightarrow \mathcal{O}_{q\xi}$, etc.

It is convenient to use the parameter ξ as arising from the

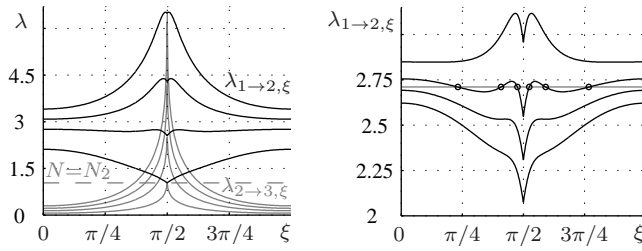


Fig. 24. Threshold functions $\lambda_{1 \rightarrow 2, \xi}$ (black) and $\lambda_{2 \rightarrow 3, \xi}$ (grey) are plotted vs ξ for capacity of the channel with the Ω -model of environment. The values of parameters at the left are $N_{\text{env}} = 0.01$, $s = 1$, η (from bottom to top): 0.15, 0.35, 0.55, 0.75. The values of parameters at the right are $N_{\text{env}} = 0.01$, $s = 1$, η (from bottom to top): 0.29, 0.32, 0.35, 0.4. Horizontal lines correspond to particular chosen values of input energy.

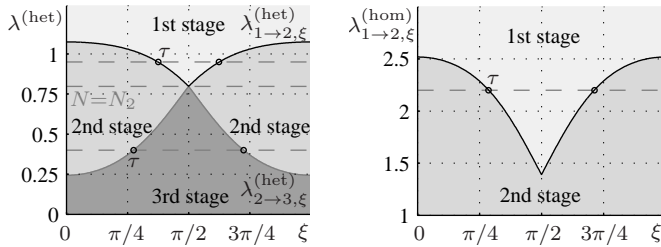


Fig. 25. Threshold functions for heterodyne (left) and homodyne (right) rates are plotted for the parameters $N_{\text{env}} = 0.5$, $s = 1$, $\eta = 0.65$ (channel environment is given by Ω -model). Horizontal lines correspond to particular chosen values of input energy. These lines cross threshold functions at the points (marked by τ if $\xi \in [0, \frac{\pi}{2}]$) corresponding to stage change.

spectrum of V_{env} -matrix [11]

$$\mathcal{E}_{u\xi} = \left(N_{\text{env}} + \frac{1}{2} \right) e^{\pm 2s \cos \xi}, \quad (176)$$

labeling both modes (if $\xi \in [0, \pi]$) and eigenvalues (if $\xi \in [0, 2\pi]$). Plus and minus in Eq. (176) stand for $u = q$ and $u = p$, respectively. Due to the mirror symmetry of eigenvalues (176) over quadratures, the symplectic spectrum and the distribution of modes across stages have to be symmetric with respect to the point $\frac{\pi}{2}$, therefore we restrict ourselves to consider spectral densities only defined in the interval $[0, \frac{\pi}{2}]$.

Threshold functions $\lambda_{1 \rightarrow 2, \xi}$ and $\lambda_{2 \rightarrow 3, \xi}$ (and also their analogs for rates) for Ω -model are shown in Figs. 22, 24 and 25. In general, the equation $\lambda_{1 \rightarrow 2, \xi} = \lambda$ (for the variable ξ) can have up to three different roots in the interval $[0, \frac{\pi}{2}]$. Below we will calculate the capacities $\underline{C}^{(0)}$ and $\underline{C}^{(1)}$ which are essentially simpler as the equation $\lambda_{1 \rightarrow 2, \xi} = \lambda$ has at maximum a single root τ which marks the boundary between the modes belonging to the first and second stages (the equation $\lambda_{2 \rightarrow 3, \xi} = \lambda$ has at most one root).

Suppose that all modes belong to the third stage, which holds true if (it can be obtained, e.g., from Eq. (75) or (81) by combining it with Eq. (176), see also Appendix in Ref. [11])

$$w := \frac{1}{2|s|} \ln \frac{\eta(2N+1) + (1-\eta)(2N_{\text{env}}+1)I_0(2s)}{\eta + (1-\eta)(2N_{\text{env}}+1)} \geq 1,$$

where I_0 is the modified Bessel function of the first kind and zero-order. The capacity \underline{C} in this case is given by Eq. (76),

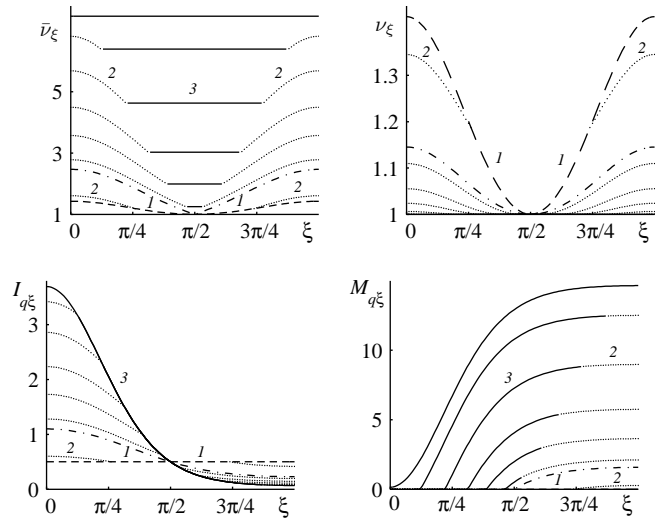


Fig. 26. Going from top-left clockwise the spectral densities $\bar{\nu}_\xi, \nu_\xi, \mathcal{M}_{q\xi}, \mathcal{I}_{q\xi}$ (for $\Omega_{ij} = \delta_{i,j+1} + \delta_{i,j-1}$) are plotted vs the parameter ξ for $N = 0, 0.05, 0.67, 1, 2, 3.5, 6, 9, 11$ (from bottom to top curve for quantities $\bar{\nu}_\xi, \mathcal{M}_{q\xi}, \mathcal{I}_{q\xi}$, and from top to bottom curve for quantity ν_ξ). Solid, dotted and dashed parts of curves correspond to third, second and first stages, respectively. Dash-dotted curve corresponds to the case of all modes belonging to the second stage. The values of other parameters used are $N_{\text{env}} = s = 1$, $\eta = 0.5$. Numbers 1, 2 and 3 are used to indicate the regions with corresponding stages.

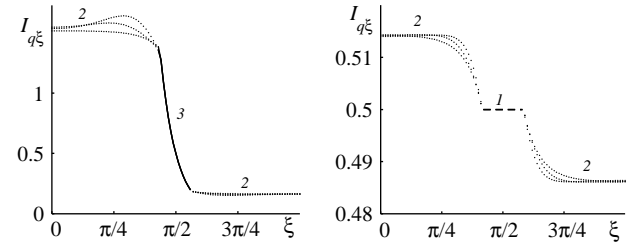


Fig. 27. Exact solution, first-order and zeroth-order approximations for spectral density $\mathcal{I}_{q\xi}$ vs ξ for $N = 1$ (left) and $N = 0.01$ (right). The values of other parameters are $N_{\text{env}} = 0.5$, $s = 2.5$, $\eta = 0.95$. Solid, dotted and dashed parts of curves correspond to third, second and first stages, respectively. Functions with maximum and minimum variations correspond to exact solution and zeroth-order approximation, respectively.

where the amount of environment photons N_{env} is given by Eq. (34) after a formal replacement $\cosh s \rightarrow I_0(2s)$. This example explicitly shows the possibility of an enhancement of the capacity with increasing degree of memory s (however, at the cost of increasing the amount of environment photons N_{env}).

If $w < 1$ we can have one of the following distributions of modes across stages according to the properties of the threshold functions $\lambda_{1 \rightarrow 2, \xi}^{(0)}$ and $\lambda_{2 \rightarrow 3, \xi}^{(0)}$ (see Fig. 23):

- i) a mixture of the second and the third stages (2,3,2);
- ii) a mixture of the second and the first stages (2,1,2);
- iii) all modes belonging to the second stage (2,2,2) which happens for a single value³² N_2 of the parameter N , given s, η and N_{env} .

If $N > N_2$ or $N < N_2$ we have the (2,3,2) or (2,1,2) case with the center of the interval $[0, \pi]$ filled by the third or the

³²Do not confuse this definition of N_2 with that used in Subsec. VI-A.

first stage, respectively. We label by $\tau \in [0, \frac{\pi}{2}]$ the point corresponding to the boundary between the regions of modes corresponding to different stages. The possible distributions of modes across stages and the dependence of τ from N are sketched in Fig.23. Notice, that at the point τ we must have $\overline{\mathcal{O}}_{u\tau} = \mathcal{O}_{u\tau}$ which can be rewritten as

$$x = x(\tau) = \eta \mathcal{I}_{u\tau} + (1 - \eta) \mathcal{E}_{u\tau}. \quad (177)$$

Here $u = q$ gives $\mathcal{I}_{q\tau} = e^{2s \cos \tau} / 2$ (see Eq. (74)) for (2,3,2) case and $u = p$ gives $\mathcal{I}_{p\tau} = \frac{1}{2}$ for (2,1,2) case (we use different quadratures in these cases because of either q or p quadrature changes its stage in the interval which contains τ).

Then, the transcendental equation for x (see Eqs. (171) and (172)) can be rewritten as an equation for τ

$$\eta \left[N + \frac{\tau_1}{\pi} - \frac{1}{\pi} \int_0^\tau \mathcal{I}_{q\xi} d\xi \right] + \frac{1 - \eta}{\pi} \int_0^{\tau_2} \mathcal{E}_{p\xi} d\xi = \frac{\tau_2}{\pi} x, \quad (178)$$

where (τ_1, τ_2) is equal to (τ, τ) for (2,1,2) and to $(\frac{\pi}{2}, \pi - \tau)$ for (2,3,2). Moreover, x is given by Eq. (177) and $\mathcal{I}_{q\xi}$ is the spectral density for the second stage which can be found as solution of functional equation obtained from Eq. (100) (or Eq. (103) in the case of $\underline{C}^{(1)}$) after the replacements discussed at the beginning of this subsection. By substituting $\tau = \frac{\pi}{2}$ in Eq. (178) we find N_2 . Comparing it with the actual energy restriction N we get the correct value of $\lambda^{(0)}$ and the distribution of modes across stages. Then, solving Eq. (178) with the found distribution of modes across stages we arrive at τ and x . Finally, $\underline{C}^{(0)}$ is expressed through these parameters as follows (see Eqs. (8), (9) and (14)):

$$\underline{C}^{(0)} = \left(1 - \frac{2}{\pi} \tau_3 \right) \left[g \left(x - \frac{1}{2} \right) - g \left((1 - \eta) N_{\text{env}} \right) \right] + \frac{2}{\pi} \int_0^\tau \left[g \left(\sqrt{x \mathcal{O}_{q\xi}} - \frac{1}{2} \right) - g \left(\sqrt{\mathcal{O}_{q\xi} \mathcal{O}_{p\xi}} - \frac{1}{2} \right) \right] d\xi,$$

where

$$\begin{aligned} \mathcal{O}_{q\xi} &= \eta \mathcal{I}_{q\xi} + (1 - \eta) \mathcal{E}_{q\xi}, \\ \mathcal{O}_{p\xi} &= \frac{\eta}{4} \mathcal{I}_{q\xi}^{-1} + (1 - \eta) \mathcal{E}_{p\xi}, \end{aligned}$$

τ_3 is equal to $\pi/2$ for (2,1,2) and to τ for (2,3,2).

The solution of the optimization problem for multiple channel uses can be interpreted as ‘‘quantum waterfilling’’ in analogy with usual (classical) ‘‘waterfilling’’ introduced for classical Gaussian channels with memory (see e.g. [22], [30] and [35]). The dependence of the found spectral densities (also symplectic ones) from N is similar to filling a vessel with water. The form of the vessel is defined by the model V_{env} and transmissivity η . The symplectic spectral density $\overline{\nu}_\xi$ goes always up by increasing N (with respect to $\nu_\xi(N = 0)$), while ν_ξ goes always down (or does not change). For environment models showing correlation (memory) among modes, the presence of the second stage gives rise to capillary effects on the edges of the vessel resulting to a ‘‘water level’’ with meniscus form. This ‘‘quantum water filling’’ effect for the considered model is shown in Fig.26 for symplectic spectral densities $\overline{\nu}_\xi$, ν_ξ and spectral densities $\mathcal{M}_{q\xi}$, $\mathcal{I}_{q\xi}$. Graphs of $\mathcal{I}_{q\xi}$ calculated through exact mode transcendental equation, zeroth-order and

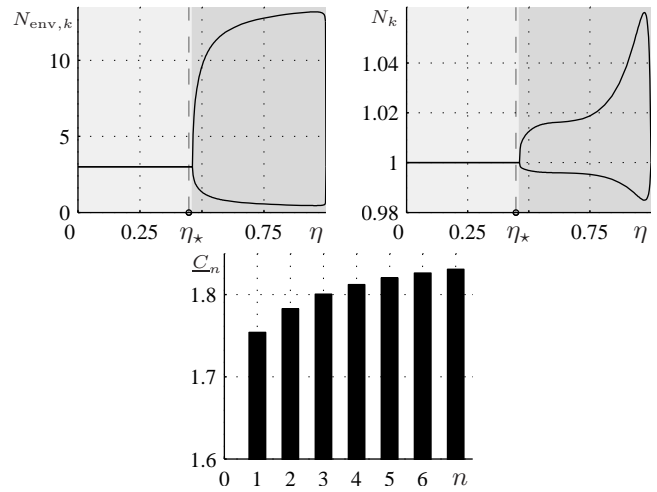


Fig. 28. Nontrivial behavior of optimal memory for capacity. Amounts of photons $N_{\text{env},k}$ (top-left) and N_k (top-right) corresponding to optimal memory for capacity are plotted as functions of transmissivity η . The values of other parameters are $N_{\text{env}} = 3$, $N = 1$ and $n = 5$. The lighter and the darker backgrounds indicate the additive and superadditive regions of transmissivity, correspondingly. Vertical dashed lines at $\eta = \eta_*$ mark the analytically estimated boundary between additive and superadditive regions. Bottom: capacity for optimal memory model is plotted vs amount of channel uses n . The values of other parameters are $N_{\text{env}} = 3$, $N = 1$ and $\eta = 0.8$.

first-order approximations are shown in Fig.27. Despite some visible difference between exact and approximate spectral densities the corresponding symplectic spectral densities are almost equal, thus resulting to the difference less than 0.05% between the capacities. The small value of this difference comes from the fact that the Holevo- χ has zero derivative with respect to the eigenvalues of V_{in} and V_{mod} in the neighborhood of the solutions of Lagrange equations (as they are equations for optimization problem).

In Fig.30-left the capacity $\underline{C}^{(1)}$ for Ω -model is plotted versus s for different values of η . The universal limit (110) for $s \rightarrow \infty$ is still valid.

D. Optimal channel memory and superadditivity

Finally, let us discuss the role of squeezing and memory in lossy bosonic channel. Considering the capacity (76) as a function on the set of environment models with fixed N_{env} , one can see that it shows *violation of quadrature symmetry*. In fact despite the symmetry of all equations over quadratures, the maximum of \underline{C} is achieved when $e_q \neq e_p$ (see also [30]). This also follows from the environment purity theorem proved for the single channel use (see Appendix D). By applying this theorem to each channel use for the case of memory channel one can see that optimal environment can always be chosen pure.

Now let us analyze the symmetry of the capacity over modes. Suppose, that the average (per mode) amount of photons in the environment N_{env} is fixed and the capacities for the single use of memoryless channel and multiple uses of memory channel (e.g. for Ω -model) are compared. As far as the Holevo- χ quantity (14) is symmetric over modes, one can expect that the capacity for the single channel use will always

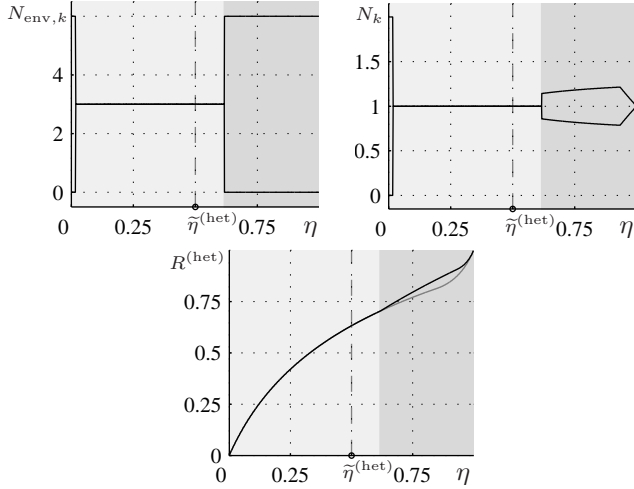


Fig. 29. Nontrivial behavior of optimal memory for heterodyne rate. Amounts of photons $N_{\text{env},k}$ (top-left) and N_k (top-right) corresponding to optimal memory for heterodyne rate are plotted as functions of transmissivity η . Bottom: heterodyne rate for memoryless model (grey curve) and for optimal memory model (black curve). The values of other parameters for all three graphs are $N_{\text{env}} = 3$, $N = 1$ and $n = 2$. The lighter and the darker backgrounds indicate the additive and superadditive regions of transmissivity, correspondingly. Vertical dashed lines at $\eta = \tilde{\eta}^{(\text{het})}$ mark the analytically estimated boundary between additive and superadditive regions.

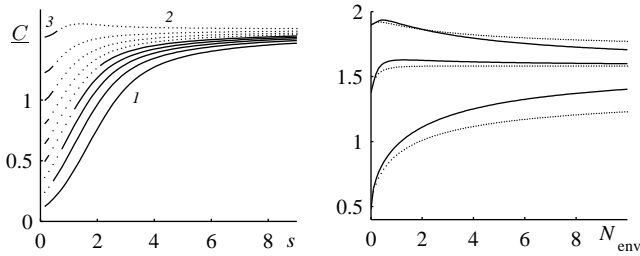


Fig. 30. On the left, the quantity $\underline{C}^{(1)}$ is plotted vs s for values of η going from 0.1 (bottom curve) to 0.9 (top curve) with step 0.1. The values of the other parameters are $N = N_{\text{env}} = 1$. Solid parts of curves correspond to the third and first stages, respectively. Dotted part of curves correspond to the second stage. Numbers 1, 2 and 3 are used to indicate the regions corresponding to the cases (2,1,2), (2,3,2) and (3,3,3), respectively. On the right, the maximum of $\underline{C}^{(1)}$ over V_{env} (i.e. over parameters s and N_{env}) is plotted vs N_{env} for values of $\eta = 0.1, 0.5, 0.9$ going from bottom to top curve. Solid and dotted curves corresponds to $\Omega = \delta_{ij}$ and $\Omega_{ij} = \delta_{i,j+1} + \delta_{i,j-1}$, respectively. The value of the other parameter is $N = 1$.

be higher. However, this is not true as results from the *violation of mode symmetry*. Indeed, this can be seen in Fig.30-right where the capacity $\underline{C}^{(1)}$ maximized over parameters s and N_{env} (thus, we have always $N_{\text{env}} = 0$) for memory and for memoryless cases is plotted versus N_{env} . We can see that the Ω -model for some parameters values provides higher capacity than memoryless model. Unfortunately the form of the *optimal* (in terms of capacity) memory for the channel is still unknown. We consider the finding of the optimal channel memory to be important and challenging problem.

As far as the optimal environment V_{env} can be always chosen in pure state, each its k th mode can be completely characterized by its squeezing s_k . Hence, the problem of finding optimal channel memory can be reformulated as finding

the form of the function $s(k)$ (or $s(\xi)$ for the case of $n \rightarrow \infty$). This function is not a constant, but numerical study of this problem in simplest situations shows that only two different values of $s(k)$ are possible for all k and given values of η , N and N_{env} .

The above properties can be also treated from the superadditivity viewpoint. First, let us discuss the memoryless channel capacity. It was proved in Subsec. IV-K that the one-shot capacity is monotonically increasing and concave function of N . In this case convex separable programming method (see Subsec. VI-A) guarantees that optimal input state is the direct sum of identical single-use matrices. It automatically implies additivity of memoryless capacity. As far as concavity was also proved for rates, the conclusions valid for capacity are also applicable for the rates.

However, the problem of additivity can be posed in another way. Quite generally one can compare different multi-mode environments containing (in average) the same amount of photons and having the same purity. In particular, the case of pure states is the most optimal as it is supported by environment purity theorem. In this case it straightforwardly follows from the dependence $\underline{C}(s)$ studied in Sec. V that the dependence of $\underline{C}(N_{\text{env}})$ (e.g. for pure environment state, see Eq. (34)) is in general non-monotonic, which guarantees optimality of non-homogeneous distribution of photons N_{env} over environment modes for some channel parameters.

In particular, one can expect that if $\eta < \eta_{\infty}$ and $N \geq \tilde{N}(0) \approx 0.3578$, then capacity is additive. In fact, in this case the dependence $\underline{C}(N_{\text{env}})$ corresponds to the concave and monotonically growing functions. Numerical calculations shows that in this region of parameters capacity is indeed additive. Similarly, if $\eta > \eta_{\infty}$, then $\underline{C}(N_{\text{env}})$ has local maximum in the interval $0 < N_{\text{env}} < \infty$ and numerical calculations shows that capacity is superadditive (non-homogeneous distribution of environment energy of modes is optimal) for some values of input energy. This allows us to conjecture, that the transitions between superadditive and additive cases happen at critical and supercritical parameters of single channel use. Notice, that heterodyne rate is in general also non-monotonic function of N_{env} , therefore it is also subjected to superadditivity property (see Fig.29).

The value of transmissivity η corresponding to transition from additive to superadditive region for given parameters N , N_{env} can be qualitatively estimated in the following way. In the case of capacity, this transition may happen close to the point $\eta = \eta_{\star}$ corresponding to the maximum of $\underline{C}(N_{\text{env}})$ (or $\underline{C}(s)$ because of purity) for fixed value of N . Similarly, in the case of heterodyne rate, one can roughly use $\eta = \tilde{\eta}^{(\text{het})}$ (see Eq. (158)) to estimate the transition point.

VII. CONCLUSION

IN this paper, we have developed powerful and versatile optimization methods for the estimation of Gaussian quantum channels' capacities and rates. We have applied them to the lossy bosonic channel in both memoryless and memory setting by restricting to Gaussian states.

First, we have thoroughly characterized the memoryless channel, thus generalizing the results of [3], [7]. To do that we

have exploited the single-mode channel whose environment's covariance matrix V_{env} can be described by two parameters: squeezing s and average amount of thermal photons \mathcal{N}_{env} . Then, to completely specify the channel usage we have fixed the values of transmissivity η and input energy N . It is the latter value that defines the kind of solution for the capacity C . For N increasing from 0 to $+\infty$ we have found three different *stages*, each characterized by a solution of a given form.

We have proved that the one-shot capacity is a concave and monotonically increasing function of N . Thus, as byproduct we have gotten the additivity of the memoryless capacity assuming covariance matrices for modulation, channel environment and input states to be mutually commuting. Moreover, due to this property the derivative $dC(N)/dN$ can be used as the equivalent replacement for the amount N of photons granted for channel input, thus providing another channel's representation. Within this representation (called λ -representation) is easily visualizable the geometry of the stages transitions.

The one-shot capacity turns out to be a monotonic function of all parameters, except of environment squeezing. This makes the latter a special parameter. In particular taking the limit $s \rightarrow +\infty$ we have defined different *regimes* depending on how the capacity tends this limit. This is determined by the value of transmissivity and amount of environment thermal photons. *Critical* values for these parameters can be defined at boundary of different regimes. Similarly, other regimes and critical parameters can be considered analyzing the other properties of $C(s)$ function. Totally we have defined five different regimes and four triads of critical parameters, which characterize the existence and values of specific points of $C(s)$.

Already from that we can draw some general conclusions about the channel's properties. For instance, if

$$N \geq [\sqrt{3/2 + 5/(2\sqrt{3})} - 1]/2 \approx 0.3578, \quad (179)$$

then $C(s)$ is always monotonic over $0 < s < +\infty$ if

$$\eta \leq 1 - 1/\sqrt{3} \quad (180)$$

and has no more than one maximum in this interval otherwise. Also, $C(s)$ has no more than one maximum if

$$\mathcal{N}_{\text{env}} \geq [(\sqrt{3} - 2/\sqrt{5})^{-1} - 1]/2 \approx 0.0969. \quad (181)$$

Another example is the case of $C(0) = C(\infty)$ for $N \rightarrow \infty$, which is possible only if

$$\eta \geq 2/e, \quad (182)$$

where inequality is saturated by pure environment state.

As far as the critical parameters in general depend on N , \mathcal{N}_{env} (or N, η — depending on the parameter varied in analyzing the behavior of $C(s)$) and not all of them exist in all the regimes, we have defined three *domains*. Each domain is characterized by existence and/or relations among critical parameters. In turn, *supercritical* values for N and \mathcal{N}_{env} can then be defined at boundary of different domains. The nontrivial global maximal or minimal values of critical and supercritical parameters must be intended as

fundamental constants characterizing the channel. Few of such constants which can be expressed in radicals are the above numbers (179), (181) for supercritical and (180), (182) for critical parameters.

Summarizing, in the space of parameters N , \mathcal{N}_{env} we have defined two functions and by equating them to zero we have divided the space into three parts (domains). The boundaries of domains define the supercritical parameters. In turn domains define the possible regimes (five at maximum). Critical parameters come out at the boundaries of regimes (this time in the space of parameters η , N , \mathcal{N}_{env}). Then, the towering achievement is the following route to determine the channel's "state":

- find the channel *domain* by comparing the actual N , \mathcal{N}_{env} with their supercritical values (it gives the set of possible *regimes*);
- find the channel *regime* by comparing the actual η , \mathcal{N}_{env} with their critical values;
- find the relevant values of squeezing parameter for the given channel *regime* and compare them with the actual s ;
- find the channel *stage*.

The above steps tell us the type of the curve $C(s)$, how many extremal and specific points it has, in which interval we are in this curve and what is the type of solution (stage). This is particularly relevant to characterize channels and might be useful in practical situations to determine the optimal 'work point' of a channel by having some freedom in its parameters values.

Then, we have presented the solution for the memory channel, thus generalizing the results of [10], [11], [12], [24]. Here, the problem of finding the capacity has been reformulated in a multi-mode setting as a total optimization problem split in two tasks: the first task is the "internal optimization", *i.e.* optimization inside each mode and the second task is the "external optimization", *i.e.* finding the optimal distribution of the total input energy $\sum_{k=1}^n N_k$ over "boxes" (modes) to get maximal output sum $\sum_{k=1}^n C_k(N_k)$. Then, the first task has been addressed using the techniques developed for the single-mode channel, while the second one using convex separable programming techniques [19], [20]. For the latter we have also given formal proofs of both the uniqueness of the solution and the convergence of the proposed algorithm.

The above splitting has become possible because we were confined to the class of memory models which make the optimization problem spectral.

In the case of single-mode channel we have derived theorems about the optimality of pure states showing that for any given V_{env} the optimal input channel state is pure, and for any fixed $\text{Tr}(V_{\text{env}})$ the optimal V_{env} is pure. In particular, purity of V_{env} once $\text{Tr}(V_{\text{env}})$ is fixed, results in a violation of quadrature symmetry. When this result is extended to the memory channel (*i.e.* non identical multiple modes environment), with optimization over distribution of input energies, we have discovered violation of mode symmetry too. That is to say, optimization inside each box gives us "violation of quadrature symmetry" with "input and environment purity

theorems"; then, maximization over our blackboxes gives us "violation of mode symmetry" and "optimal channel memory".

In this context the enhancement (superadditivity) of classical capacity is possible (for only some values of the memory channel parameters), if energy is redistributed between environment modes to become (in general) different in different modes. This possible violation of mode symmetry points out the existence of nontrivial optimal channel's environment (memory). Such environment can always be chosen pure. One can also say that capacity is superadditive if mode symmetry is violated and additive otherwise, where transition between additive and superadditive cases happens at critical and supercritical parameters found for the single-use of the single-mode channel.

Notice that the main feature of the considered memory model is to be symbol independent, *i.e.* the action of the channel at a given use does not depend on the previous inputs, and without a causal structure. That made its characterization a daunting task, which nevertheless has been accomplished.

Transmission rates for heterodyne and homodyne measurements have been treated parallelly to the capacity because they can be considered as its logarithmic approximations. In the case of heterodyne it has done by introducing heterodyne variables. Thus, most of the capacity properties can be also found analyzing the rates. In particular, it was shown that homodyne measurement for the single-use of the single-mode channel gives a rate which is always monotonically growing function of environment squeezing. However, this is not the case for heterodyne measurement which is monotonically growing function of squeezing only in neighborhood of $s \rightarrow \infty$, therefore its critical parameters were also calculated and its regimes were studied to provide complete characterization.

Finally, besides a thorough characterization of the lossy channel, we have provided mathematical techniques for the solution of optimization problems in information transmission with Gaussian channels. The machinery developed herein seems applicable to other capacities and other Gaussian channels as witnessed by the similarities with a recent study on additive Gaussian noise channel [22], which can be characterized as well by critical parameters [34]. Above all extension to the amplification channel seems within reach and is planned as a future work.

APPENDIX A

PROOF OF THE INPUT PURITY THEOREM FOR CAPACITY

Let us prove the theorem 1. Since the dimension of matrices is 2×2 , there is a symplectic transformation S which is orthogonal and diagonalizes V_{env} . Let us apply S to matrices V_{out} and \bar{V}_{out} (see Eqs. (23) and (24)). The transformation S preserves energy constraint (25), symplectic eigenvalues³³ $\nu, \bar{\nu}$ and does not change the Holevo function. If $V_{\text{in}}, V_{\text{mod}}$ and

V_{env} are taken in the form

$$V_{\text{in}} = \begin{pmatrix} i_q & i_{qp} \\ i_{qp} & i_p \end{pmatrix}, \quad V_{\text{mod}} = \begin{pmatrix} m_q & m_{qp} \\ m_{qp} & m_p \end{pmatrix}, \\ V_{\text{env}} = \begin{pmatrix} e_q & e_{qp} \\ e_{qp} & e_p \end{pmatrix}$$

we get for symplectic eigenvalues the relations

$$\bar{\nu}^2 = [\eta(i_q + m_q) + (1 - \eta)e_q] \times \\ [\eta(i_p + m_p) + (1 - \eta)e_p] - \eta^2(i_{qp} + m_{qp})^2, \\ \nu^2 = [\eta i_q + (1 - \eta)e_q][\eta i_p + (1 - \eta)e_p] - \eta^2 i_{qp}^2.$$

By setting m_{qp} to zero we cannot violate positivity of V_{mod} or change energy constraint (25), which is equivalent to write

$$i_q + i_p + m_q + m_p = 2N + 1, \quad (183)$$

but we always increase maximum in the Holevo function. Thus, the optimal V_{mod} must have $m_{qp} = 0$.

Also, it is evident that the case of mixed input ($i_q i_p - i_{qp}^2 > \frac{1}{4}$) is not optimal. Indeed, in this case there is a value $i'_{qp} > i_{qp}$ which gives $i_q i_p - i_{qp}^2 = \frac{1}{4}$ and does not change the constraint (183). Because of the monotonic behavior and the concavity over y of function $g(\sqrt{y} - \frac{1}{2})$, the matrix V_{in} with i_{qp} replaced by i'_{qp} gives higher maximum for capacity. Thus, optimal input state must be pure.

Following [22], [36] one can consider the Lagrange equations for the variables $i_q, i_p, i_{qp}, m_q, m_p, m_{qp}$ with constraints (183) and $i_q i_p - i_{qp}^2 = \frac{1}{4}$. This is reasonable because the case of N higher than some threshold value always gives the solution with positive values of i_q, i_p, m_q, m_p and positive matrix V_{mod} , therefore the corresponding constraints (requiring positivity) can be omitted. In particular, the derivative of the Lagrange function with respect to m_{qp} gives $i_{qp} + m_{qp} = 0$. Taking into account that the optimal m_{qp} is 0, we get that $i_{qp} = 0$ is also optimal.

Analogously, if N is below that threshold, either the value of m_q or m_p found according to the above approach is negative. It means that for a given N , the solution with positive values of both m_q and m_p does not exist and single zero-equal m -value is the only possibility allowed by the restriction $m_q, m_p \geq 0$ (the trivial case $m_q = m_p = 0$ gives zero capacity and therefore is excluded from consideration).

Let us consider the case of $m_q = 0$ (the case $m_p = 0$ can be proved analogously). Notice, that $m_q = 0$ implies that the covariance m_{qp} is not defined, *i.e.* matrix $V_{\text{mod}} \equiv m_p$ is a scalar. Then, one can consider the Lagrange equations for the variables i_q, i_p, i_{qp}, m_p with constraints (183) and $i_q i_p - i_{qp}^2 = \frac{1}{4}$ (one can show that the solution always gives $i_q, i_p > 0$). Taking the Lagrange function in the form

$$L = g\left(\bar{\nu} - \frac{1}{2}\right) - g\left(\nu - \frac{1}{2}\right) \\ - \lambda(i_q + i_p + m_p - 2N - 1) - \gamma\left(i_q i_p - i_{qp}^2 - \frac{1}{4}\right),$$

where λ and γ are the Lagrange multipliers, one can get, from $\partial L / \partial i_{qp} = 0$, that

$$i_{qp} \left(\frac{g_1(\bar{\nu})}{\bar{\nu}^2} - \frac{g_1(\nu)}{\nu^2} - 2\gamma \right) = 0. \quad (184)$$

³³As far as only the single-mode case is discussed, index k (see Eq. (14)) is omitted for symplectic eigenvalues.

By expressing γ from Eq. (184) and substituting it in the relation

$$\frac{\partial L}{\partial i_q} - \frac{\partial L}{\partial i_p} = 0$$

we arrive at

$$\frac{g_1(\bar{\nu})}{\bar{\nu}^2} (\beta - \eta^2 m_p) = \frac{g_1(\nu)}{\nu^2} \beta, \quad (185)$$

where

$$\beta = \eta(1 - \eta)(e_q - e_p) - (1 - \eta^2)(i_q - i_p).$$

As far as the function $y^{-2}g_1(y)$ is monotonically decreasing and $m_p > 0$, Eq. (185) results not consistent. Thus, $i_{qp} = 0$ is the only possibility in Eq. (184).

APPENDIX B

PROOF OF THE INPUT PURITY THEOREM FOR RATES

Let us prove the theorem 2. If quadrature p is measured for homodyne rate (31) (the case of q -quadrature is analogous), then one needs to maximize the quantity

$$R^{(\text{hom})} = \frac{1}{2} \log_2 \bar{o}_p - \frac{1}{2} \log_2 o_p, \quad (186)$$

where \bar{o}_p and o_p are diagonal elements of matrices $\bar{V}_{\text{out}} = \text{diag}(\bar{o}_q, \bar{o}_p)$ and $V_{\text{out}} = \text{diag}(o_q, o_p)$ (see Eqs. (23) and (24)). Similarly, we shall denote input and modulation matrices as $V_{\text{in}} = \text{diag}(i_q, i_p)$ and $V_{\text{mod}} = \text{diag}(m_q, m_p)$. Analogously, to find the heterodyne rate (30) one needs to maximize the quantity

$$R^{(\text{het})} = \log_2 \sqrt{(\bar{o}_q + 1/2)(\bar{o}_p + 1/2)} - \log_2 \sqrt{(o_q + 1/2)(o_p + 1/2)}. \quad (187)$$

The maximum for both functions (186) and (187) is taken over the variables i_q, i_p, m_q and m_p .

Suppose, that the maximum is achieved with a non pure state having $i_q i_p > \frac{1}{4}$. This means that some real number $\varepsilon > 0$ exist, such that $i_p = i'_p + \varepsilon$, where $i'_p = (4i_q)^{-1}$. New variables denoted with primes and defined by transformations

$$\begin{aligned} i'_p &= i_p - \varepsilon, & i'_q &= i_q, \\ m'_p &= m_p + \varepsilon, & m'_q &= m_q, \end{aligned}$$

make V_{in} pure and preserve the energy constraint (25). They also preserve the values of the first terms and decrease the values of the second terms in Eqs. (186) and (187), thus providing higher maximum than initial variables. Hence, the theorem is proved by contradiction.

APPENDIX C

PROOF OF THE PROPOSITION 2

Let us prove the proposition 2. Suppose, that $m_u > 0$ and $m_{u_*} = 0$ are optimal for $e_u > e_{u_*}$ in second stage. We will consider three possible cases $\bar{o}_u > \bar{o}_{u_*}$, $\bar{o}_u < \bar{o}_{u_*}$ and $\bar{o}_u = \bar{o}_{u_*}$ separately. If $\bar{o}_u > \bar{o}_{u_*}$, then our assumption leads to contradiction due to proposition 1. In what follows we will

use the equivalence between $\bar{o}_u \leq \bar{o}_{u_*}$ and $i_{u_*} \geq i_{u_* \text{min}}$, where

$$i_{u_* \text{min}} = N + \frac{1}{2} + \frac{1 - \eta}{2\eta} (e_u - e_{u_*}).$$

Notice, that our condition $e_u > e_{u_*}$ leads to $i_u < i_{u_*}$, where the latter is equivalent to $i_u < \frac{1}{2}$ due to optimality of pure input state (see theorem 1). For the interval $i_u < \frac{1}{2}$ one can show that ν^2 is a decreasing function of i_u . In addition, for $i_{u_*} > i_{u_* \text{min}}$ one can see that $\bar{\nu}^2$ is a decreasing function of i_{u_*} . Indeed, for these intervals the derivatives of ν^2 and $\bar{\nu}^2$ are negative:

$$\begin{aligned} \frac{d\nu^2}{di_u} &= \eta(1 - \eta) \left(e_{u_*} - \frac{e_u}{4i_u^2} \right) < 0, \\ \frac{d\bar{\nu}^2}{di_{u_*}} &= 2\eta^2 (i_{u_* \text{min}} - i_{u_*}) < 0. \end{aligned} \quad (188)$$

First, let us consider the strict inequality $\bar{o}_u < \bar{o}_{u_*}$. If the variables i_u, i_{u_*} and m_u are changed according to transformations

$$i'_u = \frac{1}{4(i_{u_*} - \varepsilon)}, \quad (189)$$

$$i'_{u_*} = i_{u_*} - \varepsilon, \quad (190)$$

$$m'_u = 2N + 1 - i_{u_*} + \varepsilon - \frac{1}{4(i_{u_*} - \varepsilon)},$$

where $0 < \varepsilon < i_{u_*} - i_{u_* \text{min}}$, then the energy constraint (65) is preserved (the variable $m_{u_*} = 0$ remains unchanged). Since $i'_u > i_u$ and $i'_{u_*} < i_{u_*}$ the new symplectic eigenvalues satisfy $\nu'^2 < \nu^2$ and $\bar{\nu}'^2 > \bar{\nu}^2$ (see Eqs. (188)). As far as g is increasing function, the new variables increase the first term in Eq. (60) and decrease the second term thus providing higher capacity.

Next, we consider the case $\bar{o}_u = \bar{o}_{u_*}$. Now we change the variables i_u, i_{u_*} according to transformations (189), (190) and variables m_u, m_{u_*} as follows:

$$m'_u = 2N + 1 - i_{u_*} - \frac{1}{4(i_{u_*} - \varepsilon)},$$

$$m'_{u_*} = \varepsilon,$$

where we choose ε (also for Eqs. (189) and (190)) from the interval $0 < \varepsilon < \frac{1}{2}(\bar{o}_{u_*} - \bar{o}_u)$. Since $i'_u > i_u$ and $i'_{u_*} < i_{u_*}$ we have $\nu'^2 < \nu^2$. In addition, the equalities $\bar{o}_u = \bar{o}_{u_*} = \bar{o}'_u = \bar{o}'_{u_*}$ lead to $\bar{\nu}'^2 = \bar{\nu}^2$. Thus, the new variables preserve the first term and decrease the second term in Eq. (60) thus providing higher capacity.

Finally, we have shown that for all possible cases ($\bar{o}_u > \bar{o}_{u_*}$, $\bar{o}_u < \bar{o}_{u_*}$ and $\bar{o}_u = \bar{o}_{u_*}$) the capacity can be increased by a suitable change of variables. Hence, the proposition is proved by contradiction.

APPENDIX D

PROOF OF THE ENVIRONMENT PURITY THEOREM

Let us prove the theorem 3. At first, notice that the following Lemma holds.

Lemma 1: Suppose one has real positive numbers a, b, c, d , where $c > a$, $b - a > d - c$ and $f(x)$ is a monotonically growing concave function in the interval $x \in (0, \infty)$, then

$$f(b) - f(a) > f(d) - f(c).$$

In the case of the first stage $\underline{C} \equiv 0$. In the case of the third stage

$$\max_{\mathcal{N}_{\text{env}}} \underline{C} = \underline{C}(\mathcal{N}_{\text{env}} = 0),$$

i.e. it is optimal to make the environment pure. Then, suppose that we have the case of second stage and environment in mixed state is optimal. Remember, that it was proved for $e_q > e_p$ that $m_q = 0$ and $o_q > \bar{o}_p > o_p$ (see proposition 2 and Eq. (68)). Let us now change the environment variables by preserving \mathcal{N}_{env} and making the new environment state pure ($\mathcal{N}'_{\text{env}} = 0$). It corresponds to the change of variables $e_q \rightarrow e'_q$, $e_p \rightarrow e'_p$ (the eigenvalues i_u and m_u remain the same), where the new value of squeezing s' is given by the relation

$$\cosh s' = (2\mathcal{N}_{\text{env}} + 1) \cosh s.$$

This results to $o'_q > o_q$ and $o'_p < o_p$, *i.e.* $o'_q - o'_p > o_q - o_p$, while $o'_q + o'_p = o_q + o_p$. It means that $\nu' < \nu$ (see analogous proofs in Subsec. IV-E). One can then write down:

$$o'_q (o'_p + \eta m_p) - o'_q o'_p > o_q (o_p + \eta m_p) - o_q o_p,$$

which is equivalent to $o'_q > o_q$. Taking into account the above inequality and applying the Lemma for $f(x) = \sqrt{x}$ one gets

$$\sqrt{o'_q (o'_p + \eta m_p)} - \sqrt{o'_q o'_p} > \sqrt{o_q (o_p + \eta m_p)} - \sqrt{o_q o_p},$$

i.e. $\bar{\nu}' - \nu' > \bar{\nu} - \nu$. Finally, applying again the Lemma for the function $f(x) = g(x - \frac{1}{2})$ one gets $\underline{C}' > \underline{C}$. Hence, the theorem is proved by contradiction.

APPENDIX E

THE SECOND DERIVATIVE OF SOLUTION OVER INPUT ENERGY

Let us show that $d^2 \underline{C} / dN^2 < 0$. In the second stage it is

$$\frac{d^2 \underline{C}}{dN^2} = \frac{\partial^2 \underline{C}}{\partial N^2} + 2 \frac{\partial^2 \underline{C}}{\partial N \partial i_u} \frac{\partial i_u}{\partial N} + \frac{\partial^2 \underline{C}}{\partial i_u^2} \left(\frac{\partial i_u}{\partial N} \right)^2 + \frac{\partial \underline{C}}{\partial i_u} \frac{\partial^2 i_u}{\partial N^2} \quad (191)$$

Taking into account that $\partial C / \partial i_u = 0$ for any values of N , we get an equality

$$\frac{d}{dN} \left(\frac{\partial \underline{C}}{\partial i_u} \right) = \frac{\partial^2 \underline{C}}{\partial N \partial i_u} + \frac{\partial^2 \underline{C}}{\partial i_u^2} \frac{\partial i_u}{\partial N},$$

which allows us to rewrite the derivative (191) as

$$\frac{d^2 \underline{C}}{dN^2} = \frac{\partial^2 \underline{C}}{\partial N^2} + \frac{\partial^2 \underline{C}}{\partial N \partial i_u} \frac{\partial i_u}{\partial N} = \frac{\partial^2 \underline{C}}{\partial N^2} - \frac{\partial^2 \underline{C}}{\partial i_u^2} \left(\frac{\partial i_u}{\partial N} \right)^2, \quad (192)$$

where

$$\frac{\partial i_u}{\partial N} = - \frac{\partial \mathcal{F}}{\partial N} \left(\frac{\partial \mathcal{F}}{\partial i_u} \right)^{-1}$$

and

$$\frac{\partial^2 \underline{C}}{\partial N^2} = [g_2(\bar{\nu}) - g_1(\bar{\nu})] \left(\frac{\eta}{\bar{o}_{u_*}} \right)^2.$$

One can show that

$$\frac{\partial^2 \underline{C}}{\partial N \partial i_u} = \frac{\eta^2}{2} \mathcal{L}, \quad \frac{\partial \mathcal{F}}{\partial N} = \eta \mathcal{L}, \quad (193)$$

where

$$\mathcal{L} = g_1(\bar{\nu}) \left(\frac{1}{\bar{\nu}^2} + \frac{1}{\bar{o}_{u_*}^2} \right) + g_2(\bar{\nu}) \left(\frac{1}{\bar{\nu}^2} - \frac{1}{\bar{o}_{u_*}^2} \right).$$

Since it always is $\bar{\nu}^2 > \bar{o}_{u_*}^2$, $g_1 > 0$ and $g_2 < 0$ (see Eqs. (19)), the quantity \mathcal{L} and the derivatives (193) are positive. Also it can be found that

$$\begin{aligned} \frac{\partial \mathcal{F}}{\partial i_u} = & -\frac{\eta}{2} \left[g_1(\bar{\nu}) \left(\frac{1}{o_u} + \frac{1}{\bar{o}_{u_*}} \right)^2 - g_1(\nu) \left(\frac{1}{o_u} + \frac{1}{4i_u^2 o_{u_*}} \right)^2 \right. \\ & - g_2(\bar{\nu}) \left(\frac{1}{o_u} - \frac{1}{\bar{o}_{u_*}} \right)^2 + g_2(\nu) \left(\frac{1}{o_u} - \frac{1}{4i_u^2 o_{u_*}} \right)^2 \\ & \left. + \frac{g_1(\nu)}{\eta o_{u_*} i_u^3} \right]. \end{aligned}$$

It was shown in [22] for additive noise channel that

$$\frac{\partial i_u}{\partial N} > 0, \quad \frac{d^2 \underline{C}}{dN^2} < 0$$

in the second stage, which can be similarly proved also for lossy channel. In addition, it is evident from Eq. (92) that $\partial i_u / \partial N > 0$ in the zeroth-order approximation. Then, in the third stage we have

$$\frac{d^2 \underline{C}}{dN^2} = \frac{\partial^2 \underline{C}}{\partial N^2} = \frac{\eta^2}{\bar{\nu}^2} g_2(\bar{\nu}) < 0. \quad (194)$$

Thus, we have shown that the second derivative of capacity is negative in the case of both the second and the third stages.

The derivative (194) also holds for rates if the replacement (56) is applied. Besides it, for the heterodyne rate the replacement (55) must be applied.

ACKNOWLEDGMENT

The research leading to these results has received funding from the European Commission's seventh Framework Programme (FP7/2007-2013) under grant agreement no. 213681. O. P. thanks Zborovskii V. G., Karpov E. A. and Schäfer J. for fruitful discussions.

REFERENCES

- [1] Holevo A. S., "On the mathematical theory of quantum communication channels", *Probl. Inf. Transm.* vol. 8, pp. 62–71, 1972.
- [2] Bennett C. H., and Shor P. W., "Quantum information theory", *IEEE Trans. Inf. Th.* vol. 44, pp. 2724–2742, 1998.
- [3] Holevo A. S., and Werner R. F., "Evaluating capacities of bosonic Gaussian channels", *Phys. Rev. A* vol. 63, pp. 032312-1–032312-14, 2001.
- [4] Braunstein S. L., and Pati A. K., *Quantum Information Theory with Continuous Variables*, Dordrecht, Kluwer Academic, 2003.
- [5] Navascues M., Grosshans F., and Acin A., "Optimality of Gaussian attacks in continuous-variable quantum cryptography", *Phys. Rev. Lett.* vol. 97, pp. 190502-1–190502-4, 2006; Garcia-Patron R., and Cerf N. J., "Unconditional optimality of Gaussian attacks against continuous-variable quantum key distribution", *Phys. Rev. Lett.* vol. 97, pp. 190503-1–190503-4, 2006.
- [6] Eisert J., and Wolf M. M., "Gaussian quantum channels", *Quantum Information with Continuous Variables of Atoms and Light*, Imperial College Press, London, pp. 23–42, 2007.

- [7] Giovannetti V., Guha S., Lloyd S., Maccone L., Shapiro J. H., and Yuen H. P., “Classical capacity of the lossy bosonic channel: the exact solution”, *Phys. Rev. Lett.* vol. 92, pp. 027902-1–027902-4, 2004.
- [8] Giovannetti V., Lloyd S., Maccone L., and Shor P. W., “Entanglement assisted capacity of the broadband lossy channel”, *Phys. Rev. Lett.* vol. 91, pp. 047901-1–047901-4, 2003.
- [9] Wolf M. M., Perez-Garcia D., and Giedke G., “Quantum capacities of bosonic channels”, *Phys. Rev. Lett.* vol. 98, pp. 130501-1–130501-4, 2007.
- [10] Giovannetti V., and Mancini S., “Bosonic memory channels”, *Phys. Rev. A* vol. 71, pp. 062304-1–062304-6, 2005.
- [11] Pilyavets O. V., Zborovskii V. G., and Mancini S., “A lossy bosonic quantum channel with non-Markovian memory”, *Phys. Rev. A* vol. 77, pp. 052324-1–052324-8, 2008.
- [12] Lupo C., Pilyavets O. V., and Mancini S., “Capacities of lossy bosonic channel with correlated noise”, *New J. Phys.* vol. 11, pp. 063023-1–063023-18, 2009.
- [13] Lupo C., Giovannetti V., and Mancini S., “Capacities of lossy bosonic memory channels”, *Phys. Rev. Lett.* vol. 104, pp. 030501-1–030501-4, 2010.
- [14] Hausladen P., Jozsa R., Schumacher B., Westmoreland M., and Wootters W. K., “Classical information capacity of a quantum channel”, *Phys. Rev. A* vol. 54, pp. 1869–1876, 1996.
- [15] Schumacher B., and Westmoreland M. D., “Sending classical information via noisy quantum channels”, *Phys. Rev. A* vol. 56, pp. 131–138, 1997.
- [16] Holevo A. S., “Quantum coding theorems”, *Russ. Math. Surveys*, vol. 53, pp. 1295–1331, 1998.
- [17] Giovannetti V., Guha S., Lloyd S., Maccone L., and Shapiro J. H., “Minimum output entropy of bosonic channels: a conjecture”, *Phys. Rev. A* vol. 70, pp. 032315-1–032315-14, 2004; Giovannetti V., Lloyd S., Maccone L., Shapiro J. H., and Yen B. J., “Minimum Rényi and Wehrl entropies at the output of bosonic channels”, *Phys. Rev. A* vol. 70, pp. 022328-1–022328-8, 2004; Giovannetti V., and Lloyd S., “Additivity properties of a Gaussian channel”, *Phys. Rev. A* vol. 69, pp. 062307-1–062307-9, 2004; Lloyd S., Giovannetti V., Maccone L., Cerf N. J., Guha S., Garcia-Patron R., Mitter S., Pirandola S., Ruskai M. B., Shapiro J. H., and Yuan H., “The bosonic minimum output entropy conjecture and Lagrangian minimization”, arXiv:0906.2758v3, 2010.
- [18] Hiroshima T., “Additivity and multiplicativity properties of some Gaussian channels for Gaussian inputs”, *Phys. Rev. A* vol. 73, pp. 012330-1–012330-9, 2006.
- [19] Stefanov S. M., “Convex separable minimization subject to bounded variables”, *Comp. Opt. Appl.* vol. 18, pp. 27–48, 2001.
- [20] Stefanov S. M., *Separable Programming. Theory and Methods*, Kluwer Academic Publishers: Dordrecht-Boston-London, 2001.
- [21] Cerf N. J., Clavareau J., Roland J., and Macchiavello P., “Information transmission via entangled quantum states in Gaussian channels with memory”, *Int. J. Quant. Inf.* vol. 4, pp. 439–452, 2006.
- [22] Schäfer J., Karpov E., and Cerf N. J., “Gaussian capacity of the quantum bosonic memory channel with additive correlated Gaussian noise”, *Phys. Rev. A* vol. 84, pp. 032318-1–032318-16, 2011.
- [23] Yuen H. P., and Shapiro J. H., “Optical communication with two-photon coherent states — Part III: Quantum measurements realizable with photoemissive detectors”, *IEEE Trans. Inf. Th.* vol. 26, pp. 78–92, 1980.
- [24] Lupo C., and Mancini S., “Entanglement enhanced bit rate over multiple uses of a lossy bosonic channel with memory”, *Optics & Spectroscopy* vol. 108, pp. 319–325, 2010.
- [25] De Gosson M., *Symplectic Geometry and Quantum Mechanics: Operator Theory, Advances and Applications* vol. 166, Birkhäuser, 2006.
- [26] Simon R., Mukunda N., and Dutta B., “Quantum-noise matrix for multimode systems: $U(n)$ invariance, squeezing, and normal forms”, *Phys. Rev. A* vol. 49, pp. 1567–1583, 1994.
- [27] Hastings M. B., “Superadditivity of communication capacity using entangled inputs”, *Nature Physics* vol 5, pp. 255–257, 2009.
- [28] Bowen G., and Mancini S., “Quantum channels with a finite memory”, *Phys. Rev. A* vol. 69, pp. 012306-1–012306-6, 2004.
- [29] Kretschmann D., and Werner R. F., “Quantum channels with memory”, *Phys. Rev. A* vol. 72, pp. 062323-1–052324-19, 2005.
- [30] Holevo A. S., Sohma M., and Hirota O., “Capacity of quantum Gaussian channels”, *Phys. Rev. A* vol. 59, pp. 1820–1828, 1999.
- [31] Lupo C., Pirandola S., Aniello P., and Mancini S., “On the classical capacity of quantum Gaussian channels”, *Phys. Scr.* vol. T143, pp. 014016-1–014016-6, 2011.
- [32] Caves C. M., and Drummond P. D., “Quantum limits on bosonic communication rates”, *Rev. Mod. Phys.* vol. 66, pp. 481–537, 1994.
- [33] Shapiro J. H., “Optical waveguide tap with infinitesimal insertion loss”, *Opt. Lett.* vol. 5, pp. 351–353, 1980.
- [34] Schäfer J., Karpov E., and Cerf N. J., “Quantum water-filling solution for the capacity of Gaussian information channels”, *Proc. of SPIE* vol. 7727 (Bellingham, WA), pp. 77270J-1–77270J-12, 2010.
- [35] Cover T. M., and Thomas J. A., *Elements of Information Theory*, New York, Wiley-Interscience, 1991.
- [36] Schäfer J., Daems D., and Karpov E., “Capacity of a bosonic memory channel with Gauss-Markov noise”, *Phys. Rev. A* vol. 80, pp. 062313-1–062313-11, 2009.
- [37] Corless R. M., Gonnet G. H., Hare D. E. G., Jeffrey D. J., and Knuth D. E., “On the Lambert W function”, *Adv. Comp. Math.* vol. 5, pp. 329–359, 1996.
- [38] Lupo C., and Mancini S., “Transitional behavior of quantum Gaussian memory channels”, *Phys. Rev. A* vol. 81, pp. 052314-1–052314-8, 2010.
- [39] Williamson J., “On the algebraic problem concerning the normal forms of linear dynamical systems”, *Am. J. Math.* vol. 58, pp. 141–163, 1936.
- [40] Holevo A. S., “Single-mode quantum Gaussian channels: structure and quantum capacity”, *Probl. Inf. Transm.* vol. 43, pp. 3–14, 2007.

Oleg Pilyavets was born in Frunze, USSR in 1983. He received his B.Sc. and M.Sc. degree in Applied Physics and Mathematics from Moscow Institute of Physics and Technology, the department of Problems of Physics and Power Engineering. In 2009 he earned the Ph.D. in Physics from the P. N. Lebedev Physical Institute, Moscow. In 2010 he received the Ph.D. in Physics also from the University of Camerino, Italy. Then he spent one year at University of Camerino as a PostDoctoral fellow.

Now he has a postdoctoral position at Centre for Quantum Information and Communication of the Université Libre de Bruxelles, Belgium. During the last years his research interest was mainly on information transmission through Gaussian quantum channels.

Cosmo Lupo received the Ph.D. degree in Fundamental and Applied Physics from the University of Napoli “Federico II”, Italy, in 2007. He was Marie Curie Fellow at the Research Center for Quantum Information (RCQI) in 2008. From 2008 he is a PostDoctoral fellow at the School of Science and Technology, University of Camerino, Italy. He has been engaged in geometric quantum computation, then in entanglement characterization and more recently in quantum channels capacities.

Stefano Mancini received the Ph.D. degree in physics from the University of Perugia, Italy, in 1998. He was Postdoctoral Fellow at the University of Milan for three years. Subsequently, with temporary lecturer positions held at University of Milan and at University of Camerino, Italy, he have contributed to establish the first Italian academic courses on quantum information and computation.

From 2004 to 2010 he has been researcher of theoretical physics and mathematical methods at Faculty of Science, University of Camerino. Since September 2010 he is professor of theoretical physics and mathematical methods at School of Science and Technology, University of Camerino. He has been involved in the fields of theoretical quantum optics, quantum control theory and quantum information theory. He has given significant contributions to the characterization of entanglement, to the formalism of quantum feedback, to the models of quantum memory channels and to the development of quantum cryptographic protocols.

He has authored or coauthored more than 150 papers published in leading international journals. He has been Editor of four journals for special issues devoted to quantum information topics. He is currently a member of the Editorial Board of the International Journal of Quantum Information. Dr. Mancini was awarded two times by the Italian Ministry of Research under Young Researchers Program.